# DEVELOPMENT OF A SULFATE REDUCING PACKED BED BIOREACTOR FOR USE IN A SUSTAINABLE HYDROGEN PRODUCTION PROCESS

by

Matthew James Lee McMahon

A thesis submitted to the Department of Chemical Engineering

In conformity with the requirements for

the degree of Master of Science (Engineering)

QUEEN'S UNIVERSITY

Kingston, Ontario, Canada

September, 2007

# Abstract

**Matthew J.L. McMahon**: Development of a Sulfate Reducing Packed Bed Bioreactor For Use In A Sustainable Hydrogen Production Process

A two-stage process is proposed that is based on the biological production of $H_2S$ from organic waste and its subsequent overall conversion to $H_2$ via an exothermic reaction. The current study examined the first step of this process, namely, the design and operation of a packed bed bioreactor with high volumetric $H_2S$ production ($mol/m^3.d$) and its comparison to analogous methanogenic technology.

A novel method of inoculum design was developed by evaluating the kinetics and immobilization potential of *Desulfovibrio desulfuricans* (ATCC 7757) and a sulfate reducing bacteria (SRB) consortium. The consortium's kinetics, as measured by the specific rate of sulfate reduction (1.2 g $SO_4^{2-}$/g CDW.h), were approximately twice as fast as those of *D. desulfuricans*. The pure strain however exhibited superior immobilization potential. Studies revealed that a mixed inoculum containing 96 % *D. desulfuricans* and 4 % consortium facilitated the rapid immobilization of a highly active SRB biomass and contributed to improved bioreactor performance.

Diatomaceous earth (DE) pellets, porous glass beads, polyurethane foam, and bone char were evaluated as potential carrier materials for SRB immobilization. The DE pellets immobilized the most biomass, were well suited for use at the industrial scale, and were thus employed in all continuous flow bioreactor experiments.

Using the designed inoculum and DE pellets, a 615 mL bioreactor achieved a volumetric productivity of 493 mol $H_2S/m^3.d$ (at $D$ = 1.6 $h^{-1}$) and a dissolved sulfide concentration of 9.9 mM. This occurred after 8 d of operation and represents a tenfold reduction in the required start-up period compared to similar bioreactors in the literature.

An $N_2$ strip gas was later used to remove the dissolved sulfide to the gas phase and enhance sulfate conversion. Shifting the medium pH from 7 to 6 increased the fraction of strippable sulfide and improved the strip gas composition from 3.6 to 5.8 mol % $H_2S$. The strip gas to liquid feed ratio ($G/L$, $m^3/m^3$) was investigated in the range of 0-14 and was found to be a suitable basis for scale-up indicating that productivities of up to 830 $mol/m^3.d$ were readily achievable. This represents a considerable improvement over current methanogenic bioreactor productivities.

**Key words**: sulfate reducing bacteria (SRB), packed bed bioreactor, *Desulfovibrio desulfuricans*, consortium, hydrogen

# Acknowledgments

I would like to thank my advisor Dr. Andrew Daugulis for his involvement in this unique project and for his enthusiasm in revisiting the peculiarities of packed bed bioreactors. His knowledge and advice have been invaluable. I am fortunate to consider him both a mentor and a friend.

Many thanks are also extended to Dr. Boyd Davis and Alain Roy for recognizing my early interest in this project and providing me with my first glimpse into the world of industrial research.

Dr. Gerrit Voordouw and Brenton Buziak were gracious hosts at the University of Calgary and provided valuable assistance with sulfate reducing bacteria cultures and anaerobic microbiological methods. The technical assistance and academic insights provided by Dr. Kunal Karan over the past few years are also greatly appreciated.

Finally, I am most thankful to God and my parents for their endless love and support throughout my academic career and beyond.

Research grants and scholarships were generously provided by the Natural Sciences and Engineering Research Council of Canada (NSERC), Kingston Process Metallurgy Inc., BioCap, and Queen's University.

# Table of Contents

**Abstract** ii

A**cknowledgements** iv

**List of Tables** ix

**List of Figures** xii

**Chapter 1: Introduction** 1

**Chapter 2: Literature Review** 3

2.1 Anaerobic Degradation of Organic Matter 3

2.2 Direct Biological Production of $H_2$ 4

2.3 Photosynthetic $H_2$ Production 5

2.4 Overview of Biological Methane Production 5

2.5 Overview of Biological Sulfate Reduction 6
- 2.5.1 Classification of Sulfate Reducing Bacteria 7
- 2.5.2 Ecological Context of Sulfate Reduction 8
- 2.5.3 Electron Donors and Reaction Stoichiometry 9
- 2.5.4 Complex Substrates 11
- 2.5.5 Sulfite and $SO_2$ as Alternative Electron Acceptors 12
- 2.5.6 Factors Affecting Growth 13
  - 2.5.6.1 pH 13
  - 2.5.6.2 Sulfide 14

2.6 Methanogenesis and Sulfate Reduction Comparison 17
- 2.6.1 Overall Volumetric Performance 18
- 2.6.2 Process Operability 23
- 2.6.3 $H_2$ and $CO_2$ Balance 24
- 2.6.4 Sulfate/Sulfite Reduction with $H_2S$ Splitting 24
- 2.6.5 Methanogenesis with Steam Methane Reforming and Water-Gas Shift 25

2.7 Practical Applications of Biological Sulfate Reduction 26

2.8 Sulfate Reducing Packed Bed Reactors 27
- 2.8.1 Rationale for Biofilm Immobilization 27
- 2.8.2 Biofilm Immobilization Fundamentals 29
- 2.8.3 Recent Literature 30

2.9 Scope of Thesis 40

**Chapter 3: Materials and Analytical Methods 42**

3.1 Chemicals 42

3.2 Analytical Methods 42
3.2.1 Total Dissolved Sulfide (TDS) 42
3.2.2 Dissolved Sulfate 43
3.2.3 Gas Phase $H_2S$ 44
3.2.4 Lactate and Acetate 44
3.2.5 Suspended Biomass Concentration 45
3.2.6 Phase Contrast Microscopy 46
3.2.7 Scanning Electron Microscopy 46
3.2.8 pH Measurement 46

3.3 Culture and Fermentation Methods 47
3.3.1 Postgate B Medium and Stock Culture Maintenance 47
3.3.2 Postgate C Medium 47
3.3.3 Serum Bottle Culture 48
3.3.4 2 L Bioflo Fermentations 48
3.3.5 Packed Bed Bioreactor (PBR) Fermentations 49

3.4 Sulfate Reducing Bacteria Cultures 52
3.4.1 *Desulfovibrio desulfuricans* (ATCC 7757) 52
3.4.2 Sulfate Reducing Bacteria Consortium 52

3.5 Carrier Materials 53
3.5.1 Polyurethane Foam Plugs 55
3.5.2 Poraver™ Porous Glass Beads 55
3.5.3 Bone Char 55
3.5.4 Celite™ R-635 56

**Chapter 4: Experimental Methods 57**

4.1 Microbial Systems Characterization Experiments: 57

4.2 Comparison of Carrier Materials Experiments 58

4.3 Comparison of *Desulfovibrio desulfuricans* and SRB Consortium Immobilization Potential Experiments 59

4.4 Continuous Packed Bed Reactor Experiments 60
4.4.1 PBR Fermentation Experiment 1: System Characterization 60
4.4.2 PBR Fermentation Experiment 2: Sustained Operation and Recovery After Shutdown 61
4.4.3 PBR Fermentation Experiment 3 (with Stripping): System Characterization 62
4.4.4 Basic Model for PBR Operation with Stripping 64
4.4.5 PBR Fermentation Experiment 4 (with Stripping): Performance Enhancement 64
4.4.5.1 Stripping with pH 6 Buffered System 65
4.4.5.2 Stripping with pH 7 Buffered System 66

**Chapter 5: Results and Discussion** **67**

5.1 Microbial Systems Characterization Experiments 67
5.1.1 Stoichiometry 67
5.1.2 Microbial Kinetics 70

5.2 Comparison of Carrier Materials 72
5.2.1 Bone Char Pellets 73
5.2.2 Poraver™ Porous Glass Beads 74
5.2.3 Polyurethane Foam Plugs 76
5.2.4 Celite™ R-635 Diatomaceous Earth Pellets 77

5.3 Immobilization Potential 80

5.4 PBR Fermentation #1 86

5.5 PBR Fermentation #2 94

5.6 PBR Fermentation #3 100

5.7 Basic Model for PBR Operation with Stripping 105

5.8 PBR Fermentation Experiment #4 107

**Chapter 6: Sulfide Product Recovery Considerations** **113**

6.1 $H_2S$ and $CO_2$ Partitioning Simulation 113
6.1.1 Sulfide Equilibrium 114
6.1.2 Carbonate Equilibrium 116
6.1.3 Simulation Results 119

6.2 Downstream Sulfide Product Recovery 122
6.2.1 Design Equations and Mass Balance 122
6.2.2 Gas to Liquid (*G/L*) Requirements for Dissolved Sulfide Recovery 125
6.2.2.1 Use of Fresh $N_2$ Strip Gas 125
6.2.2.2 Use of Bioreactor Strip Gas 126

**Chapter 7: Conclusions** **131**

**Chapter 8: Future Work** **135**

**Chapter 9: References** **138**

**Chapter 10: Appendices** **154**

10.1 Appendix A: Prediction of Volumetric $CH_4$ Production 155

10.2 Appendix B: Volumetric Sulfate Reduction Rates from Literature 156

10.3 Appendix C: Calibration Curves for Analytical Methods 158
10.3.1 Calibration Curve for Dissolved Sulfide 158
10.3.2 Calibration Curve for Dissolved Sulfate 159

10.3.3 Calibration Curve for Gas Phase $H_2S$ 160
10.3.4 Calibration Curves for Dissolved Lactate and Acetate 161
10.3.5 Calibration Curve for Suspended Cell Concentration 162
10.4 Appendix D: Basic PBR Model Description 163

# List of Tables

**Table 2.1:** Reaction stoichiometry for the formation of methane from various substrates by methanogenic bacteria (Madigan et al., 1997 as cited by Metcalf and Eddy, 2003). **.....6**

**Table 2.2:** Order of magnitude most probable number (MPN) count of sulfate reducing bacteria in environmental samples as cited by Hao et al. (1996). MPN per 100 mL unless otherwise stated. **.....9**

**Table 2.3:** Reaction stoichiometry and Gibbs free energy for the incomplete oxidation of lactate and the mineralization of acetate by SRB (Widdel et al., 1988). **.....10**

**Table 2.4:** Stoichiometry of SRB metabolic functions with lactate as the incompletely oxidized substrate. Biomass is approximated by the ratio $C_5H_7NO_2$. The balanced overall metabolism is based on experimental values (D'Alessandro et al., 1974 and Traore et al., 1982 as cited by Okabe and Characklis, 1992). **.....11**

**Table 2.5:** Complex substrates utilized by mixed cultures of fermentative heterotrophs and sulfate reducing bacteria. **.....12**

**Table 2.6:** Summary of literature reporting the effects of sulfide on growth and activity on sulfate reducing bacteria (adapted from Okabe et al., 1995). **.....16**

**Table 2.7:** Summary of microbial kinetic parameters for *Desulfovibrio desulfuricans* grown at 35 $^oC$ on lactate media. **.....17**

**Table 2.8:** Typical organic loading rates and predicted $CH_4$ production in methanogenic anaerobic bioreactors (adapted from Metcalf and Eddy, 2003). Abbreviations: CSTR - continuous stirred tank reactor; SBR, -sequential batch reactor; UASB - upflow anaerobic sludge blanket; ABR - anaerobic baffled reactor; AMBR - anaerobic migrating blanket reactor; PBR - packed bed reactor; AEBR - anaerobic expanded bed reactor; WW -wastewater. **.....19**

**Table 2.9:** Organic loading rates and associated $CH_4$ production in recent methanogenic literature. All bioreactors were run at mesophilic conditions (25-37 $^oC$). Abbreviations: SBR - sequential batch reactor; UASB - upflow anaerobic sludge blanket; ABR - anaerobic baffled reactor; PBR - packed bed reactor; AEBR - anaerobic expanded bed reactor; FBR - fluidized bed reactor; UASFF - upflow anaerobic sludge fixed film; WW - wastewater. **.....20**

**Table 2.10:** Volumetric sulfate reduction rates (mol $SO_4^{2-}/m^3$.d) from recent SRB literature. Abbreviations: CSTR- continuous stirred tank reactor; UASB - upflow anaerobic sludge blanket; PBR - packed bed reactor; FBR - fluidized bed reactor; WW - wastewater. All bioreactors were run at mesophilic conditions (20-37 $^oC$). **.....21**

**Table 2.11:** Summary of $H_2$ and $CO_2$ yields for production of $H_2$ via biologically produced $CH_4$ and $H_2S$ precursor molecules. **.....25**

**Table 2.12:** Characteristics of support materials evaluated by Silva et al. (2006). Abbreviations: PU -

polyurethane foam; AC- activated carbon; CE - alumina ceramic; PE - polyethylene. ..... **40**

**Table 3.1:** Composition of sulfate assay conditioning fluid (per 1000 mL). ..... **44**

**Table 3.2:** General carrier material dimensions and prices. ..... **54**

**Table 4.1:** List of 2 L batch BioFlo fermentations and their inoculum composition used in microbial kinetics and stoichiometry experiments. ..... **58**

**Table 4.2:** List of inoculum compositions and carrier materials used in immobilization potential experiments. ..... **59**

**Table 4.3:** Liquid feed rates, feed duration, and respective hydraulic residence times (HRT), dilution rates (*D*), and equivalent column volumes (CV) for this first PBR fermentation experiment (no stripping). ..... **61**

**Table 4.4:** Liquid feed rates, feed duration, and respective hydraulic residence times (HRT), dilution rates (*D*), and equivalent column volumes (CV) for this second PBR fermentation experiment. ..... **62**

**Table 4.5:** List of stripping ratios *(G/L)* evaluated for PBR fermentation at constant 80 mL/h liquid feed. *L* = liquid feed rate; *G* = $N_2$ strip gas rate. ..... **63**

**Table 4.6:** List of stripping conditions (*G/L*) at which strip gas samples were taken for gas phase $H_2S$ analysis. ..... **63**

**Table 4.7:** List of stripping ratios *(G/L)* evaluated for PBR fermentation using media buffered to pH 6.1. *L* = liquid feed rate; *G* = nitrogen strip gas rate. ..... **66**

**Table 4.8:** List of stripping conditions *(G/L)* evaluated for PBR fermentation using media buffered to pH 7. *L* = liquid feed rate; *G* = nitrogen strip gas rate. ..... **66**

**Table 5.1:** Summary of yield coefficients (*Y*) for serum bottle batch cultures of *Desulfovibrio desulfuricans* and an SRB consortium. Parameters measured were sulfate reduced ($SO_4^{2-}$), total dissolved sulfide (TDS), lactate oxidized, and cell dry weight (CDW) produced. At the experimental conditions (pH ~ 7.5) the majority of sulfide was in the dissolved phase. ..... **67**

**Table 5.2:** Batch growth kinetic properties for *Desulfovibrio desulfuricans* and an SRB enriched consortium as measured in 2 L batch fermentations. ..... **67**

**Table 5.3:** Summary of relevant volumetric productivities reported in literature for sulfate reducing bioreactors. ..... **94**

**Table 5.4:** Summary of highest volumetric productivities observed for PBR fermentations #1 and #2. ..... **95**

**Table 5.5:** Maximum theoretical suspended biomass concentrations assuming complete conversion of substrate to biomass according to the equation [$X = (Y_{X/S})(S_0)$]. The initial sulfate concentration is 32 mM but only 27 mM can be reduced due to a stoichiometric limiting amount of lactate. ..... **98**

**Table 5.6:** Results of a PBR experiment with stripping at various *G/L* ratios and the resulting partitioning of sulfide between dissolved and gas phases. The molar sulfur mass balance is also reported as total sulfide produced per sulfate reduced (mol/mol). ..... **104**

**Table 5.7:** Distribution of 20 mM total dissolved sulfide and the equilibrium $H_2S$ partial pressure at 37 $^oC$

for the pH range 6-8. **105**

**Table 5.8:** Observed changes in pH during the fourth PBR fermentation with potassium phosphate buffered media. **107**

**Table 5.9:** Summary of highest volumetric productivities (based on total reactor volume and port 3 outlet concentrations) from separate fermentations in this study. The volumetric productivity for the fourth fermentation accounts for both dissolved and gas phase sulfide product streams. **111**

**Table 6.1:** Nomenclature for sulfide equilibrium calculations. **114**

**Table 6.2:** Nomenclature for carbonate equilibrium equations **117**

**Table 6.3:** Nomenclature for stripping column analysis. It is assumed that the solute is sufficiently dilute in the liquid phase that its molar fraction and mole concentration are equivalent (i.e. $C_i = x_i$). **123**

**Table 10.1:** Volumetric sulfate reduction rates (mol $SO_4^{2-}/m^3.d$) from recent SRB literature. Abbreviations: CSTR - continuous stirred tank reactor; UASB, upflow anaerobic sludge blanket; PBR - packed bed reactor; FBR - fluidized bed reactor; WW - wastewater. **156**

**Table 10.2:** Nomenclature for basic PBR model for volumetric productivity based on equilibrium relationships. **163**

# List of Figures

**Figure 1.1:** Simplified process flow diagram for the proposed process of producing $H_2$ from organic waste via biogenic $H_2S$. Full details of the $H_2S$ converter are omitted due to its proprietary nature. **.....2**

**Figure 2.1:** Pathways of anaerobic degradation of organic compounds under methanogenic and sulfidogenic conditions (Colleran et al., 1995). Fermentation intermediates includes short chain organic acids and alcohols. Abbreviations: FB – fermentative bacteria; OHPA – obligate hydrogen-producing bacteria; MPB – methane producing bacteria; SRB – sulfate reducing bacteria; HAc – hydrogenotrophic acidogenic bacteria. **.....4**

**Figure 2.2:** General metabolic process of sulfate reducing bacteria. As in other anaerobic bacteria, the main fraction of the electron donor is oxidized for energy conservation, and only a minor fraction is assimilated into cell mass. Catabolism (energy conservation) is shown in white-outline; anabolism (cell synthesis) is shown in heavy black lines (adapted from Rabus et al., 2000). **.....7**

**Figure 2.3:** Phylogenetic tree reflecting the relationship of sulfate reducing bacteria to other organisms on the basis of 16S rRNA sequences. The three domains of life are labeled (1) Eubacteria; (2) Archaebacteria; and (3) Eukaryotes (adapted from Rabus et al., 2000). **.....8**

**Figure 2.4:** Fraction of total dissolved sulfide (TDS) present as $H_2S_{(aq)}$ as a function of pH at 25 $^oC$ and 37 $^oC$. The balance of TDS is present as $HS^-_{(aq)}$. **.....15**

**Figure 2.5:** Effect of total sulfide concentration on maintenance coefficient (*m*) for *Desulfovibrio desulfuricans* growing on lactate medium (Okabe et al., 1995). **.....17**

**Figure 2.6:** Typical configuration for an upflow, packed bed reactor. Attached cells and biofilms remain immobilized on inert carrier materials while high liquid flow rates are applied to improve volumetric productivity. **.....28**

**Figure 2.7:** Conceptual model of a single species biofilm in a flowing environment. Microcolony structure is varied and convective fluid flow occurs around and below these microstructures within biofilms (Costerton et al., 1995). **.....29**

**Figure 3.1:** Diagram of 615 mL (4.5 cm x 38 cm) packed bed bioreactor (PBR) used for continuous SRB fermentations. The PBR contained barbed fittings for liquid and gas inlet/outlet, butyl rubber sampling ports, and was surrounded with Tygon tubing heat coils and foam insulating material (not shown). The column of the PBR was packed with biomass carrier material while the end pieces contained a polyethylene mesh to improve gas/liquid dispersion. **.....51**

**Figure 3.2:** Photographs of carrier materials (ruler for scale). A) Poraver™ porous glass beads; B) polyurethane foam plug; C) bone char; D) Celite™ R-635 diatomaceous earth pellets. **.....54**

**Figure 4.1:** Diagram of experimental setup for the evaluation of carrier material immobilization potential. 2 L stationary phase *Desulfovibrio desulfuricans* cultures were circulated from a BioFlo bioreactor to

a column packed with carrier material at ambient conditions at flow rate of 200 mL/h. **.....59**

**Figure 5.1:** Specific growth rate ($\mu$, $h^{-1}$) of 2 L batch fermentations as a function of inoculum composition. 0 % consortium corresponds to 100 % *Desulfovibrio desulfuricans*. **.....71**

**Figure 5.2:** Quantities of immobilized *Desulfovibrio desulfuricans* biomass (mg CDW per reactor) on different carrier materials after 20 h circulation of 2 L stationary phase cultures through 615 mL packed bed reactors. Abbreviations: BC - bone char; PPG - Poraver porous glass beads; PF - polyurethane foam; R-635 - Celite diatomaceous earth pellets**.....73**

**Figure 5.3:** Scanning electron micrograph (100x) of the surface of Celite™ R-635 carrier material. Scale bar shows 100 $\mu$m. **.....79**

**Figure 5.4:** Scanning electron micrograph (2000x) of the surface Celite™ R-635 carrier material. Scale bar shows 20 $\mu$m. **.....79**

**Figure 5.5:** Biomass immobilized (mg CDW per reactor) to carrier material in a packed bed as a function of inoculum composition. 0 % consortium corresponds to 100 % pure culture (*Desulfovibrio desulfuricans*). Diamonds represent results obtained using polyurethane foam as the carrier material. Squares represent results obtained using Celite™ R-635 as the carrier material. **.....82**

**Figure 5.6:** *Desulfovibrio desulfuricans* (A) and SRB consortium (B) cultures grown under identical conditions. Detached biofilm 'streamers' are clearly visible in (A). The SRB consortium cultures contained only a small amount of floc particles that settled to the bottom of the tube (not visible). **...82**

**Figure 5.7:** Volumetric sulfide productivity-time course plot for PBR fermentation #1. **.....86**

**Figure 5.8:** Concentration-time course plot for total dissolved sulfide (A), sulfate (B), and suspended biomass (C) concentrations for PBR fermentation #1. Port 3 corresponds to the reactor's outlet. **.....87**

**Figure 5.9:** Scanning electron micrograph (5000x) of the surface of a Celite™ R-635 pellet retrieved from the bioreactor inlet after an 11 d fermentation. Scale bar shows 2 $\mu$m. **.....90**

**Figure 5.10:** Scanning electron micrograph (5000x) of the surface of a Celite™ R-635 pellet retrieved from the midpoint of the bioreactor after an 11 d fermentation. Scale bar shows 2 $\mu$m. **.....91**

**Figure 5.11:** Scanning electron micrograph (5000x) of the surface of a Celite™ R-635 pellet retrieved from the bioreactor outlet after an 11 d fermentation. Scale bar shows 2 $\mu$m. **.....91**

**Figure 5.12:** Volumetric sulfide productivity-time course plot for PBR fermentation #2. **.....95**

**Figure 5.13:** Concentration-time course plot for total dissolved sulfide (A), sulfate (B), and suspended biomass (C) concentrations for PBR fermentation #2. Port 3 corresponds to the bioreactor's outlet. **96**

**Figure 5.14:** Results of a PBR experiment at constant liquid flow (80 mL/h) and a varying $N_2$ strip gas flow rate (reported as a normalized *G/L* ratio). pH (A), total dissolved sulfide (B), sulfate conversion (C), and suspended biomass concentration (D) were measured at port 3 (outlet) of the bioreactor. **...102**

**Figure 5.15:** Predicted volumetric sulfide production ($mol/m^3.d$) for a PBR with reactor volume of 600 mL and liquid feed rate of 80 mL/h. Effluent conditions were assumed to be 37 $^oC$ and 20 mM TDS. *G/L* is the ratio of strip gas to liquid feed. Volumetric productivities were calculated using total

reactor volume. ..... **106**

**Figure 5.16:** Results of a PBR fermentations at various feed rates and pH values showing the effect of *G/L* ratio on sulfate conversion (A) and total dissolved sulfide concentration (B). All measurements were based on port 3 (outlet) samples. ..... **108**

**Figure 6.1:** Diagrammatic representation of a closed system model describing sulfide and carbonate dissolved phase ionization and vapour-liquid equilibrium. ..... **114**

**Figure 6.2** Effect of temperature and pH on the mol % of $H_2S$ (A) and mol % of $CO_2$ (B) in a closed system. The system was assumed to have a liquid volume of 100 mL, headspace volume of 100 mL (with $N_2$ at 1 atm), and 20 mM of total sulfide ($H_2S_{(g)}$, $H_2S_{(aq)}$, $HS^-_{(aq)}$) and 40 mM total carbonate ($CO_{2(g)}$, $H_2CO_{3(aq)}$, $HCO_3^-$(aq), $CO_3^{2-}{}_{(aq)}$). ..... **119**

**Figure 6.3:** Temperature dependence of the first dissociation equilibrium constants for $H_2S_{(aq)}$ and $CO_2/H_2CO_{3(aq)}$ (B). ..... **120**

**Figure 6.4:** Diagram for mass balance analysis of a counter-current gas stripping column (adapted from Metcalf and Eddy, 2003). Nomenclature described in Table 6.3. ..... **123**

**Figure 6.5:** Gas to liquid ratios *(G/L*, $m^3/m^3$) required to remove varying % dissolved sulfide from a liquid stream (20 mM) at 20 $^oC$ (293 K) and 37 $^oC$ (310 K). It was assumed that the pH was sufficiently low (pH < 5.0) that all of the dissolved sulfides were in the strippable $H_2S_{(aq)}$ form and that temperature dependent ionization was negligible. ..... **125**

**Figure 6.6:** Process flow diagram of a possible process where an $H_2S$ free strip gas is first fed to bioreactor to strip a portion of $H_2S$ *in situ*. The liquid is then acidified to convert the residual total dissolved sulfides (TDS) to the strippable $H_2S_{(aq)}$ species which are removed in a countercurrent stripping column using gas from the bioreactor. $C_i$ = liquid phase concentration (mM); $P_i$ = gas phase $H_2S$ partial pressure (atm). ..... **127**

**Figure 6.7:** Gas to liquid (*G/L*, $m^3/m^3$) ratios required to remove 100% dissolved sulfide from a liquid stream (20 mM) using strip gases of varying initial $H_2S$ partial pressures (atm). *G/L* values were evaluated at 20 $^oC$ (293 K) and 37 $^oC$ (310 K). The equilibrium $H_2S$ partial pressure in the exiting gas ($P_e = P_3$) is 0.17 atm at 293 K (vertical dotted line) and 0.25 atm at 310 K (vertical dotted-dashed line). It was assumed that the pH was sufficiently low (pH < 5.0) that all of the dissolved sulfides were in the strippable $H_2S_{(aq)}$ form and that temperature dependent ionization was negligible. $H_2S$ partial pressure of entering strip gas will likely be in the range of 0.04-0.21 atm. ..... **128**

**Figure 10.1:** Linear relationship between $A_{480\ nm}$ and total dissolved sulfide concentration (mM). Data points are mean values of triplicate analysis and the vertical error bars are standard deviation. ..... **158**

**Figure 10.2:** Relationship between $A_{420\ nm}$ and total dissolved sulfide concentration (mM). Data points are mean values of triplicate analysis and the vertical error bars are standard deviation. ..... **159**

**Figure 10.3:** Relationship between square root peak height (counts) and gas phase $H_2S$ concentration (PPM, v/v). Data points are mean values of triplicate analysis and the vertical error bars are standard

deviation. **.....160**
**Figure 10.4:** Relationship between peak area and dissolved lactate concentration (mM). **.....161**
**Figure 10.5:** Relationship between peak area and dissolved acetate concentration (mM). **.....161**
**Figure 10.6:** Relationship between $A_{600\ nm}$ and suspended cell biomass measured as cell dry weight (CDW g/L). **.....162**

# Chapter 1: Introduction

In response to the world's growing energy demands, it has become clear that there must be an eventual shift away from the current fossil fuels based energy infrastructure. $H_2$, as a clean and potentially renewable fuel source, has been the focus of much research at all levels of an alternative energy infrastructure, including its efficient production, storage, and use. The potential for $H_2$ as a 'green' fuel will only be realized if it can be produced from a renewable source.

Today's highly industrialized and populous society produces larges volumes of solid and liquid organic wastes that contain significant amounts of recoverable energy. The traditional method of recovering $H_2$ from organic waste has been to produce $CH_4$ via anaerobic degradation followed by thermochemical conversion to $H_2$. The most common process for the conversion of $CH_4$ to $H_2$ is a combination of steam methane reforming and the water gas shift reaction. Despite being an established process for $H_2$ production, steam methane reforming has the disadvantages of being highly endothermic and requiring considerable plant infrastructure.

A proposed alternative is the production of $H_2S$ gas (by sulfate reducing bacteria) with organic waste as the energy feedstock. Several methods for converting $H_2S$ to $H_2$ are currently under investigation (Luinstra, 1995; Ohashi et al., 1998). The industrial sponsor for this study (Kingston Process Metallurgy Inc.) has developed a proprietary technology that converts $H_2S$ to $H_2$ via an exothermic reaction. This catalytic, thermochemical conversion process has rapid kinetics, nearly complete yields and

appears to be competitive with steam methane reforming.

A simplified process flow diagram of the proposed process is outlined in Figure 1.1 and shows the two primary unit operations. An organic feedstock is combined with sulfur oxides (e.g. $SO_4^{2-}$, $SO_3^{2-}$, $SO_2$) and fed to a sulfate reducing bioreactor. The biologically produced $H_2S$ is then fed to the thermochemical reactor which produces $H_2$ and regenerates the sulfur oxide electron acceptor.

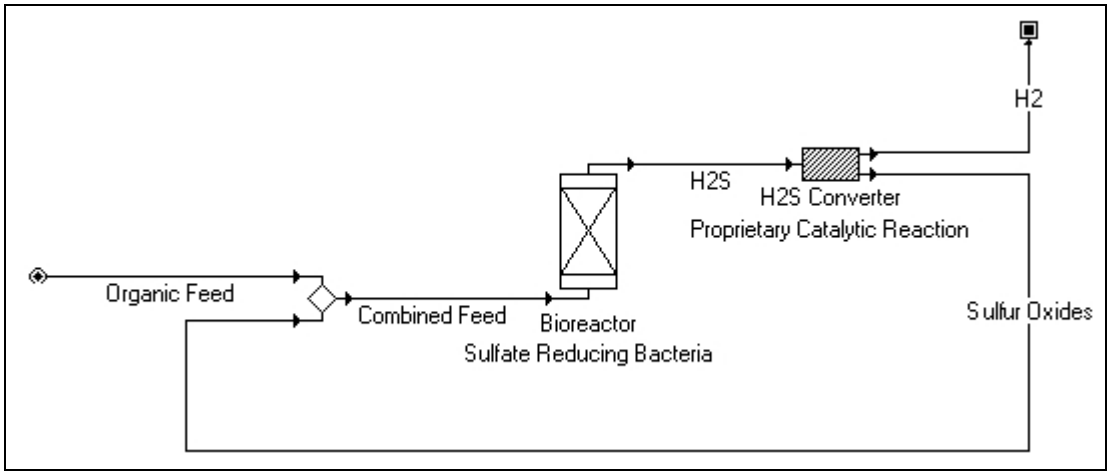


**Figure 1.1:** Simplified process flow diagram for the proposed process of producing $H_2$ from organic waste via biogenic $H_2S$. Full details of the $H_2S$ converter are omitted due to its proprietary nature.

The present study's focus was the design and development of a bench scale, sulfate reducing packed bed reactor. Factors such as inoculum composition, carrier materials for biomass immobilization, process feed rates, and pH were evaluated to improve upon current bioreactor technology and provide a suitable source of $H_2S$ for conversion to $H_2$. Comparisons were also made with methanogenic technology by a review of the relevant literature.

# Chapter 2: Literature Review

## 2.1 Anaerobic Degradation of Organic Matter

Anaerobic degradation is the basis for most methods of biological $H_2$ production. It can broadly be described as the process by which complex organic matter is sequentially degraded by microorganisms, in the absence of oxygen, to produce $CO_2$ and other terminal products such as $CH_4$ and $H_2S$. Each step of this process involves syntrophic relationships between different trophic levels of anaerobic bacteria. Figure 2.1 illustrates the sequential nature of anaerobic degradation. Hydrolysis of the large, insoluble, polymeric organic matter (e.g. fats, polysaccharides, and proteins) is accomplished by extra-cellular enzymes. The soluble monomers (e.g. sugars, long chain fatty acids, and amino acids) are further degraded by fermentative bacteria to intermediate products (e.g. alcohols and organic acids). The most common terminal step in anaerobic degradation is methanogenesis, but sulfate can become a significant alternative terminal pathway in the presence of sulfate or similar sulfur oxide electron acceptor.

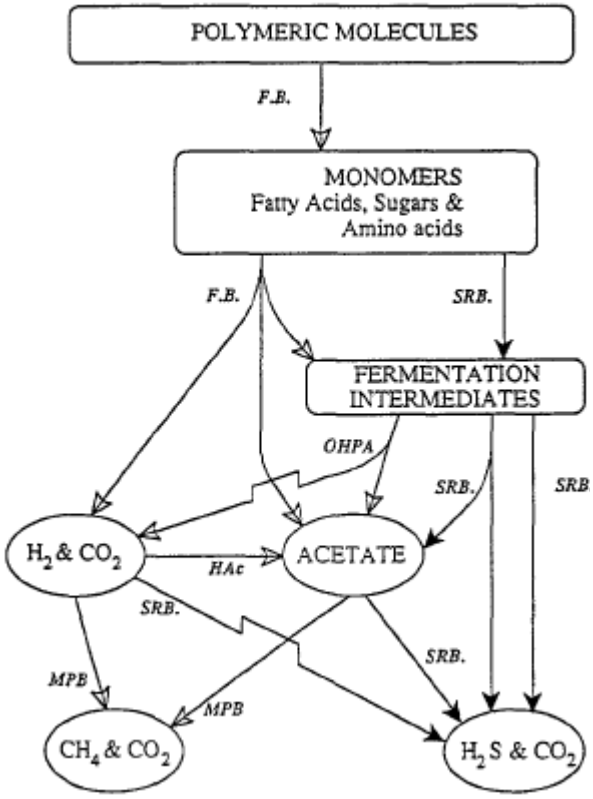


**Figure 2.1:** Pathways of anaerobic degradation of organic compounds under methanogenic and sulfidogenic conditions (Colleran et al., 1995). Fermentation intermediates includes short chain organic acids and alcohols. Abbreviations: FB – fermentative bacteria; OHPA – obligate hydrogen-producing bacteria; MPB – methane producing bacteria; SRB – sulfate reducing bacteria; HAc – hydrogenotrophic acidogenic bacteria.

## 2.2 Direct Biological Production of $H_2$

Figure 2.1 reveals that $H_2$ is produced as an intermediate product of anaerobic degradation before it is consumed in either the methanogenic or sulfate reduction steps. The direct production of $H_2$ via anaerobic processes (dark fermentation) is an active area of research. Recent review papers (Kapdan and Kargi, 2006; Ni et al., 2006) have reported volumetric $H_2$ productivities as high as 470 mol $H_2/m^3.d$ (Lin and Jo, 2003) which is within the same range of methane and sulfate reduction volumetric rates. Despite high volumetric productivities, dark fermentation suffers from low yields. $H_2$ is a by-product of acidogenic fermentation and only a fraction of the total electron

equivalents are channeled into $H_2$ with the balance being directed to organic acid products (acetic, propionic, butyric, lactic, etc.). Due to thermodynamic limitations and the numerous metabolic pathways that are simultaneously active in anaerobic degradation, dark fermentation is unable to convert any more than 15 % of the electron equivalents in a carbohydrate rich wastewater to $H_2$ (Angenent et al., 2004). The balance of the electron equivalents (as organic acids) can be further degraded by sulfate reducing bacteria (SRB) or eventually methanogens. $H_2$ itself is a substrate for SRB and methanogens and will eventually be converted to $CH_4$ or $H_2S$ if the anaerobic degradation process is allowed to reach either of these terminal steps.

## 2.3 Photosynthetic $H_2$ Production

Photosynthetic organisms such as the purple non-sulfur bacteria have been shown to convert lactate and other fermentation intermediates, with input of light, into $H_2$ (Lee et al., 2002; Koku et al., 2002; Kondo et al., 2002 as cited by Nath and Das, 2004). The high capital costs associated with photo-bioreactors and current gas recovery methods renders this process cost-prohibitive until major advances are made in the relevant technology areas.

## 2.4 Overview of Biological Methane Production

Biological methane production is carried out by a group of strict, obligate anaerobic prokaryotes classified as archaea. Methanogens, as they are more commonly known, convert the penultimate products of anaerobic degradation to $CH_4$. The two most common substrates are acetate and $H_2$ (Table 2.1) of which the former accounts for 72 %

of methane production.

**Table 2.1:** Reaction stoichiometry for the formation of methane from various substrates by methanogenic bacteria (Madigan et al., 1997 as cited by Metcalf and Eddy, 2003).

| Substrate | Methane Formation Stoichiometry |
|---|---|
| $H_2$ | $4H_2 + CO_2 \rightarrow CH_4 + 2H_2O$ |
| Acetate | $CH_3COO^- + H_2O \rightarrow CH_4 + HCO_3^-$ |
| Methanol | $4CH_3OH \rightarrow 3CH_4 + CO_2 + 2H_2O$ |
| Carbon monoxide | $4CO + 2H_2O \rightarrow CH_4 + 3CO_2$ |
| Formate | $4HCOO^- + 4H^+ \rightarrow CH_4 + 3CO_2 + 2H_2O$ |
| Methylamine | $4(CH_3)_3N + H_2O \rightarrow 9CH_4 + 3CO_2 + 6H_2O + 4NH_3$ |

Although thermophilic (50-60 $^oC$) methanogenesis is possible, the majority of industrial methanogenic processes occur in the mesophilic range (30-35 $^oC$) (Metcalf and Eddy, 2003).

## 2.5 Overview of Biological Sulfate Reduction

"Sulfate reducing bacteria" (SRB) is a broad term that is applied to a diverse collection of obligate anaerobic bacteria that utilize sulfate and similar sulfur oxides as terminal electron acceptors for the production of $H_2S$. More precisely, it is the dissolved disulfide $S^{2-}$ ion that is produced and is rapidly hydrolyzed in solution to a mixture of dissolved $HS^-$ and $H_2S$ (Postgate, 1984). The term sulfide will be used in this study to refer to all sulfide moieties in the gas and dissolved phases ($S^{2-}$, $HS^-$, $H_2S$). Sulfate reduction is a dissimilatory process in that only negligible amounts of sulfur species are incorporated into cellular components. Figure 2.2 illustrates the basic metabolic principles of SRB whereby organic substrates are oxidized and sulfate is reduced according to the generalized Equation (1) (Hao et al., 1996).

$$SO_4^{2-} + \text{organic matter} \xrightarrow{\text{SRB}} HS^- + HCO_3^- + H_2O \qquad (1)$$

Energy conservation occurs via substrate-level phosphorylation and electron transport phosphorylation. The latter metabolic step is accomplished via respiratory sulfate reduction. An important consequence of sulfate reduction is the production of $HS^-$ and $HCO_3^-$ ions which will increase the solution pH if allowed to hydrolyze to $H_2S$ and $CO_2$ (Hao et al., 1996). The biochemistry and molecular biology of SRB have been previously reviewed in detail by Rabus et al. (2000).

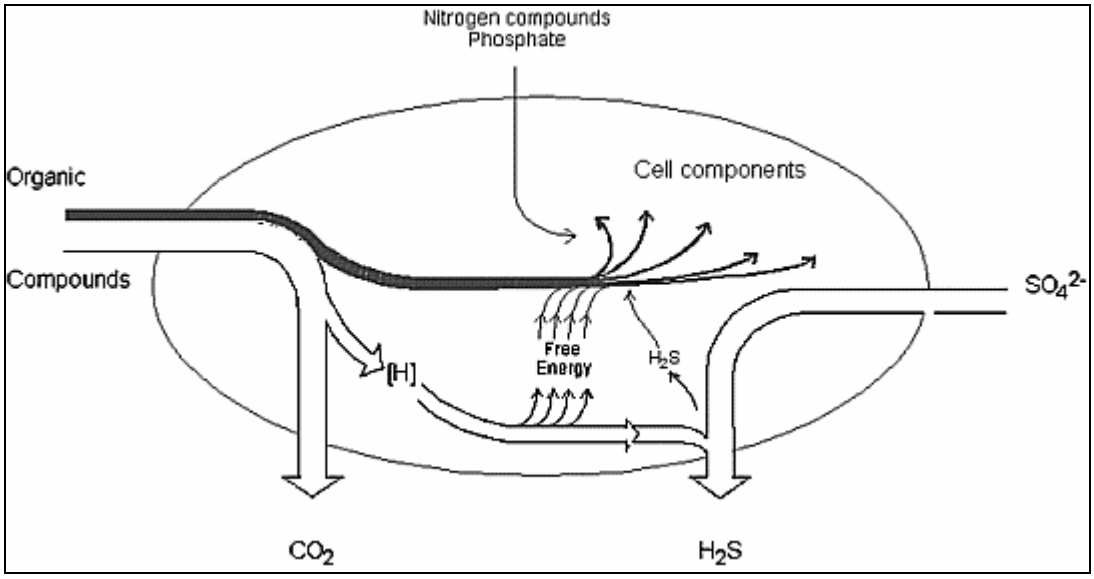


**Figure 2.2:** General metabolic process of sulfate reducing bacteria. As in other anaerobic bacteria, the main fraction of the electron donor is oxidized for energy conservation, and only a minor fraction is assimilated into cell mass. Catabolism (energy conservation) is shown in white-outline; anabolism (cell synthesis) is shown in heavy black lines (adapted from Rabus et al., 2000).

### 2.5.1 Classification of Sulfate Reducing Bacteria

Sulfate reducing bacteria have been studied since the mid 19$^{th}$ century but it was not until the 1960s when a coherent system of classification was developed (Rabus et al., 2000). SRB were divided into two basic groups, the non spore-forming genus *Desulfovibrio* (Gram negative) and the spore-forming genus *Desulfotomaculum* (Gram positive). The *Desulfovibrio* genus remains the best studied group due to the relative ease with which it

is cultured and isolated. The archetypical species are the curved, motile cells of *Desulfovibrio desulfuricans* that incompletely oxidize the preferred substrate lactate (or pyruvate) to acetate (Widdel, 1988). During the 1970s and early 1980s the discovery of significantly distinct groups of SRB, including complete oxidizers that were capable of mineralizing acetate, lead to the creation of further genera (*Desulfobacte*r, *Desulfococcus*, *Desulfonema*, *Desulfobulbus*, and *Desulfosarcina*). Until the mid-1980s, classification had been accomplished largely by observation of microbial nutrition, morphology and some biochemical markers such as desulfoviridin protein, specific lipid fatty acids, or menaquinones (Rabus et al., 2000). Recent advances in 16S rRNA sequence analysis has allowed for a more thorough and systematic classification of SRB (Figure 2.3).

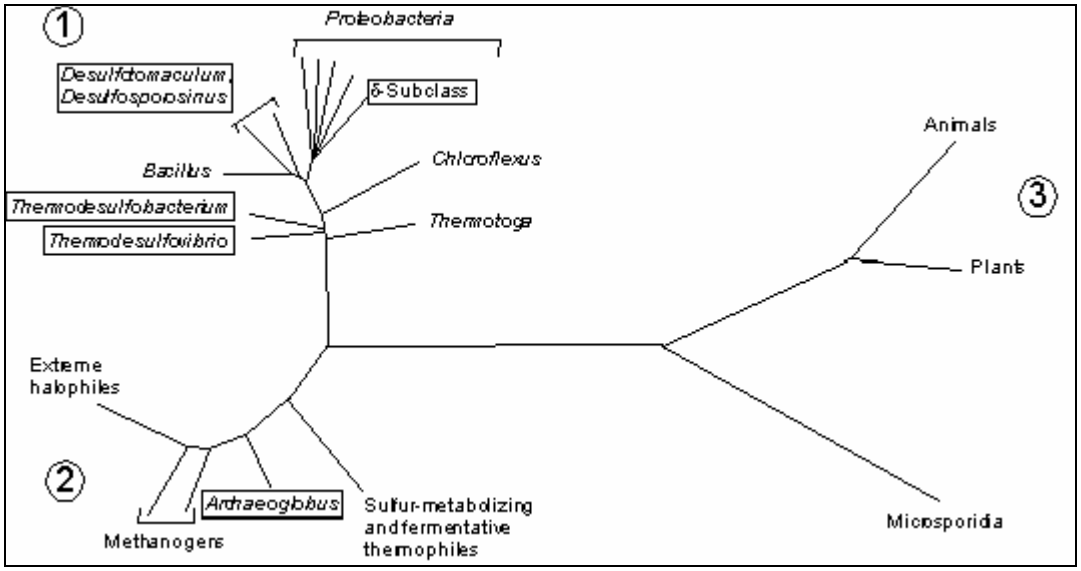


**Figure 2.3:** Phylogenetic tree reflecting the relationship of sulfate reducing bacteria to other organisms on the basis of 16S rRNA sequences. The three domains of life are labeled (1) Eubacteria; (2) Archaebacteria; and (3) Eukaryotes (adapted from Rabus et al., 2000).

### 2.5.2 Ecological Context of Sulfate Reduction

Sulfate reducing bacteria are remarkably adaptable microorganisms and can be found in numerous aquatic and terrestrial environments that have been depleted of oxygen via

aerobic decomposition of organic matter. SRB are found in soils; fresh, marine, and brackish waters; hot springs; oil and gas wells; estuaries; sewage; and mammalian intestines (Postgate, 1984). Incomplete oxidizing species such as *Desulfovibrio* are frequently found in freshwater environments while marine environments contain larger numbers of acetate mineralizing species. The well known *Desulfovibrio* species can generally be found in any waterlogged area that contains sufficient sources of organic matter and sulfate (Hao et al., 1996; Postgate, 1984). Table 2.2 provides an indication of the relative number of SRB found in various environmental samples.

**Table 2.2:** Order of magnitude most probable number (MPN) count of sulfate reducing bacteria in environmental samples as cited by Hao et al. (1996). MPN per 100 mL unless otherwise stated.

| **Sample Type** | **MPN Count (per 100 mL)** | **Sample Type** | **MPN Count (per 100 mL)** |
|---|---|---|---|
| aerobic fixed film | $10^6$-$10^8$ (per g VSS) | marine sediment | $10^5$ |
| activated sludge | $10^5$ (per g VSS) | estuary sediment | $10^7$ |
| anaerobic sludge | $10^7$-$10^8$ (per g VSS) | raw wastewater | $10^8$ |
| stream water | 550 | primary wastewater | $10^8$ |
| methanogenic sewage sludge | $10^6$ | secondary wastewater | $10^2$ |
| pond water | $10^4$ | activated sludge (aerobic) | $10^5$ |
| gravel pit water | $10^4$ | activated sludge (anaerobic) | $10^5$ |
| SRB pure culture | $10^9$ | anaerobic digested sludge | $10^7$ |
| clay stratum groundwater | $10^5$ | anaerobic sludge (enriched) | $10^8$ |
| stagnant water | $10^5$ | harbour silt | $10^5$ |
| polluted stream water | $10^3$ | estuary mud | $10^5$ |
| stream water downriver from a paper mill | $10^5$ | primary wastewater effluent | $10^7$ |

### 2.5.3 Electron Donors and Reaction Stoichiometry

Sulfate reducing bacteria are capable of using a wide range of substrates as electron donors. SRB are divided into two broad nutritional groups based on their metabolic products. One group comprises the SRB that incompletely oxidizes its carbon substrates

to acetate. The second group is capable of mineralizing select carbon substrates (including acetate) to $CO_2$ (Widdel, 1988). The incomplete oxidizers include the genera *Desulfovibrio* and *Desulfotomaculum*. Incomplete oxidizers have significantly faster growth rates than complete oxidizers and can achieve doubling times of 3-4 h if provided with preferred substrates such as lactate and $H_2$ under ideal conditions. Doubling times for slower growing complete oxidizers are often greater than 20 h (Widdel, 1988). The incomplete oxidation of lactate and the mineralization of acetate are described in Table 2.3.

**Table 2.3:** Reaction stoichiometry and Gibbs free energy for the incomplete oxidation of lactate and the mineralization of acetate by SRB (Widdel et al., 1988).

| **Reaction** | **Stoichiometry** | **$\Delta G^{o\prime}$ (kJ)** |
|---|---|---|
| Incomplete lactate oxidation | $2CH_3CHOHCOO^- + SO_4^{2-} \rightarrow 2CH_3COO^- + 2HCO_3^- + HS^- + H^+$ | -160.1 |
| Acetate mineralization | $CH_3COO^- + SO_4^{2-} \rightarrow 2HCO_3^- + HS^-$ | -47.6 |

Typical completely oxidizing species capable of mineralizing acetate are *Desulfobacter postgatei* (from saltwater) and *Desulfotomaculum acetoxidans* (from freshwater) (Widdel, 1988). Other common substrates for SRB are propionate, butyrate, and monovalent alcohols (all products of fermentative degradation). Specialized species of SRB are capable of oxidizing aromatics, saturated cyclic organic acids, amino acids, and glycerol, usually at slower growth rates (Widdel, 1988).

Lactate was used as the carbon source and electron donor for the present study due to it being a preferred substrate for SRB. It is also a significant product of the fermentative degradation of organic waste and is thus considered a renewable feedstock (Hofvendahl and Hahn-Hagerdal, 2000; Sreenath et al., 2004; Alvarez et al., 2007; Yumiko and Inoue, 2007). The anabolic, catabolic, and overall metabolic stoichiometries for the incomplete

oxidation of lactate by SRB are listed in Table 2.4. The catabolic growth yields ($Y_{acetate/lactate}$, $Y_{SO4/lactate}$) have been found to be largely independent of culture conditions (Okabe et al., 1995; Konishi et al., 1996). The anabolic growth yields ($Y_{X/S}$) are not constant and a function of maintenance energy requirements due to inhibitory sulfide conditions.

**Table 2.4:** Stoichiometry of SRB metabolic functions with lactate as the incompletely oxidized substrate. Biomass is approximated by the ratio $C_5H_7NO_2$. The balanced overall metabolism is based on experimental values (D'Alessandro et al., 1974 and Traore et al., 1982 as cited by Okabe and Characklis, 1992).

| Reaction | Stoichiometry |
|---|---|
| Catabolism | $CH_3CHOHCOOH + 0.5\ H_2SO_4 \rightarrow CH_3COOH + CO_2 + 0.5\ H_2S + H_2O$ |
| Anabolism | $CH_3CHOHCOOH + 0.6\ NH_3 \rightarrow 3CH_{1.4}N_{0.2}O_{0.4} + 1.8\ H_2O$ |
| Overall metabolism | $CH_3CHOHCOOH + 0.47\ H_2SO_4 + 0.036\ NH_3 \rightarrow$ $0.18\ CH_{1.4}N_{0.2}O_{0.4} + 0.47\ H_2S + 0.94\ CO_2 + 0.94\ CH_3COOH + 1.05\ H_2O$ |

### 2.5.4 Complex Substrates

Several studies have achieved sulfate reduction in bioreactors containing a mixed culture of SRB and fermentative heterotrophs that were fed a variety of complex substrates. Both raw plant matter and organic waste have been used with favourable results. Recent examples are listed in Table 2.5 and indicate that there are several cheap, renewable, and abundant feedstocks that could eventually be used in the proposed process for $H_2$ production. Liamleam and Annachhatre (2007) provide a recent review of substrates suitable for SRB.

**Table 2.5:** Complex substrates utilized by mixed cultures of fermentative heterotrophs and sulfate reducing bacteria.

| Complex Substrate | Reference |
|---|---|
| wild type grass, bagasse, fresh blue gum prunings, fresh pine prunings, molasses, blue buffalo grass, wattle prunings, blue gum chips, *Eragrostis* grass, wattle sawdust, pine chips | Coetser et al., 2006 |
| raw sewage sludge | Yeh, 1999 |
| cheese whey | Deswaef et al., 1996 |
| tannery effluent | Boshoff et al., 2004a |
| algae | Boshoff et al., 2004b |
| mushroom compost | Hammack and Ednborn, 1992 |
| oak chips, spent mushroom compost, waste newspaper recycling plant sludge | Chang et al., 2000 |
| whey | Christensen et al., 1996 |
| maple wood chips, sphagnum peat moss, leaf compost, conifer compost, poultry manure, and conifer sawdust | Zagury et al., 2006 |
| cow manure | La et al., 2003 |
| leaf mulch, wood chips, sludge | Waybrant, 2002 |
| landfill leachate | Nedwell and Reynolds, 1996 |
| landfill leachate | Henry and Prasad, 2000 |
| molasses | Annachhatre and Suktrakoolvait, 2001 |
| anaerobically digested municipal sewage sludge | Selvaraj et al., 1997 |

### 2.5.5 Sulfite and $SO_2$ as Alternative Electron Acceptors

The reduction of sulfate to sulfide is a complex biochemical process involving numerous enzymes and electron carriers. Among the first steps in sulfate reduction is the activation of sulfate with ATP to produce the intermediate adenosine-5'-phosphosulfate (APS). APS is reduced to sulfite and then to the terminal product sulfide (Rabus et al., 2001). As an intermediate in the sulfate reduction process, sulfite can also be provided in solution as an alternative electron acceptor.

Sulfur dioxide gas is highly soluble in solution (Henry's constant, $H$ = 36 atm at 20 $^{o}$C) and is hydrolyzed to form sulfurous acid according to Equation (2). Sulfurous acid then dissociates to form bisulfite and sulfite ions according to Equations (3) and (4).

$$SO_{2(aq)} + H_2O_{(l)} \leftrightarrow H_2SO_{3(aq)} \quad (2)$$

$$H_2SO_{3(aq)} \leftrightarrow H^+_{(aq)} + HSO_3^-{}_{(aq)} \quad (3)$$

$$HSO_3^-{}_{(aq)} \leftrightarrow H^+_{(aq)} + SO_3^{2-}{}_{(aq)} \quad (4)$$

The $H_2S$ conversion technology developed by the industrial sponsor has $H_2$ and $SO_2$ as its products. It is proposed that eventually the $SO_2$ stream will be recycled to the SRB bioreactor as the terminal electron acceptor sulfite. In this manner the sulfur species is retained in a closed process loop (Figure 1.1). The process of dissolving $SO_2$ in solution to form sulfite ions has been shown in the literature to be a suitable substitute for sulfate ions. The use of $SO_2$ has been reported with pure culture SRB grown on lactate (Dutta et al., 2007) and in coculture with an anaerobic consortium grown on anaerobically digested sewage sludge (Selvaraj et al., 1997). The later study experimentally confirmed the stoichiometric conversion of $SO_2$ to $H_2S$ with a COD requirement of 48 g COD/mol $SO_3^{2-}$.

### 2.5.6 Factors Affecting Growth

#### 2.5.6.1 pH

The preferred pH range of SRB is around pH 7 with inhibition occurring at pH values below 6.5 and above 8.5 (Widdel, 1988; Reis et al., 1992; Konishi et al., 1996; Azabou et al., 2005). SRB however can survive acidic conditions and are commonly used to treat acid mine drainage (AMD) wastewaters with pH values initially as low as 3. Metabolically produced bicarbonate alkalinity neutralizes AMD to more favourable pH

conditions (Tsukamoto et al., 2004; Kolmert and Johnson, 2001; Glombitza, 2000).

#### 2.5.6.2 Sulfide

The toxic effects of sulfide on bacteria, including SRB are well known and reported qualitatively in the literature (Okabe et al., 1995). Not surprisingly, SRB have a greater tolerance towards sulfide than most bacteria but the exact nature of the toxicity and microbial inhibition continues to be the subject of investigation (Icgen and Harrison, 2006).

$H_2S$ is a weakly acidic gas when dissolved in solution and its aqueous concentrations are governed by both pH and gas phase equilibria. Under the normal range of culture pH values (6 to 8), sulfide is present in solution as either the $HS^-_{(aq)}$ or $H_2S_{(aq)}$ forms. The first acid dissociation constant $K_{a1}$ is a function of temperature and the second dissociation ($K_{a2} = 10^{-19}$ mol/L, 25 $^oC$) may be considered negligible at typical microbial culture conditions. The dissolved phase equilibrium is described by Equation (5). The fraction of total dissolved sulfide (TDS) present in the $H_2S_{(aq)}$ form is a function of pH is shown in Figure 2.4.

$$H_2S_{(aq)} \xleftrightarrow{K_{a1}} HS^-_{(aq)} + H^+_{(aq)} \quad (5)$$

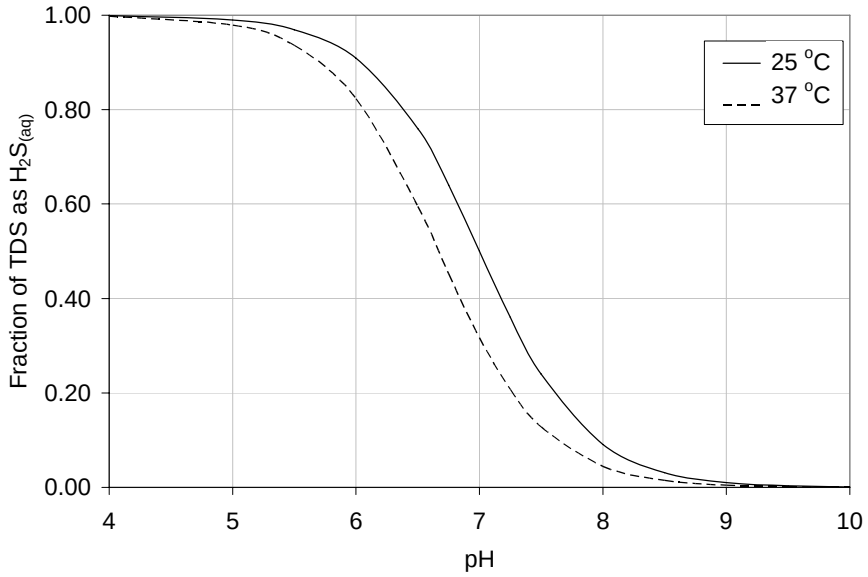


**Figure 2.4:** Fraction of total dissolved sulfide (TDS) present as $H_2S_{(aq)}$ as a function of pH at 25 °C and 37 °C. The balance of TDS is present as $HS^-_{(aq)}$.

Ambiguity exists regarding which form of sulfide is most inhibitory and what the quantitative effects of sulfide are on growth and activity. It has been proposed from observation that the molecular form $H_2S$ is most toxic to microorganisms as the uncharged molecule more readily passes through the cell membrane and reacts with cell components (Hauser and Holder, 1986; Tursman and Cork, 1989 as cited by Stucki et al., 1992). Although the exact biochemistry of sulfide inhibition has not been fully characterized, it is known that sulfide inhibition of SRB is a reversible phenomenon (Reis et al., 1992). Some genera and species of SRB are more vulnerable to sulfide inhibition than others. Mixed culture acetotrophic SRB have been reported to be completely inhibited at $H_2S$ concentrations as low as 1.2-1.5 mM (40-50 mg/L) (Stucki et al., 1993) while lactate using *Desulfovibrio* spp. experiences complete inhibition at an $H_2S$ concentration of 16.1 mM (547 mg/L) (Reis et al., 1992). The effects of sulfide on growth and activity are summarized in Table 2.6.

**Table 2.6:** Summary of literature reporting the effects of sulfide on growth and activity on sulfate reducing bacteria (adapted from Okabe et al., 1995).

| Microbe | Substrate | Conc. (mM) | pH | Temp. ($^oC$) | Reactor | Observation | References. |
|---|---|---|---|---|---|---|---|
| *Desulfovibrio desulfuricans* | lactate | 16.1 | 7.0 | 35 | chemostat | 50% decrease in lactate oxidation. Decreased biomass yield and cell size. | Okabe et al., 1992 |
| *Desulfovibrio* spp. | lactate | 16.2 | 6.2-6.6 | 37 | batch | Ceased sulfate reduction. $H_2S$ was most toxic form. | Reis et al., 1991 |
| *Desulfovibrio* spp. | lactate | 16.1 | 6.2-6.6 | 37 | batch | Completely inhibited growth. Reversible toxicity | Reis et al, 1992 |
| *Desulfovibrio desulfuricans* | lactate | 7.84 | 7.0 | 35 | chemostat | 50% decrease in biomass yield. | Okabe et al., 1995 |

Studies evaluating the effect of sulfide inhibition of *Desulfovibrio desulfuricans* growing on lactate media were carried out by Okabe et al. (1995). Microbial kinetics were described by a non-competitive inhibition model [Equation (6)] where the specific growth rate ($\mu$) is decreased by the presence of sulfide, but the substrate half-saturation ($K_{Lac}$,) coefficient is unaffected. Sulfide was found to increase the maintenance coefficient value as shown in Figure 2.5. Other model parameters were: $\mu_{\max}$ - maximum specific growth rate; $S$ – lactate substrate concentration; $K_i$ - inhibition coefficient; and $i$ - sulfide product concentration. Typical parameter values are summarized in Table 2.7.

$$\mu = \frac{\mu_{\max} S K_i}{(K_{Lac} + S)(K_i + i)} \tag{6}$$

**Table 2.7:** Summary of microbial kinetic parameters for *Desulfovibrio desulfuricans* grown at 35 °C on lactate media.

| Kinetic Parameter | Value | Unit | Reference |
|---|---|---|---|
| $\mu_{max}$ | 0.34 | $h^{-1}$ | Okabe et al., 1995 |
| $K_{Lac}$ | 3.08 | mg/L | Okabe and Characklis, 1992 |
| $Y_{X/Lac}^{intrinsic}$ | 0.03 | g cell/g lactate | Okabe et al., 1995 |
| $m$ | 0-11.5 | g lactate/g cell.h | Adapted from Okabe et al., 1995 |
| $K_i$ | 251 | mg/L | Okabe et al., 1995 |

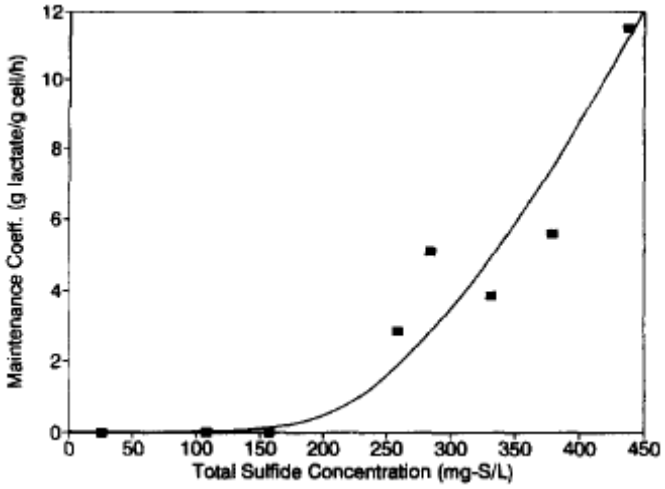


**Figure 2.5:** Effect of total sulfide concentration on maintenance coefficient (*m*) for *Desulfovibrio desulfuricans* growing on lactate medium (Okabe et al., 1995).

## 2.6 Methanogenesis and Sulfate Reduction Comparison

The production of $H_2$ from organic waste via $H_2S$ is a novel proposal that compels a comparison with the established $CH_4$ based route. What follows is a comparison between the two biological processes and a brief analysis of overall process yields.

As shown in Figure 2.1, sulfate reduction and methanogenesis are parallel pathways that occupy roughly the same trophic level in the sequential anaerobic degradation of organic matter. Due to their ecological overlap, methanogens and SRB often coexist wherever anaerobic degradation occurs. The flow of electrons to a specific pathway is dictated

largely by the availability of a suitable terminal electron acceptor. SRB activity in nature is often limited by the relative scarcity of sulfate in terrestrial environments. Methanogenesis, in comparison, commonly use $CO_2$ as a terminal electron acceptor (Table 2.1). In the presence of sufficient sulfate concentrations, the metabolic pathway of anaerobic degradation will often shift to toward sulfate reduction (Yamguchi et al., 1999; Henry and Prasad, 2000).

### 2.6.1 Overall Volumetric Performance

In performing an overall comparison of methanogenesis and sulfate reduction, a useful metric is bioreactor volumetric productivity (i.e. volumetric rate - the rate of substrate consumption or product formation normalized with respect to reactor volume; mol/$m^3$.d, g/L.d). Volumetric productivity is an overall performance indicator that represents the collective effect of various intrinsic system parameters such as microbial population, kinetics, mass transfer, substrate type, residence times, and bioreactor design. Due to the general similarity between the two microbial groups, overall volumetric productivities for methanogenic and sulfate reducing bioreactors reported in literature are within the same range with upper values in the range of 500-700 mol/$m^3$.d. Typical methanogenic volumetric productivities are summarized in Table 2.8. Volumetric COD removal rates (kg COD/$m^3$.d) were converted to volumetric methane production rates (mol $CH_4$/$m^3$.d) using the theoretical methane yield coefficient ($Y_{COD/CH4}$ = 64 g COD/mol $CH_4$) as described in Appendix A. A review of recent methanogenic literature was also performed (Table 2.9) and, expectedly, the values were within the same range of those listed in Table 2.8.

A survey of volumetric productivities for sulfate reducing bioreactors was conducted and is presented in Table 2.10. Values are listed as the volumetric rate of sulfate reduction (mol $SO_4^{2-}/m^3.d$) which is theoretically equivalent to the volumetric rate of sulfide production (mol $H_2S/m^3.d$). Reported values vary greatly between 3 and 677 $mol/m^3.d$ due to differences in bioreactor design and operating conditions. The values listed were from papers published within the last five years (2002-2007) or with volumetric rates greater than 100 $mol/m^3.d$. A more exhaustive listing of lower volumetric rates prior to 2002 is listed in Appendix B.

**Table 2.8:** Typical organic loading rates and predicted $CH_4$ production in methanogenic anaerobic bioreactors (adapted from Metcalf and Eddy, 2003). Abbreviations: CSTR - continuous stirred tank reactor; SBR, -sequential batch reactor; UASB - upflow anaerobic sludge blanket; ABR - anaerobic baffled reactor; AMBR - anaerobic migrating blanket reactor; PBR - packed bed reactor; AEBR - anaerobic expanded bed reactor; WW -wastewater.

| Substrate | Reactor Type | Temp. ($^oC$) | Organic Loading ($kg\ COD/m^3.d$) | Fractional COD Removal | $CH_4$ Production ($mol\ CH_4/m^3.d$) |
|---|---|---|---|---|---|
| **Suspended Growth Bioreactors** | | | | | |
| typical WW | CSTR | 25 | 5 | 0.90 | 62 |
| typical WW | anaerobic contact | 25 | 8 | 0.90 | 100 |
| typical WW | SBR | 25 | 2.4 | 0.90 | 30 |
| **Granular Sludge Bioreactors** | | | | | |
| typical WW | UASB | 35 | 24 | 0.95 | 316 |
| molasses | ABR | 35 | 28 | 0.88 | 341 |
| nonfat dry milk | AMBR | 20 | 2 | 0.95 | 26 |
| **Attached Growth Bioreactors** | | | | | |
| typical WW | PBR (upflow) | 37 | 6 | 0.90 | 75 |
| typical WW | AEBR | 20 | 4.4 | 0.89 | 54 |
| typical WW | FBR | 37 | 20 | 0.90 | 249 |
| typical WW | PBR (downflow) | 37 | 10 | 0.90 | 125 |

**Table 2.9:** Organic loading rates and associated $CH_4$ production in recent methanogenic literature. All bioreactors were run at mesophilic conditions (25-37 $^oC$). Abbreviations: SBR - sequential batch reactor; UASB - upflow anaerobic sludge blanket; ABR - anaerobic baffled reactor; PBR - packed bed reactor; AEBR - anaerobic expanded bed reactor; FBR - fluidized bed reactor; UASFF - upflow anaerobic sludge fixed film; WW - wastewater.

| Substrate | Reactor Type | Organic Loading ($kg/m^3.d$) | Fractional COD Removal | $CH_4$ Production ($mol/m^3.d$) | Reference |
|---|---|---|---|---|---|
| tannery liquor | UASB | 0.5 | 0.78 | 5 | Lefebvre et al., 2006 |
| food and sewage sludge | SBR | - | - | 24 | Kim et al., 2006 |
| potato leachate | PBR | 4.7 | 0.90 | 27 | Parawira et al., 2006 |
| pulp and paper liquor | ABR | - | - | 35 | Grover et al., 1999 |
| potato leachate | UASB | 6.1 | 0.90 | 50 | Parawira et al., 2006 |
| olive mill WW | SBR | 5.3 | 0.80 | 59 | Ammary, 2005 |
| sunflower extract WW | FBR | 9.3 | 0.80 | 97 | Borja et al., 2001 |
| synthetic dairy WW | FBR | 10.0 | 0.85 | 129 | Haridas et al., 2005 |
| dairy wastewater | UASB | 13.5 | 0.86 | 161 | Ramasamy et al., 2004 |
| food waste | UASB | 12.9 | 0.96 | 161 | Han et al., 2005 |
| palm oil mill WW | UASFF | 23.2 | 0.90 | 266 | Zinatizadeh et al., 2006 |
| landfill leachate | PBR | 23.5 | 0.85 | 277 | Calli et al., 2006 |
| slaughterhouse WW | PBR | 30.0 | 0.71 | 295 | del Pozo et al., 2000 |
| slaughterhouse WW | FBR | 54.0 | 0.75 | 561 | Borja et al, 1995 |

**Table 2.10:** Volumetric sulfate reduction rates (mol $SO_4^{2-}/m^3.d$) from recent SRB literature. Abbreviations: CSTR- continuous stirred tank reactor; UASB - upflow anaerobic sludge blanket; PBR - packed bed reactor; FBR - fluidized bed reactor; WW - wastewater. All bioreactors were run at mesophilic conditions (20-37 $^oC$).

| Substrate | Reactor Type | Carrier Material | Sulfate Reduction (mol $SO_4^{2-}/m^3.d$) | Reference |
|---|---|---|---|---|
| lactate | PBR | glass beads | 3 | Baskaran and Nemati , 2006 |
| methanol | UASB | - | 4 | Weijma et al., 2003 |
| ethanol, toluene | horizontal PBR | polyurethane foam | 7 | Cattony et al., 2005 |
| acetate | CSTR | - | 19 | Moosa et al., 2005 |
| lactate | FBR | silicate | 21 | Kaksonen et al., 2003a |
| lactate | PBR | scouring pad foam | 29 | Baskaran and Nemati , 2006 |
| lactate | PBR | pool filter silica sand | 32 | Jong and Parry, 2003 |
| sewage sludge | PBR | k-carrageenan gel | 41 | Selvaraj et al., 1997 |
| acetate | CSTR | - | 43 | Moosa et al., 2002 |
| ethanol | FBR | silicate | 45 | Kaksonen et al., 2004 |
| sewage sludge | CSTR with recycle | - | 50 | Selvaraj et al., 1997 |
| lactate | PBR | sand | 57 | Baskaran and Nemati , 2006 |
| acetate, ethanol | membrane | - | 69 | Vallero et al., 2005 |
| acetate | EGSB | - | 100 | de Smul, 1998 |
| $H_2/CO_2/CO$ | FBR/gas lift | pumice | 104 | van Houten et al., 1996 |
| ethanol | EGSB | - | 131 | de Smul et al., 1999 |
| acetate | UASB | - | 146 | Muthumbi et al., 2001 |
| acetate | PBR | textile fiber | 155 | Stucki et al., 1993 |
| acetate | PBR | porous lava rock | 156 | Stucki et al., 1993 |
| $H_2/CO_2$ | FBR/air lift | basalt | 186 | van Houten et al., 1994 |
| $H_2/CO_2$ | FBR/air lift | pumice | 260 | van Houten et al., 1995 |
| $H_2/CO_2$ | FBR/air lift | pumice | 313 | van Houten et al., 1994 |
| molasses | PBR | granular activated carbon | 320 | Gasiorek, 1994 |
| sewage sludge | PBR | BioSep | 456 | Selvaraj et al., 1997 |
| acetate | PBR | polyurethane foam | 576 | Stucki et al., 1993 |
| acetate | PBR | sintered glass beads | 677 | Stucki et al., 1993 |

The similar volumetric rates between methanogenesis and sulfate reduction are not surprising considering that both $CH_4$ and $H_2S$ have an identical COD requirement of 64 g COD/mol $CH_4$ or $H_2S$ (Speece, 1996). Henry and Prasad (2000) performed a direct, experimental comparison of sulfate reduction and methanogenesis using a series of anaerobic bioreactors to treat landfill leachate. Bioreactors were inoculated with an anaerobic consortium and supplemented with varying concentrations of sulfate. The study confirmed that by varying the COD/$SO_4^{2-}$ ratio, the degradation pathway could be directed towards either $CH_4$ or $H_2S$ production. Volumetric COD removal rates (kg COD/$m^3$.d) remained similar across all the COD/$SO_4^{2-}$ ratios, verifying the equivalence of the degradative pathways.

Due to the intrinsic similarity between methanogenesis and sulfate reduction, the most significant differences between the two processes may arise from factors such as bioreactor design, operability, and $H_2/CO_2$ mass balances. Methanogenic bioreactors are an established and well characterized technology while sulfate reduction is a younger, nascent technology (Colleran et al., 1995). Much of the past research in anaerobic bioreactor design has focused on optimizing $CH_4$ production by retention (i.e. immobilization) of methanogenic biomass. SRB are known to exhibit inferior immobilization properties compared to methanogens under certain circumstances (Speece, 1996). It is foreseeable that improvements in volumetric sulfate reduction rates will be accomplished via bioreactor designs that increase the immobilization of highly active SRB biomass.

### 2.6.2 Process Operability

Minor process operability distinctions exist between methanogenic and sulfate reducing bioreactors. Substrate overloading of anaerobic digesters can frequently lead to the accumulation of organic acid intermediates decreasing the pH in a phenomenon known as 'souring'. The souring process disrupts methanogenesis and can lead to total process failure (Torre and Stephanopolous, 1986). In contrast, SRB are known for their ability to treat highly acidic wastewaters. A tolerance to a greater range of pH values and decreased sensitivity towards temperature disturbances (Sarner, 1990) suggests that SRB are more resilient to potential process upsets.

The ideal feedstock for anaerobic processes is a high-COD wastewater such as industrial effluent from food processing industries. These wastewaters are a source of easily degradable and relatively innocuous organic substrates. SRB have the advantage of being able to accept a wider range of substrates including recalcitrant aromatics that might be otherwise toxic and/or resistant to methanogenic degradation (Chen and Taylor, 1997; Boopathy et al., 1998; Chang et al., 2002). Sulfate reducing processes are also more tolerant to heavy metals exposure, sequestering the metal cations as recoverable sulfide precipitates. These advantages could be exploited if the feedstock was landfill leachate which in addition to high COD levels, contains significant concentrations of heavy metals and xenobiotics (Wiszniowski et al., 2007).

Both SRB and methanogens are obligate anaerobes and biologically inactive under aerobic conditions. In the event of an oxygen incursion to an SRB bioreactor, the sulfide

product acts as a reducing agent to remove the oxygen. Methanogenic systems would have to have oxygen removed by either aerobic depletion or gas scrubbing.

### 2.6.3 $H_2$ and $CO_2$ Balance

For the sustainable production of $H_2$ it is desirable to minimize $CO_2$ generation while maximizing the $H_2$ recovered from the organic feedstock. The $CO_2$ and $H_2$ yields for the overall methanogenic and sulfate reducing processes are presented below using lactate as a representative carbon source (1 mol lactate = 96 g COD). Yield values are summarized in Table 2.11.

### 2.6.4 Sulfate/Sulfite Reduction with $H_2S$ Splitting

Assuming that lactate is oxidized completely to $CO_2$ the net reaction is described by Equation (7).

$$2\,CH_3CHOHCOOH + 3\,H_2SO_4 \rightarrow 6\,CO_2 + 6\,H_2O + 3\,H_2S \qquad (7)$$

The thermochemical conversion process produces $H_2$ from $H_2S$ at a 1.0 mol/mol ratio. The overall $H_2$ yield for the sulfate reduction process is thus 1.5 mol $H_2$/mol lactate or 15.6 mol $H_2$/kg COD.

The theoretical COD demand for sulfite reduction is 48 g COD/mol $SO_3^{2-}$ (compared to 64 g COD/mol $SO_4^{2-}$) which provides a small advantage to using $SO_2$ (i.e. sulfite) over sulfate as the electron acceptor [Equation (8)]. The overall $H_2$ yield becomes 2.0 mol $H_2$/mol lactate or 20.8 mol $H_2$/kg COD.

$$CH_3CHOHCOOH + 2\,H_2SO_3 \rightarrow 3\,CO_2 + 3\,H_2O + 2\,H_2S \quad (8)$$

### 2.6.5 Methanogenesis with Steam Methane Reforming and Water-Gas Shift

Degradation of lactate to $CH_4$ is a multi-step process involving $H_2$ and acetate intermediates; the net reaction is shown in Equation (9).

$$2\,CH_3CHOHCOOH \rightarrow 3\,CH_4 + 3\,CO_2 \quad (9)$$

The steam methane and water gas shift reactions are shown in Equations (10) and (11) respectively. The net reforming equation is shown in Equation (12).

$$CH_4 + H_2O \rightarrow 3\,H_2 + CO \quad (10)$$

$$CO + H_2O \rightarrow H_2 + CO_2 \quad (11)$$

$$3\left[CH_4 + 2\,H_2O \rightarrow 4\,H_2 + CO_2\right] = \left[3\,CH_4 + 6\,H_2O \rightarrow 12\,H_2 + 3\,CO_2\right] \quad (12)$$

The sum of Equation (9) and Equation (12) is the net reaction for production of $H_2$ via a methane based process [Equation (13)].

$$2\,CH_3CHOHCOOH + 6\,H_2O \rightarrow 6\,CO_2 + 12\,H_2 \quad (13)$$

The overall $H_2$ yield is thus 6 mol $H_2$/mol lactate or 62.5 mol $H_2$/kg COD.

**Table 2.11:** Summary of $H_2$ and $CO_2$ yields for production of $H_2$ via biologically produced $CH_4$ and $H_2S$ precursor molecules.

| **Reactions** | **$H_2$ Yield (mol $H_2$/mol lactate)** | **$H_2$ Yield (mol $H_2$/kg COD)** | **$CO_2$ Yield (mol $CO_2$/mol $H_2$)** |
|---|---|---|---|
| Sulfate reduction with $H_2S$ splitting | 1.5 | 15.6 | 2.0 |
| Sulfite reduction with $H_2S$ splitting | 2.0 | 20.8 | 1.5 |
| Methanogenesis with steam methane and water-gas shift | 6.0 | 62.5 | 0.5 |

Initial analysis of the yield values suggests that the $CH_4$ based route for $H_2$ production is

more efficient with regard to COD utilization and $CO_2$ production. These calculations however have omitted the external energy requirements of operating the thermochemical conversion processes at elevated temperature and/or pressures. The biological reactions occur at 1 atm and ambient temperatures (20-37 $^oC$). The exothermic nature of $H_2S$ splitting and the endothermic nature of steam methane may shift the $H_2$ and $CO_2$ yields in favour of the $H_2S$ based process due to the diversion of $CH_4$ for heating requirements. There is also a significant difference in the plant and infrastructure requirements for the thermochemical conversion processes. A detailed thermodynamic and cost analysis of all the pertinent reactions and unit operations is outside the scope of this study but is required to provide a more accurate appraisal of the two $H_2$ production methods.

In summary, the biological production of $CH_4$ and $H_2S$ occurs at similar volumetric rates. Sulfate reducing bioreactors are a relatively inchoate technology that may benefit from enhancements in immobilized cell bioreactor design to improve volumetric rates. The exothermic nature of the $H_2S$ splitting process is a key advantage over endothermic $CH_4$ conversion and further analysis is required for a more accurate comparison.

## 2.7 Practical Applications of Biological Sulfate Reduction

Production of $H_2S$ as an $H_2$ precursor molecule is a novel use of sulfate reducing bioreactor technology which has conventionally been applied to the treatment of sulfate waste streams and for environmental bioremediation. Paper mills, molasses based fermentation, flue gas desulfurization, phosphate fertilizer manufacturing are common industries and processes that generate significant sulfate wastes (Colleran et al., 1995;

Lens et al, 2003; Azabou et al., 2007).

Treatment of AMD is the most common bioremediation application for SRB (Hulshoff et al., 2001; Lens et al., 2002; Luptakova and Kusnierova 2005; Kaksonen et al., 2006; Cohen, 2006; Sheoran and Sheoran, 2006). Biological sulfate reduction produces bicarbonate alkalinity that neutralizes the acidic wastewater and the biogenic sulfide complexes with heavy metals to form easily recoverable metal-sulfide precipitates. Chromium, nickel, copper, zinc, iron, aluminium, and magnesium are among the metals that have been recovered using SRB bioreactors (Jong and Parry 2003; Viera et al., 2003).

A select number of SRB are capable of degrading aromatic compounds (Widdel, 1988). This ability has been exploited for the destruction of priority pollutants such as benzene, toluene, ethylbenzene and toluene (Chen and Taylor, 1997), polycyclic aromatic hydrocarbons (Chang et al., 2002), and nitroaromatic explosives (Boopathy et al., 1998).

## 2.8 Sulfate Reducing Packed Bed Reactors

### 2.8.1 Rationale for Biofilm Immobilization

As anaerobic bacteria, SRB have intrinsically slow growth rates. This characteristic limits their use in suspended cell bioreactors where under high flow rates, cells are washed out faster than they can replicate. Biomass immobilization techniques allow the retention of a high biomass concentration with simultaneous application of high liquid throughput leading to improved volumetric rates. The solids residence time (SRT) and

hydraulic residence time (HRT) are effectively decoupled in an immobilized cell bioreactor.

Granular sludge bioreactors have previously been applied for sulfate reduction but proper granule development requires several months and is better suited for methanogenic applications (O'Flaherty, 1997, Omil et al., 1997). More recent research has focused on SRB biofilm reactors in the packed bed (Figure 2.6) and fluidized bed configurations (Cattony et al., 2005; Kaksonen et al., 2006; Silva et al., 2006; and Alvarez et al., 2006). The highest reported volumetric productivities have been accomplished in packed bed reactors (Stucki et al., 1993; Selvaraj et al., 1997).

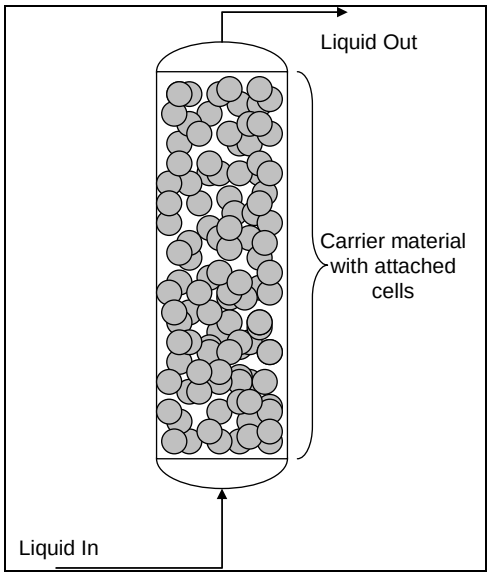


**Figure 2.6:** Typical configuration for an upflow, packed bed reactor. Attached cells and biofilms remain immobilized on inert carrier materials while high liquid flow rates are applied to improve volumetric productivity.

Packed/fluidized bed reactors offer the advantages of faster start-up times and fewer maintenance requirements compared to granular sludge bioreactors. Immobilization of SRB in biofilms provides a degree of protection against oxygen exposure (Kolmert et al.,

1997) and increased process stability (Alvarez et al., 2006). Biofilm reactors may also enhance microbial growth as it has been suggested that bacteria preferentially live in surface attached communities (Chen et al., 1994; Costerton and Wilson, 2004).

### 2.8.2 Biofilm Immobilization Fundamentals

Attached growth in flowing systems is a common phenomenon and initiated by the adhesion of a single monolayer of cells. Subsequent production of extracellular polysaccharides (EPS) aids surface attachment and promotes the formation of microbial communities surrounded by a 'slimy' matrix (Ye et al., 2005). Biofilm structure is non-homogenous with the presence of individual microcolonies (Figure 2.7). A phenotypic distinction exists between attached growth and suspended cells. Changes in genetic regulation are responsible for production of molecular signals between cells and role specialization can occur even among bacterial cells of the same species. Increased gene expression has also been observed in mixed culture biofilms which suggests syntrophic interaction between microbial species (Costerton and Wilson, 2004).

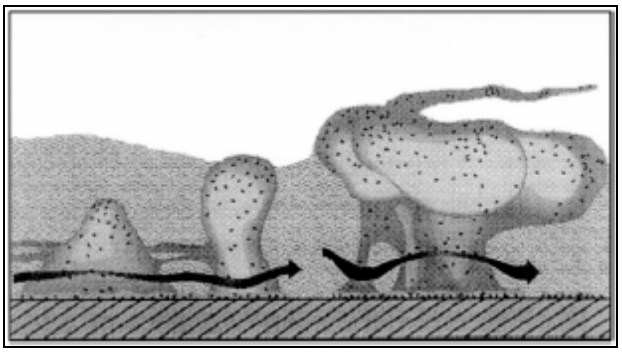

**Figure 2.7:** Conceptual model of a single species biofilm in a flowing environment. Microcolony structure is varied and convective fluid flow occurs around and below these microstructures within biofilms (Costerton et al., 1995).

In the presence of sufficient substrates and appropriate culture conditions, biofilms reach a steady state thickness when the rate of cell detachment due to sloughing equals the rate

of biofilm growth. By varying the rate of biomass sloughing, biofilm reactors are capable of operating at different steady state biomass concentrations (Van Loosdrecht and Heijnen, 1993).

There are many factors responsible for the biofilm formation and the adhesion of cells to inert surfaces. Of these factors, carrier pore size has been described as the most important having a greater effect than macroscopic surface roughness and total surface area (Huysman et al., 1983; Seth et al., 1995; Joo-Hwa et al., 1996). Optimal pore diameter is in the range of one to five times the major diameter of the microbe, such that materials with pores in the range of 1-10 $\mu$m are ideal for the immobilization of bacterial cells (Ince et al., 2000). The importance of these pores stems from their ability to provide an environment protected from fluid shear where cells can establish foundation monolayers that serve as the basis for further growth. Carrier materials can either be natural substances such as granular activated carbon (Harendranath et al., 1996) or highly engineered materials with customizable surface charges such as ion exchange resin (Krug and Daugulis, 1983).

### 2.8.3 Recent Literature

Development of improved packed bed sulfate reducing bioreactors is an active area of research. Specific topics of focus have included evaluation of different carrier materials, reactor geometry, substrate selection, and ability to treat heavy metal contaminated acidic wastewaters. A review of the literature is presented below. Unless otherwise specified, volumetric productivity is reported as volumetric sulfate reduction (mol $SO_4^{2-}$

reduced/$m^3$.d) which is theoretically equivalent to volumetric sulfide production.

Stucki et al. (1993) published a benchmark setting paper describing two acetate fed PBR capable of volumetric rates that remain the highest in literature to date. A bioreactor filled with polyurethane foam achieved a rate of 576 mol/$m^3$.d. A similar bioreactor with sintered glass packing achieved a rate of 677 mol/$m^3$.d after 150 d. Inoculum included a mix of pure strain acetotrophic SRB and biomass from anaerobic digesters exposed to elevated levels of sulfate. The weakness of this bioreactor was that volumetric sulfate loading had to be started at near zero levels and increased linearly over a period of 100 d in order to maintain stable operation. Volumetric rates of approximately 260 mol/$m^3$.d were achieved within a start-up period of 30-40 d.

Gasiorek (1994) evaluated the use of granular activated carbon (0.5 cm diameter) in a PBR for the reduction of $SO_2$ to $H_2S$. The downflow PBR was part of a larger system that combined biotic and abiotic reactors to treat gas streams containing various sulfur species. The paper did not discuss in detail the biochemical engineering aspects of their bioreactor. Relatively high volumetric rates (320 mol/$m^3$.d) were achieved using *Desulfovibrio desulfuricans* fed with molasses. It was not clear as to how a pure culture SRB was able to metabolize the complex substrate molasses without fermentative heterotrophs.

Van Houten et al. (1994) compared the performance of basalt (diameter, 0.29 mm) and pumice (diameter, 0.2-0.5 mm) particles as carrier materials and using $H_2$ and $CO_2$ for

autotrophic growth in a gas-lift bioreactor. Using granular sludge as inoculum, biofilm formation was observed on pumice but not on basalt particles. Maximum sulfate reduction was achieved on pumice particles at volumetric rate of 312 mol $SO_4^{2-}/m^3$.d (HRT 4.5 h) after 10 d of operation.

Fukui and Takii (1994) investigated *Desulfovibrio desulfuricans* attached growth on FeS precipitated particles and anion exchange resin (Dowex 1-X4, 100-200 mesh, chloride form). Under lactate and sulfate rich conditions the sulfide production of resin and FeS associated cells was found to be 2-3 % and 19-56 % respectively of suspended cells. The authors cited other instances in literature where cells associated with anion exchange resin performed at orders of magnitude less than suspended growth cells suggesting this material is not a suitable carrier material for SRB.

du Preez and Maree (1995) investigated the treatment of waste streams rich in nitrate and sulfate by SRB reactors. Using a PBR with pelletized ash, a volumetric rate of 25 $mol/m^3d$ was achieved using $H_2$ and CO as the electron and carbon sources respectively. Immobilization properties of the carrier was not the focus of the paper and the topic was largely ignored in the discussion.

Deswaef et al. (1996) proposed using two PBR reactors in series to treat gypsum (calcium sulfate) wastes. The bioreactors were packed with Plasdek™ PVC materials. Using a mixed inoculum of fermentative bacteria and SRB in the first reactor (HRT, 6 h), cheese whey was successfully applied as the carbon source. The second reactor (HRT, 12 h) was

inoculated with acetate degrading SRB. The combined reactors achieved a volumetric rate of approximately 35 mol/$m^3$.d.

Selvaraj et al. (1997) compared immobilization by coculture with floc-forming bacteria, $\kappa$-carrageenan gel beads, and Bio-Sep™ porous polymer. An earlier paper (Selvaraj et al., 1996) compared $\kappa$-carrageenan gel beads to alginate beads and found the former to be more stable. Maximum volumetric rate of the CSTR with SRB flocs was found to be only 50.4 mol $SO_2/m^3$.d. A PBR configuration with $\kappa$-carrageenan beads was unstable beyond volumetric rates of 40.8 mol $SO_2/m^3$.d Bio-Sep™ porous polymer beads in a PBR configuration achieved the highest volumetric rate of 456 mol $SO_3^{2-}/m^3$.d. Unfortunately a start-up period with gradual increases in volumetric loading over four to six months was required to attain this performance.

Cadavid et al. (1999) studied the impact of increasing the $SO_4^{2-}$/COD ratio in a horizontal-flow anaerobic immobilized sludge (HAIS) bioreactor. The biofilm carrier used was polyurethane foam cubes with dimensions of 3-5 mm. Despite elevated sulfate levels ($COD/SO_4^{2-}$ = 4.3) methanogenic bacteria were the dominant immobilized population. The authors suggested this may be due to the incompatibility of polyurethane foam with SRB. It is more likely that the origin of the inoculum, granular sludge, was the cause of high methanogenic activity. The highest volumetric rate was 12.83 mol/$m^3$.d.

Nagpal et al. (2000b) investigated the use of porous glass beads in a fluidized bed configuration. Using ethanol as the feedstock, in conjunction with $N_2$ sparging, a volumetric rate of 66 mol/$m^3$.d was achieved at HRT of 5.1 h. Inoculum was a mixture

of *Desulfovibrio desulfuricans* for ethanol degradation and *Desulfobacter postgatei* for acetate degradation. Only partial oxidation of acetate was achieved. The fluidized bed design was rationalized by its improved mass transfer characteristics over packed beds.

Christy (2001) compared the rate of sulfate reduction in column reactors with and without polypropylene pall ring packing (diameter, 15.0 mm; surface area, 10.8 $m^2/m^3$). Using mixed cultures obtained from local sewage treatment plants the lactate fed bioreactors achieved a volumetric rate of 6.97 $mol/m^3.d$ (HRT, 0.83 d). The author did not ascertain if the packing material or inoculum source was responsible for the negligible SRB immobilization that was observed.

Glombitza (2001) used crushed lava rocks successfully in a pilot scale PBR treating AMD. The bioreactor was 3.9 $m^3$ in volume achieved a volumetric rate of 33.5 mol $/m^3.d$ at HRT of 4.2 h. Methanol was the organic substrate and operation was found to be stable for a period of several months.

Kolmert and Johnson (2001) investigated sulfate reduction in PBRs packed with Poraver™ porous glass beads at pH levels representative of AMD (pH < 4). Earlier work had shown Poraver beads to have superior performance to suspended plastic carrier particles (Kolmert et al., 1997). Average volumetric rates were 2.6-3.1 $mol/m^3.d$ at HRT of 2.1 d. A mixed ethanol/lactic acid/glycerol feed was used as the organic substrate. After three months biofilm thoroughly colonized the surface and outer pores of the beads but the inner pores remained relatively bare. It is possible that absence of inner colonization was due to low inner pore connectivity.

Battaglia-Brunet et al., (2002) used a fluidized bed reactor with a volcanic ash basaltic carrier material (2-5 mm major dimension) to study the mechanism of Cr (VI) reduction by SRB. Immobilization evaluation was not the focus of this study and the presence of Cr (VI) acted as a sulfate reduction inhibitor (Smith and Gadd, 2000). An accurate appraisal of the potential of this carrier for SRB immobilization is therefore difficult. The volumetric rate achieved was 45 mol/$m^3$.d

Waybrant et al. (2002) proposed the use of a packed bed style reactor for *in situ* treatment of AMD. A reactive barrier was built into the site and incorporated crushed pyrite, silica sand, leaf mulch, wood chips, sawdust, sewage sludge, creek sediment, and limestone for the combined purposes of biofilm carrier, inoculum source and electron donor source. The mixture was also supplemented with lactate and calcium sulfate to assist in the initiation of sulfate reduction. Relatively low volumetric rates were observed (1.21 mol/$m^3$.d) and the *in situ* configuration employed would likely not be well adapted for an industrial, high-rate application.

A recent series of articles from the Kaksonen research group based in Finland has studied the use of sulfate reducing FBR for the treatment of AMD. Kaksonen et al. (2003a) reported that a silicate (diameter 0.5-1 mm) packed FBR and a UASB bioreactor both had comparable volumetric rates of 20.8 mol/$m^3$.d. A second paper (Kaksonen et al., 2003b) found that lactate as the substrate promoted rapid reactor startup. The substrate could then be switched to less costly ethanol over a period of 50 d without a significant decrease in performance. A third paper (Kaksonen et al., 2004) achieved a volumetric

rate of 44.8 mo/$m^3$.d (HRT, 6.5 h) in the ethanol fed PBR. A non-competitive model was developed to describe sulfide inhibition kinetics. Comparison of the model with the literature highlighted the need to recognize that inhibition is a function of pH, SRB species, organic substrate, and biomass morphology (biofilm, granular, or suspended). It also emphasized that sulfide inhibition has independent effects on growth, substrate utilization, and sulfate reduction. A fourth paper (Kaksonen et al., 2004) investigated the long term effect (393 d) of lactate and ethanol feeding on microbial ecology. Molecular methods were used for species identification. The ethanol fed bioreactor exhibited greater population diversity which was credited with providing greater adaptability to environmental changes. The most recent paper (Kaksonen et al., 2006) summarized the key findings from their previous papers and demonstrated the applicability of sulfate reducing FBRs for treatment of acidic metal- and sulfate-containing wastewater.

Silva et al. (2002) evaluated the treatment of a sulfate-rich wastewater using a PBR with polyurethane foam. The focus of the study was to test different parameters and operation conditions (batch, semi-continuous) for treating an industrial effluent with sulfate concentration of 12-35 g/L. In semi-continuous mode, volumetric rates of up to 22.3 mol/$m^3$.d were achieved. Inoculum was obtained from an industrial wastewater treatment plant and from granular sludge treating domestic sewage and required 83 d to adapt to sulfate reducing conditions. No clear indication of was made to the suitability of polyurethane foam for SRB immobilization.

Jong and Perry (2003) investigated the use of a PBR with commercial pool filter sand for the treatment of heavy metal contaminated water. Sulfate reduction rates reached 31.7

mol/$m^3$.d treating a lactate supplemented metal contaminated influent. Inoculum enriched from mine site water required 14 d until sufficient biofilm had developed for bioreactor operation. Observations from this paper revealed that the silica sand may be prone to clogging with excessive biomass and that high up-flow velocities will result in sloughing.

Beyenal and Lewandowski (2004) investigated the use of hematite and quartz packed flat plate reactors for treatment of dissolved $Pb^{2+}$ ions. After seven weeks of operation *Desulfovibrio desulfuricans* (G20) biofilm densities reached values of 90 g/L (hematite) and 60 g/L (quartz). Despite having a higher biomass density, the hematite system had lower sulfide concentrations due to precipitation of sulfide with $Fe^{2+}$ ions within the hematite. The iron-free quartz would likely be a better carrier material for the production of free sulfide.

Tsukamoto et al. (2004) compared the use of rock (diameter 0.64-1.9 cm), wood (major dimension 2-7 cm), and plastic packing (major dimension < 1 cm) in PBRs for the removal of iron and other metals from AMD. These materials were found to have superior characteristics compared to straw and horse manure which had been used at a field scale bioreactor. Exact volumetric rates were not reported but sulfate reduction was highest in the rock filled bioreactor. This work was consistent with that of Lyew and Sheppard (1997) that suggested rock/gravel was a suitable SRB a carrier material, although detailed quantification of biomass immobilization was not provided.

Gibert et al. (2005) attempted to treat synthetic AMD using SRB immobilized in a

column filled with crushed calcite, municipal compost, and river sediment. The compost was intended as the organic substrate and the river sediment served as the primary inoculum. Sulfate reduction was unsuccessful and sulfide was not detected in the column effluent. Metals removal was attributed to sorption onto the compost material and inorganic precipitation reactions. Municipal compost as the organic substrate was found to have insufficient and/or unsuitable organic material to support to sulfate reduction, consistent with earlier findings (Gibert et al., 2004). Due to low SRB microbial activity the applicability of calcite as a carrier material was not sufficiently evaluated. Inappropriate inoculum selection may also have played a role in sulfate reduction failure.

Cattony et al. (2005) used a horizontal-flow anaerobic immobilized biomass (HAIB) bioreactor packed with polyurethane foam to degrade ethanol and toluene. The intended application was bioremediation of Brazilian gasoline spills which contain high fractions of ethanol. A sulfate volumetric rate of 7.28 mol/$m^3$.d (HRT, 12 h) was obtained using inoculum from a poultry slaughterhouse UASB bioreactor. Immobilization of biomass on the polyurethane foam was greatest near the inlet of the reactor with loadings as high as 620 mg VSS/g PU foam.

Baskaran and Nemati (2006) evaluated sand (diameter, 225 $\mu$m), scouring pad foam (1 x 1 x. 0.5 cm), and glass beads (diameter, 3 mm) as carrier materials for a mixed SRB culture being fed lactate. The PBR packed with sand achieved the highest volumetric rate of 57 mol/$m^3$.d, followed by scouring pad foam (29 mol/$m^3$.d), and finally glass beads (3 mol/$m^3$.d). A direct relationship existed between sulfate reduction rates and available surface area. Available surface area in the sand PBR was 145 $m^2$, scouring pad foam had

3.2 $m^2$/bioreactor and glass beads had 0.6 $m^2$/bioreactor. This study provided good comparative performance data on the carrier materials, but extensive reactor run times (71-119 d) were required to obtain the listed volumetric rates.

Alvarez et al. (2006) compared the performance of Poraver™ porous glass beads (diameter 10-20 mm) and pumice (10 x 15 x 15 mm) in PBRs. Factorial design methods were used to optimize the dissolved sulfide concentration by adjusting the lactate and sulfate concentrations to 67 mM and 46 mM respectively. Effluent sulfide concentrations of 9.8 mM and 15 mM for the pumice and Poraver™ packed reactors respectively. The inoculum (brewery sludge) required a recirculation period of two months at an HRT of 100 h for satisfactory biofilm development. Volumetric rates were not reported but both carrier materials were found to be able to support stable and robust biofilms. The development of good biofilms was partially attributed to the presence of several SRB species and non-SRB heterotrophs as identified by molecular methods.

Silva et al. (2006) evaluated four carrier materials for their ability to immobilize methanogenic bacteria and SRB. The materials evaluated were polyurethane foam, activated carbon, alumina ceramic, and polyethylene (Table 2.12). Volumetric rates were not assessed, rather the paper focused on microbial ecology of the biofilms that developed on each of the carrier materials. Granular sludge from an UASB bioreactor treating poultry slaughterhouse wastewater served as the inoculum. Polyurethane foam exhibited the best specific immobilization capability of (872 mg total volatile solids/g support). Polyurethane and the activated carbon were found to be preferentially

colonized by SRB; polyethylene by hydrolytic and fermentative bacteria; and alumina ceramic by methanogens. This work was consistent with other research that had suggested that polyurethane foam (Stucki et al., 1993) and granular activated carbon type materials such as activated carbon (Gasiorek, 1994) are ideally suited for SRB immobilization.

**Table 2.12:** Characteristics of support materials evaluated by Silva et al. (2006). Abbreviations: PU - polyurethane foam; AC- activated carbon; CE - alumina ceramic; PE - polyethylene.

| **Support material characteristics** | **PU** | **AC** | **CE** | **PE** |
|---|---|---|---|---|
| **Shape** | **Cubic** | **Irregular pellet** | **Cubic** | **Cylindrical** |
| Apparent density (g/mL) | 0.023 | 0.51 | 0.46 | 0.40 |
| Equivalent diameter (cm) | 0.6 | 0.5 | 0.5 | 0.5 |
| Porosity | 0.92 | 0.43 | 0.75 | - |
| Mean pore diameter ($\mu$m) | 543 | 1.9 | 84.7 | - |
| Surface area ($m^2/g$) | 43.8 | 3.51 | - | 2.05 |

## 2.9 Scope of Thesis

Recent research in the area of sulfate reducing bioreactors has focused on the packed bed reactor configuration. High volumetric rates (~600 $mol/m^3.d$) have been achieved only after extended start-up periods in excess of 100 d. Two key design criteria that affect bioreactor performance are carrier material selection and the microbial inoculum. While numerous carrier materials have been evaluated for immobilization potential the research has been spread across individual studies under different experimental conditions. Two recent studies (Baskaran and Nemati, 2006; Silva et al., 2006) have performed meaningful evaluations of several carrier materials, but many of the materials tested have been found to be unsuitable for SRB immobilization.

The inoculum's microbial kinetics and intrinsic ability for attached growth have a considerable effect on bioreactor performance. Despite this fact, most previous studies

have used undefined consortia and neglected to investigate the potential benefit of rational inoculum composition design.

The majority of sulfate reducing bioreactor applications are wastewater treatment where the production of $H_2S$ is considered a nuisance by-product or AMD remediation where the preferred state of the sulfide product is in the dissolved phase. There has been little interest in the recovery of a gas phase product.

The objectives of the present study were to maximize the volumetric productivity of a sulfate reducing PBR and optimize conditions for recovery of a gas phase $H_2S$ product. The aspect of carrier material selection was addressed by evaluating four candidate materials under controlled experimental conditions. Polyurethane foam and Poraver™ porous glass beads were selected due to their proven ability for SRB immobilization. Bone char and Celite™ R-635 diatomaceous earth pellets had not been previously been used with SRB but were selected due their proven ability to immobilize other anaerobic bacteria. The effect of inoculum composition was investigated by comparing a benchmark pure culture (*Desulfovibrio desulfuricans*) with an undefined SRB consortium. Inoculum composition optimization was based on immobilization potential and kinetic performance criteria. Initial continuous PBR fermentations were performed to characterize the bioreactor system behaviour and decrease the start-up period required to achieve high volumetric productivities. An $N_2$ strip gas was implemented in the final PBR fermentations for $H_2S$ product recovery. pH adjustment was investigated as a method of increasing both stripping efficiency and $H_2S$ concentration in the strip gas.

# Chapter 3: Materials and Analytical Methods

## 3.1 Chemicals

All chemicals (unless otherwise specified) were analytical grade and obtained from Fisher Scientific Ltd. (Nepean, Ontario), Sigma Aldrich Canada Ltd. (Oakville, Ontario), and Alfa Aesar (Ward Hill, Massachusetts).

## 3.2 Analytical Methods

### 3.2.1 Total Dissolved Sulfide (TDS)

Total dissolved sulfide ($H_2S_{(aq)}$, $HS^-_{(aq)}$,) $S^{2-}_{(aq)}$) were determined by the spectrophotometric method of Cord-Ruwisch (1985). The assay is based on the precipitation of sulfide as colloidal copper sulfide. Samples were analyzed immediately to minimize oxidation and volatilization.

Using 1.5 mL microcentrifuge tubes, 50 $\mu$L of culture sample was mixed with 950 $\mu$L copper reagent solution (aqueous solution of 50 mM HCl and 5 mM $CuSO_4.5H_2O$) and then vortexed for 5 seconds and the relative absorbance was measured immediately at 480 nm using a Biochrom Ultrospec 3000 UV/Visible spectrophotometer.

Calibration standards from (0-20 mM, 0-641 mg/L $S^{2-}$) were prepared by diluting certified solutions of 3 % w/v $Na_2S.9H_2O$ (LabChem, Pittsburgh, Pennsylvania) in degassed, deionized water. Efforts were made to minimize contact of the standards with air. The linear calibration curve is shown in Appendix C.

### 3.2.2 Dissolved Sulfate

Sulfate concentrations were determined by the turbidimetric method of Kolmert et al. (2000). The assay is based on the precipitation soluble sulfate ions as barium sulfate. Samples to be analyzed for sulfate were treated with an excess of crushed zinc acetate dihydrate crystals to precipitate dissolved sulfide as zinc sulfide. Fixation of sulfide prevented oxidation to sulfate.

Using 1.5 mL microcentrifuge tubes, 1 mL culture samples were vortexed for 5 seconds with ~0.01 g of crushed zinc acetate dihydrate crystals. The mixture was then centrifuged for 10 min at 6000 RPM and 4 $^{o}$C using a Jouan MR 14.11 centrifuge. 50 $\mu$L of the supernatant was mixed with 950 $\mu$L of conditioning fluid (Table 3.1) in a fresh microcentrifuge tube and vortexed for 5 seconds. Finally, ~0.01 g of crushed barium chloride dihydrate crystals was added to the mixture which was then vortexed for 15 seconds and the relative absorbance was immediately read at 420 nm using a Biochrom Ultrospec 3000 UV/Visible spectrophotometer.

Calibration standards (0-48 mM) were prepared using sodium sulfate (ACS grade, Fisher Scientific) and deionized water. The relationship between sulfate concentration and $A_{420}$ was a 3$^{rd}$ order polynomial as described by Kolmert et al. (2000). The calibration curve is shown in Appendix C.

**Table 3.1:** Composition of sulfate assay conditioning fluid (per 1000 mL).

| Component | Quantity |
|---|---|
| NaCl | 150 g |
| glycerol | 100 mL (126 g) |
| concentrated HCl (12.1 M) | 60 mL |
| 90 % ethanol (histological grade) | 200 mL |
| deionized water | 640 mL |

### 3.2.3 Gas Phase $H_2S$

Gas phase $H_2S$ concentration was measured using a Varian 3400CX gas chromatograph (GC) equipped with a pulsed flame photometric detector and a Varian 1.5 % silicone Carbopack B 60-80 mesh 8'x1/8"x2.4 mm analytical column. Bioreactor strip gas samples were diluted as required with ultra high purity (UHP) $N_2$ to obtain $H_2S$ concentrations within the linear range of the GC. Helium was used as the carrier gas and the injector, column, and detector were set to 110 $^oC$, 150 $^oC$, and 60 $^oC$ respectively.

Calibration standards were prepared using 20 and 200 PPM $H_2S$ (v/v, balance $N_2$) calibration gases (Calgaz Air Liquide, Cambridge, Maryland). All injections were 250 $\mu$L using a gas tight syringe and appropriate dilutions were made using UHP $N_2$. Peaks were analyzed using the Varian Star software package and a linear calibration curve for $H_2S$ concentration and square root peak height was obtained (Appendix C)

### 3.2.4 Lactate and Acetate

Dissolved lactate and acetate were measured by high pressure liquid chromatography using the following Waters (Milford, Massachusetts) components: Model 515 HPLC

Pump, Model 2487 Dual $\lambda$ Absorbance Detector (set to 210 nm), Atlantis $dC_{18}$ 5 $\mu$m, 4.6x20 mm guard column, and Atlantis $dC_{18}$ 5 $\mu$m, 40x150 mm analytical column. The mobile phase was 20 mM $NaH_2PO_4.2H_2O$ (pH adjusted to 2.7 with 3 M $H_3PO_4$) at 1.2 mL/min. The mobile phase and calibration standards were prepared using degassed deionized water. Calibration standards were prepared using sodium lactate (60 % syrup w/w, Sigma-Aldrich) and sodium acetate trihydrate (HPLC grade, Fisher Scientific). Linear calibrations curves are shown in Appendix C.

1 mL of liquid culture samples were centrifuged at 6000 RPM for 10 min. Samples were assayed immediately after centrifugation or frozen for later analysis. 200 $\mu$L of the supernatant was mixed with 40 $\mu$L of concentrated (15 M, 86 % w/v) $H_3PO_4$ before being injected as 20 $\mu$L (measured loop) volumes.

Chromatographic data was collected using Waters Millenium[32] Chromatography Manager software and peak areas were calculated using Origin Pro 7.5 (Student Version) software.

### 3.2.5 Suspended Biomass Concentration

Suspended biomass concentrations were measured using a Biochrom Ultrospec 3000 UV/Visible spectrophotometer. The optical density of the culture was measured at 600 nm and correlated to cell dry weight (CDW). Samples were diluted a necessary to fit within the range of the linear calibration curve as shown in Appendix C.

### 3.2.6 Phase Contrast Microscopy

Phase contrast microscopy was performed using a Nikon Eclipse E600 microscope with 100x oil immersion lens.

### 3.2.7 Scanning Electron Microscopy

Celite™ R-635 pellets were taken from different points along the bioreactor after it had been drained of its liquid contents. Pellets were immediately dehydrated by successive immersion in aqueous solutions of 25 %, 50 %, 75 % and 100 % v/v histological grade alcohol (90 % ethanol, 5 % methanol, and 5 % v/v isopropanol) for 20 min each and then allowed to dry overnight. The dried samples were coated with high purity, SEM grade silver paint, affixed to aluminum stubs and allowed to dry. Samples were examined using a LEO 1530 field emission SEM at an accelerator voltage of 3.5 kV and working distance of 3-6 mm.

### 3.2.8 pH Measurement

pH was measured using a Cole Parmer sulfide resistant double junction reference (Ag/AgCl) electrode with an Orion Research Expandable ionAnalyzer EA 920. The electrode was calibrated before each use using reference pH solutions (Cole Parmer Canada, Montreal, Quebec) of pH 7 and either 4 or 10 depending on the anticipated pH value of the sample.

## 3.3 Culture and Fermentation Methods

### 3.3.1 Postgate B Medium and Stock Culture Maintenance

Postgate B (PB) medium (Postgate, 1984) was used for preparing stock cultures of SRB. The medium consisted of the following components per L of tap water: 0.5 g/L $KH_2PO_4$, 1 g/L $NH_4Cl$, 1.26 g/L $CaSO_4.2H_2O$, 2 g/L $MgSO_4.7H_2O$, 5.83 g/L sodium lactate (60 % w/w syrup), 1 g/L yeast extract (BD Difco, Franklin Lake, New Jersey), 0.1 g/L ascorbic acid, 0.1 g/L sodium thioglycollate, and 0.5 g/L $FeSO_4.7H_2O$. pH was adjusted to 7.25 using 3 M NaOH and 1 M HCl.

Subcultures (3 % v/v) were made on a monthly basis using 100 mL (liquid volume) serum bottles. Subcultures were incubated statically at 33 $^oC$ for 48 h and then wrapped in aluminum foil for storage at 4 $^oC$.

### 3.3.2 Postgate C Medium

Postgate C (PC) medium (Postgate, 1984) was used for culturing SRB in batch and continuous culture. The medium consisted of the following components per L of distilled water: 0.5 g/L $KH_2PO_4$, 1 g/L $NH_4Cl$, 4.5 g/L $Na_2SO_4$, 0.06 g/L $MgSO_4.7H_2O$, 0.06 g/L $CaCl_2.H_2O$, 10 g/L sodium lactate (60 % w/w syrup), 1 g/L yeast extract (BD Difco, Franklin Lake, New Jersey), 0.1 g/L sodium thioglycollate (97 %, Alfa Aesar), 0.004 g/L $FeSO_4.7H_2O$, and 5.0 g/L sodium citrate dihydrate. pH was adjusted to 7.25 using 3 M NaOH and 1 M HCl. After autoclaving the measured pH of the media was 6.5. Nutrient, pH, and buffer concentrations were later adjusted in some experiments as noted in the

respective Experimental Methods sections.

### 3.3.3 Serum Bottle Culture

Sulfate reducing bacteria were cultured in 150 mL serum bottles for small scale batch experiments and preparation of inoculum for bioreactor experiments. The bottle head space was made anaerobic by placing the bottles in a -20" Hg abs. vacuum and restoring atmospheric pressure with an anaerobic gas mixture (5 % $CO_2$, 10 % $H_2$, 85 % $N_2$ v/v, Praxair certified standard). This process was performed 3x before the bottles were sealed with butyl rubber stoppers (Bellco Biotechnology, Vineland, New Jersey) and then autoclaved at 121 $^oC$ for 20 min. Alternatively, serum bottles with media were sparged with UHP $N_2$ for 60 s before being sealed and autoclaved. Neither method resulted in noticeably different serum bottle culture growth behaviour suggesting both methods provided equivalent anaerobic conditions. Inoculation and sampling procedures were performed using sterile, disposable 1-3 mL medical syringes. Unless otherwise specified serum bottle cultures were incubated under static conditions at 33 $^oC$ in a Forma Scientific model 3956 Reach-in incubator. Smaller volumes of cultures were revived as needed using similar methods in 20 mL (liquid volume) anaerobic culture tubes with butyl rubber stoppers.

### 3.3.4 2 L Bioflo Fermentations

2 L (liquid volume) fermentations were performed in Bioflo 1/Multigen stirred tank bioreactors (New Brunswick Scientific, Edison, New Jersey). Bioreactors and 1680-1700 mL of medium were autoclaved at 121 $^oC$ separately, then sparged with filter sterilized (0.2 $\mu$m) UHP $N_2$ for 10 min while being agitated at 180 RPM by two Rushton turbines

to remove dissolved $O_2$. Bioflo fermentations were inoculated using 300-320 mL (at 0.200-0.240 g CDW/L) of growth phase PC SRB cultures revived from 4 $^oC$ stocks. Bioreactors were maintained at 34 ± 1 $^oC$ by circulating water from a thermostated bath through Tygon tubing coils. 3 vertical baffles and agitation by the turbines at 90 RPM maintained well mixed conditions.

### 3.3.5 Packed Bed Bioreactor (PBR) Fermentations

A 615 mL glass column bioreactor was constructed for packed bed fermentations (Figure 3.1). The overall bioreactor dimensions of the bioreactor were 38 cm x 4.5 cm and consisted of a main column to which two end pieces were clamped. The main column was fitted with three butyl rubber sampling ports located at each end (inlet/outlet) and at the column midpoint. The end pieces were each fitted with two barbed fittings for liquid and gas inlet/outlets. The main column contained the carrier material and the end pieces were filled with polyethylene mesh to improve fluid and gas dispersion. Bioreactors were maintained at 38 ± 1 $^oC$ by circulating water from a thermostated bath through Tygon tubing coils. The entire apparatus was covered in removable foam insulation.

Bioreactors were filled with carrier packing material and autoclaved at 121 $^oC$. The bioreactors were then purged with filter sterilized UHP $N_2$ before being inoculated with SRB cultures by circulating 2 L stationary phases Bioflo cultures through the bioreactor for 48 h at 200 mL/h. After inoculation, the liquid feed was switched to sterile PC media from a 12 L carboy that was maintained anaerobic by a continuous filter sterilized UHP $N_2$ purge. Liquid flowrates were adjusted using an IMED Gemini 1 digital peristaltic

infusion pump (Cardinal Health, Canada). Stripping experiments were conducted by sparging filter sterilized UHP $N_2$ to the bottom of the bioreactor. Gas flow rates were controlled by precision rotameters (Cole Parmer, Montreal, Quebec) with maximum flow rates of either 5.6 mL/min or 112.5 mL/min depending on the required flow rate. Gas and liquid sulfide waste streams were treated with 3 M NaOH and bleach before disposal.

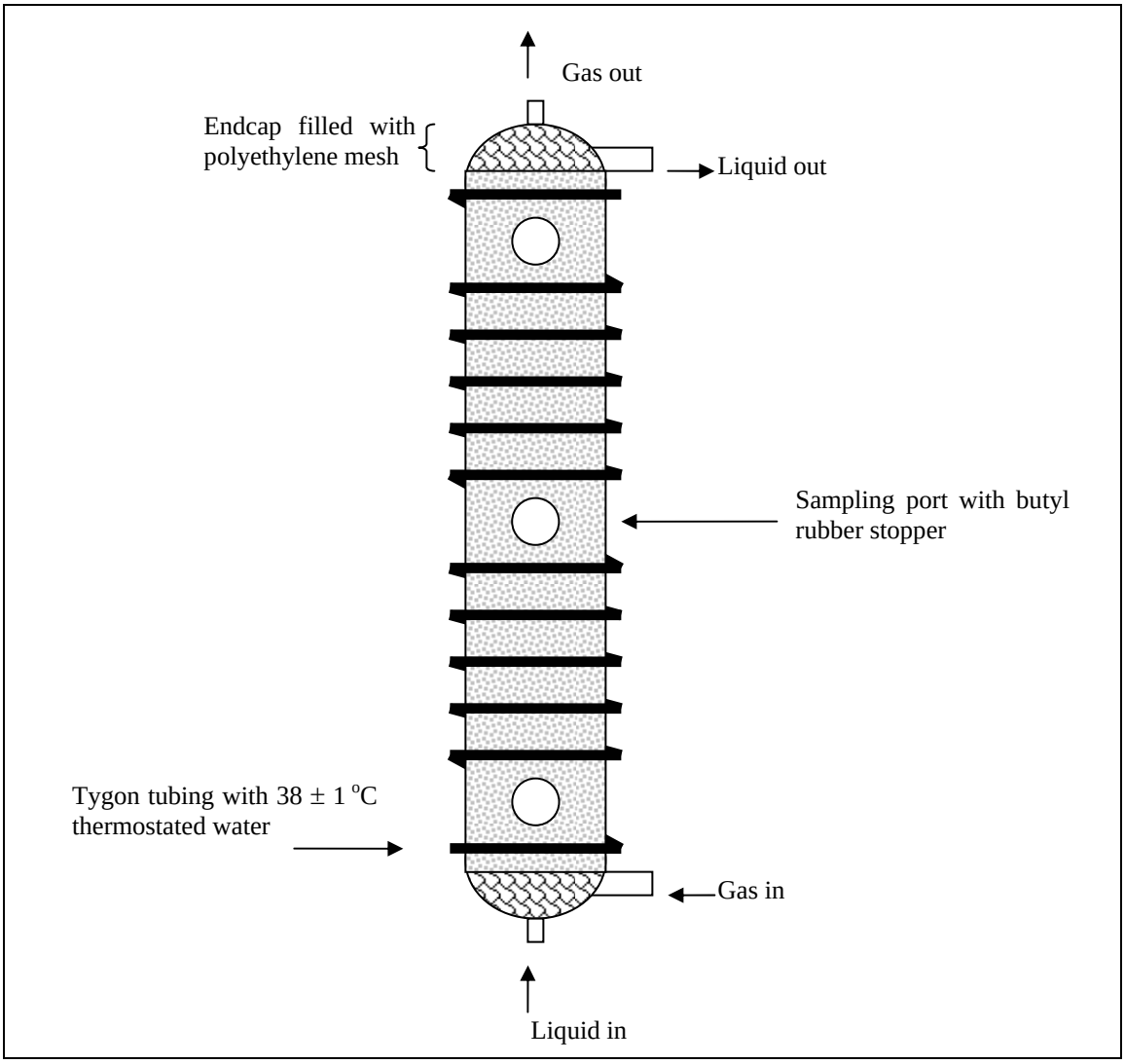


**Figure 3.1:** Diagram of 615 mL (4.5 cm x 38 cm) packed bed bioreactor (PBR) used for continuous SRB fermentations. The PBR contained barbed fittings for liquid and gas inlet/outlet, butyl rubber sampling ports, and was surrounded with Tygon tubing heat coils and foam insulating material (not shown). The column of the PBR was packed with biomass carrier material while the end pieces contained a polyethylene mesh to improve gas/liquid dispersion.

## 3.4 Sulfate Reducing Bacteria Cultures

### 3.4.1 *Desulfovibrio desulfuricans* (ATCC 7757)

*Desulfovibrio desulfuricans* subsp. *desulfuricans* (ATCC 7757) was obtained as a freeze dried specimen from the American Type Culture Collection (Manassas, Virginia). *Desulfovibrio desulfuricans* was revived as per ATCC instructions and then transferred to PB medium stocks. Phase contrast microscopy of the cultures revealed a homogenous population of motile cells with a vibrio morphology consistent with the ATCC description.

### 3.4.2 Sulfate Reducing Bacteria Consortium

A complex (undefined) consortium of sulfate reducing bacteria was enriched from landfill leachate samples collected from a municipal landfill in Calgary, Alberta at an approximate depth of 15 m. Initial enrichment work was performed at the University of Calgary by Mr. Brenton Buziak of Dr. Gerrit Voordouw's research group. 1 mL of leachate was used to inoculate 100 mL of CSB-K media. CSB-K is a defined lactate, sulfate based media in which yeast extract has been replaced with a defined trace element solution. Four successive 1 % (v/v) transfers were performed until an SRB enriched culture was obtained and confirmed by a decrease in sulfate concentration and concomitant sulfide production. The CSB-K enrichment culture was then transferred to Queen's University at Kingston for further enrichment.

Further enrichments at Queen's University were conducted using PC media in serum bottle cultures. Cultures were incubated until TDS concentrations reached approximately 15 mM and then transferred to fresh media. Eight such transfers at 2 % v/v were performed. The ratio of TDS to cell density ($Y_{P/X}$) was used as an indicator of the consortium's relative sulfate reducing activity. The initial PC transfer exhibited a $Y_{P/X}$ value of 54 mmol TDS/g CDW. An SRB enriched consortium with stable population composition was assumed to be achieved when four successive transfers exhibited similar $Y_{P/X}$ values of 95 ± 7 mmol TDS/g CDW. Six successive transfers of the culture (2 % v/v) were then performed at 24 h intervals in PB media to ensure a stable consortium composition in all future transfers from PB stock cultures.

## 3.5 Carrier Materials

Four different carrier materials (Table 3.1, Figure 3.2) were evaluated for their biomass immobilization potential. Polyurethane foam plugs and Poraver™ porous glass beads were selected based upon their previous use for SRB immobilization as reported in the recent literature (Silva et al., 2006 and Alvarez et al., 2006 respectively). Bone char and Celite™ R-635 diatomaceous earth pellets were evaluated based on their general suitability for the immobilization of anaerobic bacteria based on the recent literature (Quereshi et al., 2005 and Wright, 2005 respectively).

**Table 3.2:** General carrier material dimensions and prices.

| Material | Bulk Density (kg/L) | Shape | Dimensions | Price (per kg) | Price (per L) |
|---|---|---|---|---|---|
| Bone char | 0.604 | irregular pellet | 5 x 8 mesh | $ 3.30 | $ 1.99 |
| Poraver™ | 0.234 | spherical | 1-2 mm D | $ 1.54 | $ 0.36 |
| Polyurethane foam | 0.027 | cylindrical | 40 mm D x 45 mm H | $ 192.98 | $ 5.18 |
| Celite™ R-635 | 0.540 | cylindrical pellet | 6.35 mm D x 12.7 mm H | $ 22.00 | $ 13.30 |


**Figure 3.2:** Photographs of carrier materials (ruler for scale). A) Poraver™ porous glass beads; B) polyurethane foam plug; C) bone char; D) Celite™ R-635 diatomaceous earth pellets.

### 3.5.1 Polyurethane Foam Plugs

Identi-Plug polyurethane foam plugs were obtained from Jaece Industries Inc. (North Tonawanda, New York). The porous, open cell foam plugs are commonly used as gas permeable stoppers for Erlenmeyer flasks, are autoclavable, and are chemically inert as described by the manufacturer.

### 3.5.2 Poraver™ Porous Glass Beads

Poraver™ porous glass beads were donated by Poraver North America (Barrie, Ontario). The beads are made from recycled soda lime glass (71 % silicon dioxide, 14 % sodium oxide, 9 % calcium oxide, 3 % alumina, 2 % magnesium oxide, and 1 % w/w potassium oxide) and used as a filling material in building construction (Poraver North America, 2006). Poraver beads were rinsed in distilled water and dried at 80 $^{o}$C before use.

### 3.5.3 Bone Char

Bone char was purchased from Ebonex Corporation (Melvindale, Michigan). Bone char is a microporous material made from the carbonization of animal bones in an inert atmosphere. The resulting material is approximately 70-76 % calcium hydroxyapatite, 9-11 % elemental carbon, 7-9 % calcium carbonate, <3 % acid insoluble ash, 0.1-0.2 % calcium sulfate and <0.3 % w/w ferric oxide. Approximate total surface area is 100 $m^2/g$ of which 50 % is carbon surface and pore volume is 0.225 $cm^3/g$ as described by the manufacturer. Bone char imparts (carbonate) alkalinity to aqueous solutions and requires acid pre-treatment before use. Bone char was treated with 1 M HCl (200 mL acid/100 g

bone char) for 1 h under static ambient conditions followed by rinsing with distilled water and drying at 80 $^{o}$C.

### 3.5.4 Celite™ R-635

Celite™ R-635 diatomaceous earth pellets were donated by World Minerals Inc. (Santa Barbara, California). The pellets are a flux calcined diatomaceous earth product with composition similar to high silica glass (approximate composition: 82.3 % silica, 7.2 % alumina, 3.3 % sodium oxide, 2.6 % calcium oxide, 1.9 % ferric oxide, 1.2 % magnesium and trace inorganics). The pellets have a microporous structure with a mean pore diameter of 20 $\mu$m and a reported BET surface area of 0.27 $m^2/g$. Designed specifically for bacterial immobilization, R-635 pellets exhibit good mechanical strength, chemical stability, and resistance to microbial degradation as described by the manufacturer.

# Chapter 4: Experimental Methods

## 4.1 Microbial Systems Characterization Experiments:

A series of experiments was conducted to evaluate the reaction stoichiometry (yield coefficients) and microbial kinetics of the pure strain *Desulfovibrio desulfuricans* and an SRB consortium. Stoichiometry experiments were conducted using 150 mL serum bottles containing PC media and inoculated (1 % v/v) with SRB stocks from 4 $^{o}$C storage. Serum bottles were incubated statically at 33 $^{o}$C and sampled daily until they reached stationary phase (~48 h or TDS concentrations of ~20 mM). Samples were analyzed for lactate, sulfate, TDS, and suspended cell concentrations.

The Monod specific growth rate ($\mu$, $h^{-1}$) was used a measure of microbial kinetics. $\mu$ was calculated by periodically measuring the suspended biomass concentration of 2 L BioFlo fermentations during the exponential growth phase. $\mu$ values were taken as the slope of the linear portion of [ln ($X/X_0$) vs. $t$] plots where $X$ is the suspended biomass concentration at a given time $t$ (h). Initial and final sulfate concentrations were also measured to confirm consistent $Y_{X/SO4}$ yield coefficients.

To examine the effects of inoculum composition on stoichiometry and kinetics, various fractions of *Desulfovibrio desulfuricans* and consortium culture were used for the 300-320 mL inoculum (e.g. a 33 % consortium inoculum contained 100 mL of consortium at 0.200 g CDW/L and 200 mL of *Desulfovibrio desulfuricans* at 0.200 g CDW/L). Eight BioFlo fermentations were conducted using inoculum compositions as described in Table

4.1.

**Table 4.1:** List of 2 L batch BioFlo fermentations and their inoculum composition used in microbial kinetics and stoichiometry experiments.

| Batch Fermentation | % Consortium in Inoculum | % *Desulfovibrio desulfuricans* in Inoculum |
|---|---|---|
| 1 | 100 | 0 |
| 2 | 100 | 0 |
| 3 | 29 | 71 |
| 4 | 16 | 84 |
| 5 | 6 | 94 |
| 6 | 4 | 96 |
| 7 | 0 | 100 |
| 8 | 0 | 100 |

## 4.2 Comparison of Carrier Materials Experiments

A series of experiments was conducted to evaluate the immobilization capability of four different carrier materials. 2 L *Desulfovibrio desulfuricans* cultures were grown to stationary phase in BioFlo bioreactors as described previously and then circulated at ambient temperature through PBRs filled with carrier material at 200 mL/h for 20 h (Figure 4.1). At the specified flow rate the HRT values for bone char, Poraver™ porous glass, polyurethane foam, and Celite™ R-635 were 2.1, 1.4, 2.8, and 2.1 h respectively.

The amount of biomass immobilized on the carrier material was calculated by measuring the initial suspended biomass concentration of the culture and after 20 h of circulation. A mass balance was then performed as described by Equation (14). The amount of immobilized biomass ($X$, g CDW) was the product of the difference in suspended biomass concentration and culture volume ($V$).

$$X_{\text{immobilized}} = \left(X_{\text{t}=20\text{ h}} - X_{\text{t}=0\text{h}}\right)(V) \tag{14}$$

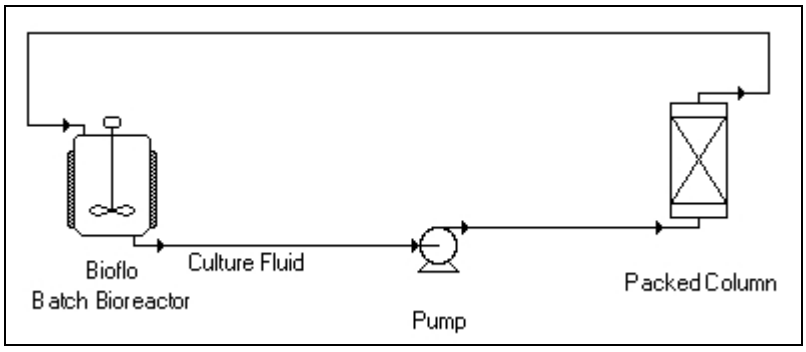


**Figure 4.1:** Diagram of experimental setup for the evaluation of carrier material immobilization potential. 2 L stationary phase *Desulfovibrio desulfuricans* cultures were circulated from a BioFlo bioreactor to a column packed with carrier material at ambient conditions at flow rate of 200 mL/h.

## 4.3 Comparison of *Desulfovibrio desulfuricans* and SRB Consortium Immobilization Potential Experiments

A series of experiments was conducted to compare the immobilization potential of *Desulfovibrio desulfuricans* and the SRB consortium. 2 L SRB cultures were grown to stationary phase in BioFlo bioreactors as described previously and then circulated at ambient temperature through a packed bed reactor filled with carrier material at 200 mL/h for 20 h. Various inoculum compositions were used to prepare the 2 L cultures and to evaluate the effect of inoculum composition on immobilization potential. Celite™ R-635 and polyurethane foam were used as carrier materials for these experiments as described in Table 4.2.

**Table 4.2:** List of inoculum compositions and carrier materials used in immobilization potential experiments.

| Batch Fermentation | % Consortium in Inoculum | % *Desulfovibrio desulfuricans* in Inoculum | Carrier Material |
|---|---|---|---|
| 1 | 100 | 0 | R-635 |
| 2 | 100 | 0 | polyurethane foam |
| 3 | 47 | 53 | polyurethane foam |
| 4 | 29 | 71 | polyurethane foam |
| 5 | 16 | 84 | polyurethane foam |
| 6 | 6 | 94 | R-635 |
| 7 | 4 | 96 | polyurethane foam |
| 8 | 4 | 96 | R-635 |
| 9 | 0 | 100 | polyurethane foam |
| 10 | 0 | 100 | R-635 |

## 4.4 Continuous Packed Bed Reactor Experiments

After Celite™ R-635 had been determined to be the best carrier material and ~4 % consortium to be the optimal inoculum composition, several continuous flow PBR fermentations were conducted using said carrier and inoculum. The experiments were divided into two general sets. The first set consisted of experiments involving only a liquid stream entering and leaving the bioreactor. Due to the high solubility of $H_2S$ and the operating pH, practically all the sulfide product emerged as dissolved sulfide in the first set of experiments. The second set of experiments involved both liquid and gas ($N_2$ stripping) streams and with the sulfide product emerging in both phases. Details and objectives of each experiment are described.

### 4.4.1 PBR Fermentation Experiment 1: System Characterization

The objective of the first PBR fermentation was to characterize the system behaviour, its ability to adapt to step changes in liquid feed rates ($L$, mL/h), and to achieve high volumetric productivity in minimal start-up time. After the bioreactor had been inoculated by circulating a stationary phase culture as described previously, a sterile feed of PC media was fed at 20 mL/h (HRT = 20 h, $D$ = 0.05 $h^{-1}$). Samples were taken daily from the bioreactor's three ports and analyzed for TDS, sulfate, and suspended biomass concentrations. When TDS concentrations had stabilized around the inhibitory concentration (15-20 mM) the liquid feed rate was increased and the system was allowed to stabilize at the new flow rate. In this manner the feed rate was increased step-wise from 20 mL/h to 640 mL/h (HRT = 39 min, $D$ = 1.6 $h^{-1}$) over a period of 200 h. After operating at a feed rate of 640 mL/h, the effect of arbitrary step changes in the feed rate

were evaluated by reducing the feed rate to 160 mL/h for 15-22 h and then restoring the feed rate to 500 mL/h. The liquid feed was decreased in two steps to 0 mL/h and restored to 500 mL/h in two steps. Details of the liquid feed step changes are listed in Table 4.3.

**Table 4.3:** Liquid feed rates, feed duration, and respective hydraulic residence times (HRT), dilution rates (*D*), and equivalent column volumes (CV) for this first PBR fermentation experiment (no stripping).

| Time (h) | Feed Rate (mL/h) | Time at Feed (h) | HRT (h) | *D* ($h^{-1}$) | CVs |
|---|---|---|---|---|---|
| 0 | 20 | 74.5 | 20 | 0.05 | 3.7 |
| 74.5 | 40 | 5 | 10 | 0.10 | 0.5 |
| 79.5 | 0 | 15 | - | - | - |
| 94.5 | 40 | 24.75 | 10 | 0.10 | 2.5 |
| 119.25 | 80 | 24.25 | 5 | 0.20 | 4.9 |
| 143.50 | 160 | 22 | 2.5 | 0.40 | 8.8 |
| 165.5 | 320 | 28.5 | 1.25 | 0.80 | 22.8 |
| 194 | 640 | 6.5 | 0.625 | 1.60 | 10.4 |
| 200.5 | 160 | 14.5 | 2.5 | 0.40 | 5.8 |
| 215 | 500 | 9.5 | 0.8 | 1.25 | 11.9 |
| 224.5 | 160 | 4.75 | 2.5 | 0.40 | 1.9 |
| 229.25 | 40 | 0.75 | 10 | 0.10 | 0.1 |
| 230 | 0 | 12.75 | - | - | - |
| 242.75 | 160 | 22.25 | 2.5 | 0.40 | 8.9 |
| 265 | 500 | 5 | 0.8 | 1.25 | 6.3 |

### 4.4.2 PBR Fermentation Experiment 2: Sustained Operation and Recovery After Shutdown

From the first PBR fermentation it was observed that biomass immobilization allowed for rapid increases in feed rates without biomass washout and attainment of high volumetric productivities. The objectives of the second PBR fermentation were to evaluate sustained bioreactor operation at high liquid feed rates (250 mL/h for periods of ~ 48 h) and the ability of the bioreactor to recover from a complete shutdown period of 24 h where both the feed rate and heating coil operation were halted. Details of the liquid feed step changes are listed in Table 4.4.

**Table 4.4:** Liquid feed rates, feed duration, and respective hydraulic residence times (HRT), dilution rates (*D*), and equivalent column volumes (CV) for this second PBR fermentation experiment.

| Time (h) | Feed Rate (mL/h) | Time at Feed (h) | HRT (h) | *D* ($h^{-1}$) | CVs |
|---|---|---|---|---|---|
| 0 | 20 | 24.75 | 20 | 0.05 | 1.2 |
| 24.75 | 40 | 42.50 | 10 | 0.10 | 4.3 |
| 67.25 | 80 | 53.75 | 5.0 | 0.20 | 10.8 |
| 121 | 160 | 19.25 | 2.5 | 0.40 | 7.7 |
| 140.25 | 250 | 47.00 | 1.6 | 0.63 | 29.4 |
| 187.25 | 0 | 25.75 | - | - | - |
| 213 | 250 | 46.25 | 1.6 | 0.63 | 28.9 |
| 259.25 | 500 | 22.50 | 0.8 | 1.25 | 28.1 |

### 4.4.3 PBR Fermentation Experiment 3 (with Stripping): System Characterization

The third PBR experiment added an $N_2$ strip gas to the bioreactor system. The purpose of implementing a strip gas was to improve volumetric productivity by *in situ* removal of the inhibitory sulfide product and to partition more of the sulfide product in to the gas phase as $H_2S_{(g)}$.

The stripping experiments were conducted by starting a PBR fermentation as previously described. The feed rate was increased step wise over a period of 66 h from 20 mL/h to 80 mL/h (HRT = 6 h, $D$ = 0.17 $h^{-1}$) where a stable TDS concentration (~20 mM) was achieved. The effects of four different stripping rates on the system were evaluated by setting the $N_2$ gas flow rate ($G$, mL/min) to specified value and allowing the system to stabilize over a 24 h period (4 CV). TDS, sulfate, and suspended biomass concentrations were measured for each condition. Gas flow rates were reported as a normalized stripping ratio ($G/L$) of gas flow rate ($G$) to liquid feed rate ($L$). $G/L$ ratios were evaluated non-sequentially as described in Table 4.5.

**Table 4.5:** List of stripping ratios *(G/L)* evaluated for PBR fermentation at constant 80 mL/h liquid feed. *L* = liquid feed rate; *G* = $N_2$ strip gas rate.

| Experimental Condition | *L* (mL/h) | *G* (mL/min) | *G/L* ($m^3/m^3$) |
|---|---|---|---|
| 1 | 80 | 5.1 | 3.8 |
| 2 | 80 | 2.4 | 1.8 |
| 3 | 80 | 3.4 | 2.6 |
| 4 | 80 | 0 | 0 |

Gas samples were analyzed at another four operating conditions as described in Table 4.6. in order to evaluate the sulfur mass balance and investigate the partitioning of the product sulfide between dissolved and gas phases.

**Table 4.6:** List of stripping conditions (*G/L*) at which strip gas samples were taken for gas phase $H_2S$ analysis.

| Experimental Condition | *L* (mL/h) | *G* (mL/min) | *G/L* ($m^3/m^3$) |
|---|---|---|---|
| 1 | 80 | 5.1 | 3.8 |
| 2 | 40 | 1.7 | 2.5 |
| 3 | 40 | 1.7 | 2.5 |
| 4 | 40 | 4.1 | 6.2 |

### 4.4.4 Basic Model for PBR Operation with Stripping

A simple steady-state model was developed to better understand the system behaviour and the interaction of variables such as substrate concentration, *G/L* ratio, volumetric productivity, and sulfide product partitioning. The model assumed that the bioreactor was capable of maintaining a constant 20 mM TDS concentration in the effluent independent of the *G/L* ratio. Dissolved sulfide speciation was then calculated using known ionization equilibrium constants and vapour liquid equilibrium was calculated using Henry's Law as described in Appendix D.

The effect of pH values of 6, 7 and 8 and *G/L* ratios of 0, 1.3, 2.4, and 3.8 on volumetric productivity and sulfide partitioning was evaluated.

### 4.4.5 PBR Fermentation Experiment 4 (with Stripping): Performance Enhancement

The objectives of the fourth PBR fermentation were to experimentally evaluate the effect of initial medium pH and higher *G/L* ratios on the bioreactor performance

Nutrient concentrations in the PC medium were doubled for this experiment and determined to be sufficient to avoid substrate limitation at the operating conditions being evaluated.

A citric acid buffer system ($pK_{a3}$ = 6.4) composed of 20 g/L sodium citrate dihydrate and

1 g/L citric acid monohydrate (73 mM total citrate ions) was initially evaluated for maintaining a pH of 6 but found to have insufficient buffering capacity.

The phosphate buffer system ($KH_2PO_4/K_2HPO_4$) was selected as an alternative due to its common use in industrial fermentations, low cost, availability as a mono/dipotassium salts (compared to the trisodium salts), and its broad buffering capacity (*pKa* values 2.15, 7.2, 12.33).

#### 4.4.5.1 Stripping with pH 6 Buffered System

Stripping experiments were conducted at initial pH 6.1 by buffering the 2x concentration PC media with 8 g/L $K_2HPO_4$ and 14.6 g/L $KH_2PO_4$ (153 mM phosphate ion). It was assumed that this would be sufficient buffering capacity if the sole alkalinity generating process occurred according to Equation (15) where 1 mol of lactate resulted in 1 mol of bicarbonate alkalinity with an initial lactate concentration of 108 mM.

$$2CH_3CHOHCOONa + Na_2SO_4 \rightarrow 2CH_3COONa + 2NaHCO_3 + H_2S \qquad (15)$$

Stripping conditions for the pH 6 buffered system were evaluated over a wide range of *G/L* ratios (0-14.1) to obtain a good representation of overall trends. Similar high value *G/L* ratios (10.5-14.1) were evaluated at different absolute liquid feed rates (50, 100, 200 mL/h) to investigate process scalability (Table 4.7). The bioreactor was allowed to stabilize at each new *G/L* ratio for at least 48 h (10 CV).

**Table 4.7:** List of stripping ratios *(G/L)* evaluated for PBR fermentation using media buffered to pH 6.1. *L* = liquid feed rate; *G* = nitrogen strip gas rate.

| Experimental Condition | *L* (mL/h) | *G* (mL/min) | *G/L* ($m^3/m^3$) |
|---|---|---|---|
| 1 | 100 | 5.1 | 3.0 |
| 2 | 100 | 1.8 | 1.1 |
| 3 | 100 | 3.2 | 1.9 |
| 4 | 100 | 0 | 0 |
| 5 | 100 | 17.5 | 10.5 |
| 6 | 200 | 43.5 | 13.0 |
| 7 | 50 | 11.8 | 14.1 |

#### 4.4.5.2 Stripping with pH 7 Buffered System

Stripping experiments were conducted at pH 7 using phosphate concentrations of 28.38 g/L $K_2HPO_4$ and 6.25 g/L $KH_2PO_4$ (208 mM phosphate ions). Four *G/L* ratios were evaluated at pH 7 as described in Table 4.8.

**Table 4.8:** List of stripping conditions *(G/L)* evaluated for PBR fermentation using media buffered to pH 7. *L* = liquid feed rate; *G* = nitrogen strip gas rate.

| Experimental Condition | *L* (mL/h) | *G* (mL/min) | *G/L* ($m^3/m^3$) |
|---|---|---|---|
| 1 | 100 | 0 | 0 |
| 2 | 100 | 5.1 | 3.0 |
| 3 | 100 | 2.6 | 1.5 |
| 4 | 100 | 3.9 | 2.3 |

# Chapter 5: Results and Discussion

## 5.1 Microbial Systems Characterization Experiments

The objectives of this experiment were to evaluate the reaction stoichiometry and microbial kinetics of the pure culture *Desulfovibrio desulfuricans* (ATCC 7757) and the SRB consortium. A summary of results from serum bottle and 2 L BioFlo bioreactor experiments are shown in Table 5.1 and Table 5.2 respectively.

**Table 5.1:** Summary of yield coefficients (*Y*) for serum bottle batch cultures of *Desulfovibrio desulfuricans* and an SRB consortium. Parameters measured were sulfate reduced ($SO_4^{2-}$), total dissolved sulfide (TDS), lactate oxidized, and cell dry weight (CDW) produced. At the experimental conditions (pH ~ 7.5) the majority of sulfide was in the dissolved phase.

| | $Y_{P/S}$ TDS/ $SO_4^{2-}$ (mol/mol) | $Y_{S/S}$ $SO_4^{2-}$/lactate (mol/mol) | $Y_{P/S}$ TDS/lactate (mol/mol) | $Y_{X/S}$ CDW/$SO_4^{2-}$ (g/g) | $Y_{X/S}$ CDW/lactate (g/g) |
|---|---|---|---|---|---|
| ***Desulfovibrio desulfuricans*** | | | | | |
| Replicate #1 | 1.07 | 0.45 | 0.48 | 0.11 | 0.053 |
| Replicate #2 | 0.99 | 0.44 | 0.44 | 0.11 | 0.052 |
| **Consortium** | | | | | |
| Replicate #1 | 0.88 | 0.48 | 0.42 | 0.12 | 0.060 |
| Replicate #2 | 0.81 | 0.48 | 0.39 | 0.11 | 0.055 |

**Table 5.2:** Batch growth kinetic properties for *Desulfovibrio desulfuricans* and an SRB enriched consortium as measured in 2 L batch fermentations.

| | $\mu$ ($h^{-1}$) | $Y_{X/S}$ CDW/$SO_4^{2-}$ (g/g) | $Q_S$ (g $SO_4^{2-}$/g CDW.h) |
|---|---|---|---|
| *Desulfovibirio desulfuricans* | 0.07-0.09 | 0.10-0.12 | 0.58-0.90 |
| SRB Consortium | 0.12-0.13 | 0.11 | 1.1-1.2 |

### 5.1.1 Stoichiometry

*Desulfovibrio desulfuricans* had been selected for this work as a benchmark SRB species as it is a well known incomplete lactate oxidizer, exhibits relatively fast kinetics, has biofilm formation tendencies, and is frequently used as a model organism in the bioengineering literature (Widdel, 1988; Okabe and Characklis, 1992; Okabe et al., 1992;

Gasiorek, 1994; Fukui and Takii, 1994; Konishi et al., 1996; Nagpal et al., 2000a; Beyenal and Lewandowski, 2004). The observed yield coefficients for *Desulfovibrio desulfuricans* (Table 5.1, Table 5.2) were similar to those reported in literature and to theoretical values. The molar ratio of total dissolved sulfide (TDS) to sulfate reduced ($Y_{TDS/\ SO4}$) was close to the theoretical value of 1.0 mol/mol. That practically all the sulfide was present in the dissolved phase at these conditions emphasized the high solubility of the desired product. The ratio of sulfate reduced to lactate oxidized ($Y_{SO4/lactate}$) was close to the theoretical value of 0.47 mol/mol. Lactate consumption is coupled with sulfate reduction for catabolic purposes at a sulfate:lactate ratio of 0.50 mol/mol. The diversion of a small amount of lactate for anabolic purposes reduces the observed yield to approximately 0.47 mol/mol. The observed biomass yield ($Y_{CDW/SO4}$ = 0.11 g/g) for *Desulfovibrio desulfuricans* was within range of values reported ($Y_{CDW/SO4}$ = 0.074-0.140 g/g) for various incomplete lactate oxidizing SRB as summarized in papers by Okabe and Characklis (1992) and Okabe et al. (1992). As discussed in the literature review, the catabolic yields (e.g. $Y_{sulfide/SO4}$, $Y_{SO4/lactate}$) are generally constant and independent of culture conditions. The anabolic biomass yields ($Y_{CDW/SO4,}$ $Y_{CDW/lactate}$) are subject to greater variability due to their dependence on culture conditions and the maintenance coefficient especially under conditions of high product sulfide inhibition. Culture conditions at the 2 L BioFlo batch bioreactor scale were similar to those at the 100 mL serum bottle scale. As anticipated, *Desulfovibrio desulfuricans* and the SRB consortium had similar biomass yields ($Y_{CDW/SO4}$ = 0.10-0.12 g/g) that were independent of liquid culture size.

The consortium had been enriched under conditions that selected for incomplete lactate oxidizing SRB. All of the observed yield coefficients for the consortium were nearly identical to those of *Desulfovibrio desulfuricans*. It was therefore assumed the consortium was composed overwhelmingly of incomplete lactate oxidizing SRB, likely of the common *Desulfovibrio* genus. The observed stoichiometric reduction of sulfate coupled to lactate oxidation for the consortium further suggested that *Desulfovibrio*-type SRB were the predominant consumers of the lactate carbon source. The serial enrichment process used to develop the consortium allowed TDS concentrations to reach inhibitory levels for several successive transfers with the assumption that non-sulfate reducing bacteria would have been unable to compete in such adverse conditions. Light micrograph examination of the pure culture *Desulfovibrio desulfuricans* had revealed a homogenous, mobile population with characteristic vibrio morphology. The consortium light micrograph revealed a population with similar members but also a small proportion of other morphologies, most noticeably elongated species several microns in length. These elongated morphologies could be further subdivided into filamentous, segmented, and spiral shapes. Other incompletely oxidizing SRB that may have been present as well include the *Desulfotomaculum* (spore formers) and *Desulfobulbus* genera which have been previously detected with the more common *Desulfovibrio* in consortia enriched from wastewater samples using PC medium (Alvarez et al., 2006). SRB are known to exhibit variable morphology even among the same species (Postgate, 1984) and ultimately these visual observations are sufficient only to suggest that a mixed population of SRB was present. Molecular identification techniques would be required to provide a more detailed picture of the SRB consortium's composition.

### 5.1.2 Microbial Kinetics

The intent of enriching for an SRB consortium was to produce a microbial system superior to the benchmark *Desulfovibrio desulfuricans* which could be used to improve bioreactor volumetric productivity. As the stoichiometry between the two microbial systems was found to be nearly identical, microbial kinetics was also used as a measure of performance. Table 5.2 shows that the observed range of specific growth rates ($\mu$, $h^{-1}$) for the consortium was generally greater than those observed for *Desulfovibrio desulfuricans.* Specific production formation rates [$Q_s$, (g $SO_4^{2-}$/g CDW.h)] were calculated as the product of $\mu$ and $Y_{SO4/CDW}$ and used as measure of the relative product sulfide formation kinetics. The results showed that the consortium had superior kinetics as measured by $Q_s$ and that under some conditions the difference was approximately twofold [0.58 vs. 1.2 (g $SO_4^{2-}$/g CDW.h)]. These results were consistent with informal observation of shorter SRB consortium lag periods in serum bottle cultures. When reviving stock cultures from 4 $^oC$ storage, the consortium often reached exponential and stationary phases in ~75 % of the time required by *Desulfovibrio desulfuricans* (data not shown). These results were anticipated as the enrichment method of serial transfers tends to select species that exhibit superior kinetics under the imposed conditions (e.g. lactate substrate with high TDS concentrations).

The observed specific growth rates (0.07-0.13 $h^{-1}$ at 34 $^oC$) were within the range of those reported in the literature for incomplete lactate oxidizing SRB (Nanninga and Gottschal, 1987). It should be noted that specific growth rates for SRB are sensitive to sulfide

inhibition and culture condition variables such as temperature, pH, and medium composition.

Additional 2 L batch experiments were conducted to evaluate the effect of inoculum composition on the observed specific growth rates. The results (Figure 5.1) illustrate a non-linear trend between specific growth rate and inoculum composition.

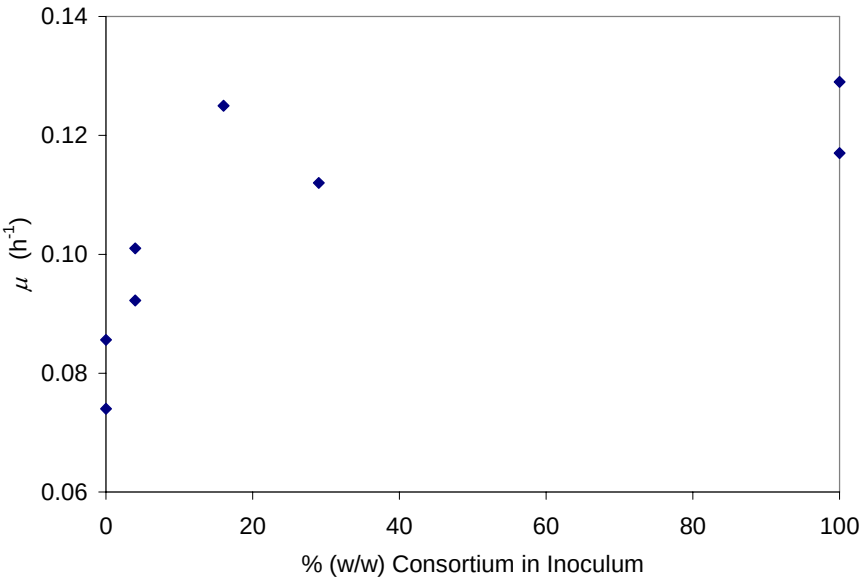


**Figure 5.1:** Specific growth rate ($\mu$, $h^{-1}$) of 2 L batch fermentations as a function of inoculum composition. 0 % consortium corresponds to 100 % *Desulfovibrio desulfuricans*.

The importance of these results was not fully appreciated until considered in conjunction with the immobilization experimental results. At this point the only clear implication was that the presence of even small fractions of consortium in the inoculum resulted in sharp increases in the specific growth rate. The non-linear relationship may be explained by the autocatalytic (i.e. exponential) growth characteristics of bacteria. It is expected that the microbial species with the greatest kinetics will rapidly become the dominate species in a closed, batch fermentation. In addition to its superior growth rate, the consortium may

have had other undetected advantages over *Desulfovibrio desulfuricans.* One possible advantage is an increased resistance to sulfide inhibition. This characteristic may have been selected for during the enrichment process by allowing the cultures to consistently reach inhibitory sulfide concentrations (> 15 mM TDS) before performing transfers. Monod saturation constants ($K_s$) were not measured but it is unlikely that the consortium would have been able to exploit a substrate affinity advantage. Initial substrate concentrations (lactate, 54 mM; sulfate, 32 mM) were both well above the $K_s$ values reported in literature for *Desulfovibrio desulfuricans* ($K_s$ < 0.1 mM for both substrates).

## 5.2 Comparison of Carrier Materials

The results of experiments to evaluate the relative biomass immobilization potential of four carrier materials is shown in Figure 5.2. *Desulfovibrio desulfuricans* was used as the model SRB for these experiments.

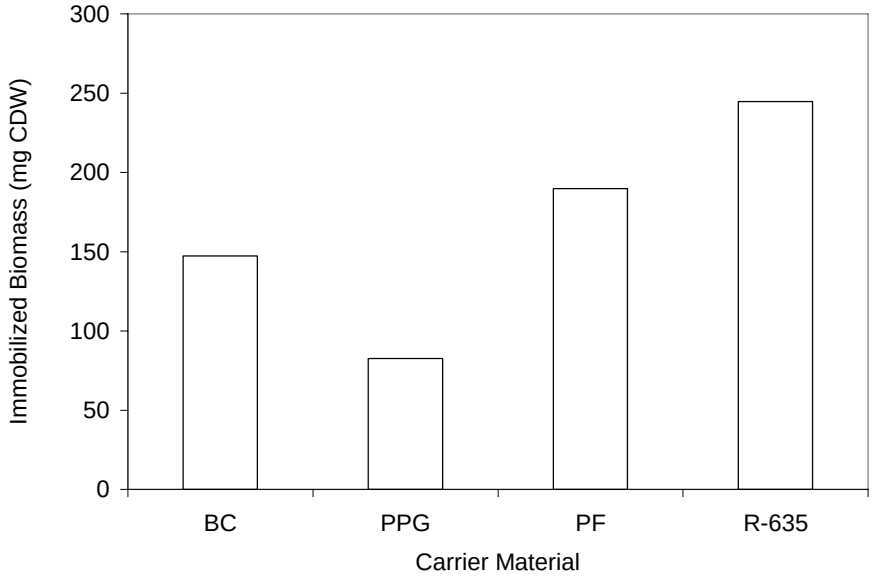


**Figure 5.2:** Quantities of immobilized *Desulfovibrio desulfuricans* biomass (mg CDW per reactor) on different carrier materials after 20 h circulation of 2 L stationary phase cultures through 615 mL packed bed reactors. Abbreviations: BC - bone char; PPG - Poraver porous glass beads; PF - polyurethane foam; R-635 - Celite diatomaceous earth pellets.

The ability for a carrier material retain large amounts of biomass is of critical importance in packed bed bioreactor design as it affects not only the volumetric productivities at which the bioreactor can operate, but also how rapidly it can be 'seeded', reducing the start-up period.

### 5.2.1 Bone Char Pellets

Bone char had been selected for evaluation as it had been reported as a suitable carrier material for immobilizing anaerobic bacteria for applications such as butanol production by *Clostridium acetobutylicum* (Qureshi et al., 2005) and treatment of petrochemical wastewaters by a mixed anaerobic consortium (Patel and Madamwar, 2002). The butanol production studies compared the performance of bone char to other carrier materials such as glass beads, glass wool, polypropylene, stainless steel wire balls, and clay brick. The

bone char was found to have measurable advantages over these other materials with respect to immobilization rates, ability to retain immobilized biomass under aggressive hydrodynamic conditions, and improved specific product formation rates. Bone char had not previously been evaluated for SRB immobilization but for the reasons mentioned it was regarded as having good potential as a carrier material.

The experimental results confirmed that bone char was capable of immobilizing the model SRB *Desulfovibrio desulfuricans* (0.147 g CDW/reactor), but not as effectively as polyurethane foam or R-635 pellets. The bone char material was found to be very brittle and crumbled under normal handling conditions, forming a fine black powder. This was undesirable as it would increase the total suspended solids in the bioreactor effluent and decrease the operational life time of the carrier material. Another significant disadvantage of the bone char was that it is known to increase the pH of process waters due to its composition of 7-9 % w/w $CaCO_3$. If the bone char was not pretreated with acid to neutralize these carbonates it was found that *Desulfovibrio desulfuricans* cells would not remain viable in the alkaline environment.

Due to its limited ability to immobilize *Desulfovibrio desulfuricans*, low durability, and carbonate alkalinity, bone char was eliminated from further consideration as a carrier material for SRB immobilization.

### 5.2.2 Poraver™ Porous Glass Beads

Poraver™ beads were selected as a benchmark carrier material as the material had been

reported suitable for both general bacterial immobilization (Zellner et al., 1994; Senthuran et al., 1999**;** Sa and Boaventura, 2001; Andersson and Bjornsson, 2002; Held et al., 2002; Lacayor et al., 2004) and SRB specific immobilization (Kolmert et al., 1997; Nagpal et al., 2000b; Kolmert and Johnson, 2001; Alvarez et al., 2006).

Of the four materials evaluated, Poraver™ was found to immobilize the least amount of *Desulfovibrio desulfuricans* (0.083 g CDW/reactor) and exhibited packing problems. Poraver may be more suited fluidized bed bioreactors as it entrains air/gas in its pores, decreasing packed bed stability. The glass material was also found to be brittle, though more durable than bone char. The crushability of the packing material would decrease its reusability and its applicability at larger scales. The low strength of Poraver™ may be due to its microporous structure. Usually the presence of micropores is beneficial for providing cells with surfaces protected from fluid shear but it has been reported that the pores in Poraver™ has low interconnectivity (Kolmert et al., 2001). The interior microporous structure therefore cannot be used for immobilization and results in the material's reduced mechanical strength.

Although considered a suitable carrier material for SRB by recent literature, Poraver™ was found to immobilize the least amount of *Desulfovibrio desulfuricans* compared to the other materials evaluated. One advantage of Poraver™ is its low cost ($1.54/kg, $0.36/L). The literature suggested that Poraver™ would provide adequate immobilization performance but this study has identified superior carrier materials and so it will not receive further consideration.

### 5.2.3 Polyurethane Foam Plugs

Polyurethane foam was selected as another benchmark carrier material that was capable of general anaerobic bacterial immobilization (Harendranath et al., 1996; Picanco et al., 2001; Oliveira et al., 2004; Yang et al., 2004; de Ory et al, 2004; and Ribeiro et al., 2005) and SRB specific immobilization (Stucki et al., 1993; Cadavid et al., 1999; Cattony et al., 2005, Silva et al., 2006).

Experimental observations from this study confirmed literature reports (Silva et al., 2006) of the suitability of polyurethane for the immobilization of SRB. Polyurethane foam immobilized the second highest amount of *Desulfovibrio desulfuricans* (0.405 g CDW/reactor) second only to Celite™ R-635. In these experiments the immobilized biomass was visible as grey particulate slime on the white foam material. Despite its high capacity for rapid biomass immobilization, polyurethane foam exhibited some disadvantages. The diameter of the foam plugs matched the bioreactor diameter (~4.5 cm) which maximized the available amount of pore surface area present. The macropores, similar to those found in synthetic sponges were large enough to seen by the unaided eye, had high interconnectivity and allowed good fluid flow, but had poor gas permeability due to bubble surface tension effects. Using the current foam plug dimensions would have prevented implementation of a strip gas in later experiments. Cutting the foam into smaller pieces may have alleviated the gas entrainment issue but would have decreased the available pore surface area for immobilization. Advantages of

the polyurethane foam were its chemical inertness, durability, and ease of handling. For these reasons the polyurethane foam plugs were used in additional experiments that evaluated the immobilization potential of mixed inoculum SRB populations. They were not considered for use in the long term packed bed fermentation experiments.

### 5.2.4 Celite™ R-635 Diatomaceous Earth Pellets

Celite™ R-635 was evaluated as carrier material as it had been reported as a suitable carrier material for aerobic and anaerobic bacteria in bioscrubber (Sorial et al., 1997; Sorial et al., 1998; and Wright, 2005) and wastewater treatment applications (Durham et al, 1994; Peres, 1999; Kim, 2002; and Bertin et al., 2004).

R-635 pellets immobilized the most *Desulfovibrio desulfuricans* biomass (0.522 g CDW/reactor) of the four materials evaluated. R-635's superior immobilization performance was attributed to it being the only carrier material that was designed for bacterial immobilization. SEM micrographs (Figure 5.3; Figure 5.4) of R-635 pellets revealed a highly microporous structure with average pore size of 20 $\mu$m as reported by the manufacturer. Pore sizes are ideally 10-20x the major diameter of the bacteria for optimal adsorption, bacterial growth, substrate/product diffusion, and protection from fluid shear forces.

Celite™ R-636 was regarded as the best of the four materials due to its combination of excellent immobilization capabilities, durability, chemical inertness, ease of handling, and previous success in other bioreactor applications. Scale-up concerns with Celite™ R-635 are minimal as its intended use is at the industrial scale as described by the

manufacturer. Although it was the most expensive of the materials tested ($22.00/kg, $13.30/L), its price was still an order of magnitude lower than more highly engineered carrier materials such as ion exchange resins (e.g. Dowex™ 1x8, $564/kg) and microcarriers (e.g. Cytoline™, $1826/L) which have been used in the literature for similar applications such as immobilization of ethanol producing bacteria (Krug and Daugulis, 1983) and anaerobic wastewater consortia (Chauhan and Ogram, 2005).

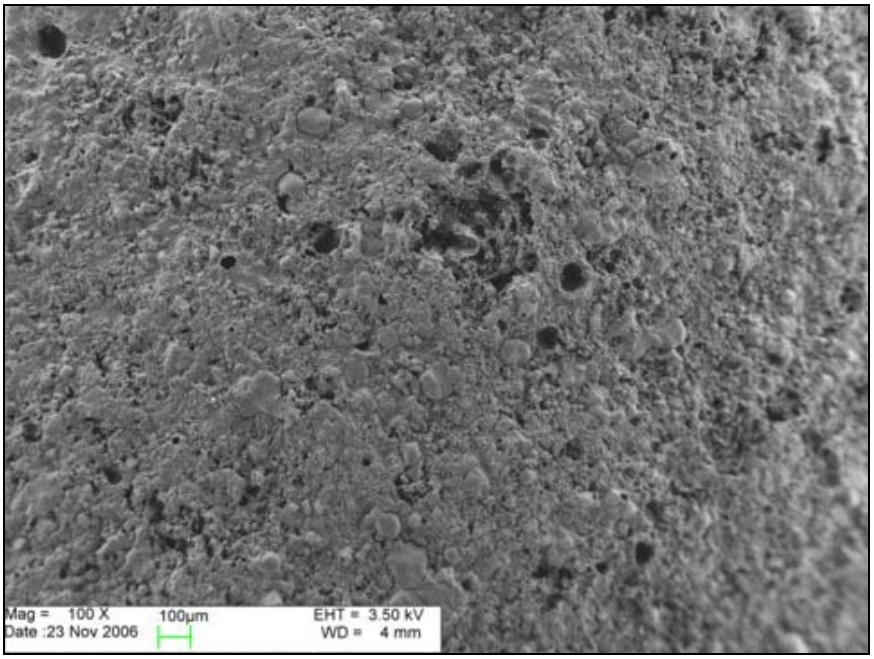


**Figure 5.3:** Scanning electron micrograph (100x) of the surface of Celite™ R-635 carrier material. Scale bar shows 100 $\mu$m.

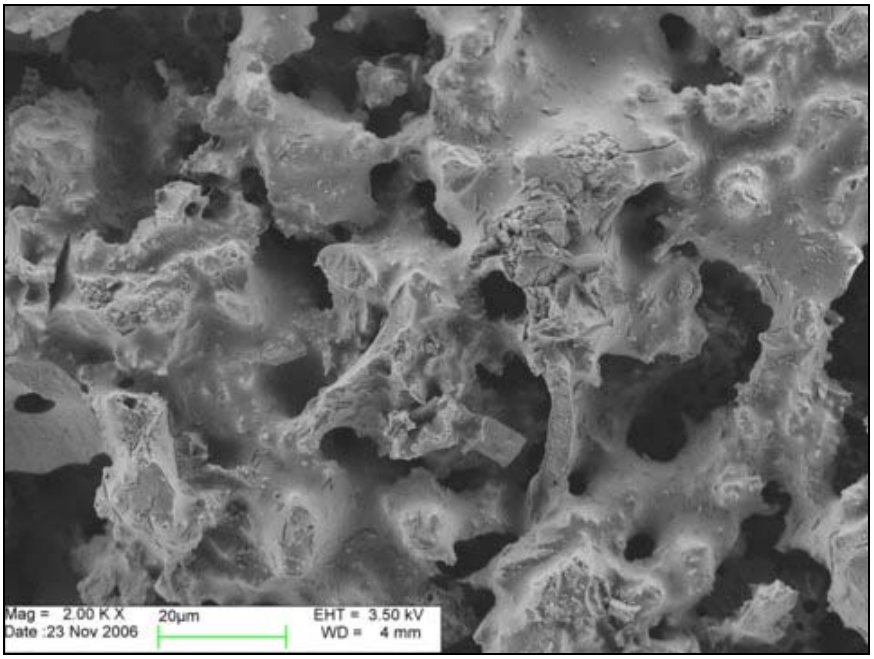


**Figure 5.4:** Scanning electron micrograph (2000x) of the surface Celite™ R-635 carrier material. Scale bar shows 20 $\mu$m.

## 5.3 Immobilization Potential

Earlier experiments in this study had compared the microbial kinetics of *Desulfovibrio desulfuricans* and the SRB consortium. The consortium exhibited superior growth rates and specific product formation rates. The immobilization potential of the two microbial systems was evaluated to determine which is more readily retained within the bioreactor. Results of immobilization experiments using varying inoculum compositions of *Desulfovibrio desulfuricans* and the SRB consortium are shown in Figure 5.5. Using both polyurethane foam and R-635 pellets as carrier materials a non-linear, inverse relationship between inoculum composition and biomass immobilized (mg CDW/reactor) was observed. *Desulfovibrio desulfuricans* appeared to have a high immobilization potential compared to the SRB consortium.

The literature had indicated that *Desulfovibrio desulfuricans* is well known for its attached growth properties and frequently used as model organism for SRB biofilm formation (Chen et al., 1994; Okabe et al., 1994; Beyenal and Lewandowski, 2004; Lopes et al., 2005; Lopes et al., 2006; Lee et al., 2006). Qualitative observations had also indicated that *Desulfovibrio desulfuricans* had superior immobilization potential compared to the consortium. *Desulfovibrio desulfuricans* serum bottle cultures were observed to form distinct biofilms on the bottle's surface 24-48 h after reaching stationary phase (Figure 5.6). Shaking the serum bottle would detach the biofilms which then aggregated into 'streamers'. The liquid medium's viscosity increased such that after agitation, gas bubbles became entrained in the liquid and slowly rose to the surface. The increased viscosity was attributed to increased extracellular polysaccharide (EPS)

formation. This phenomenon had been observed in other pure culture work using the similar *Desulfovibrio vulgaris* (Hildenborough) species. In contrast, the SRB consortium produced only small amounts of rapidly settling flocs that were less than 1 mm in diameter. Similar biofilm or EPS production was not observed for the consortium.

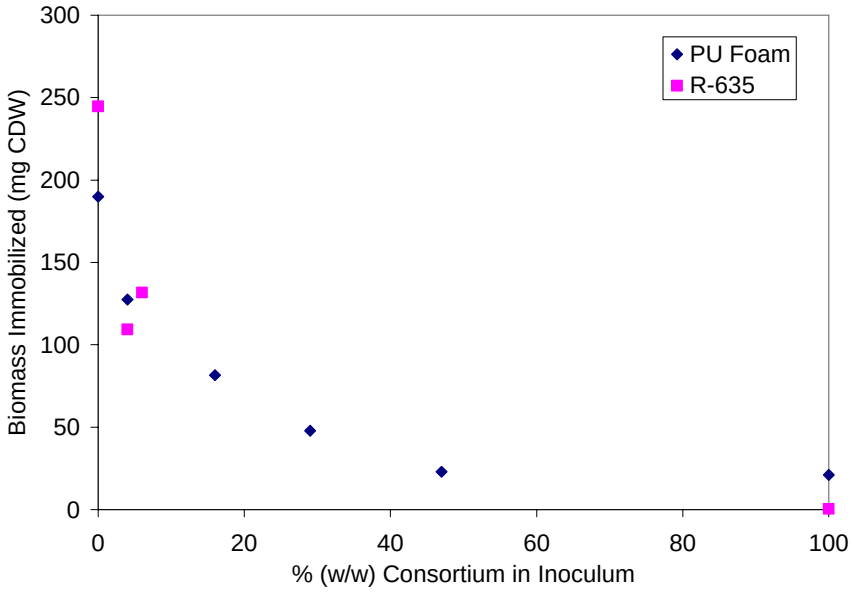


**Figure 5.5:** Biomass immobilized (mg CDW per reactor) to carrier material in a packed bed as a function of inoculum composition. 0 % consortium corresponds to 100 % pure culture (*Desulfovibrio desulfuricans*). Diamonds represent results obtained using polyurethane foam as the carrier material. Squares represent results obtained using Celite™ R-635 as the carrier material.

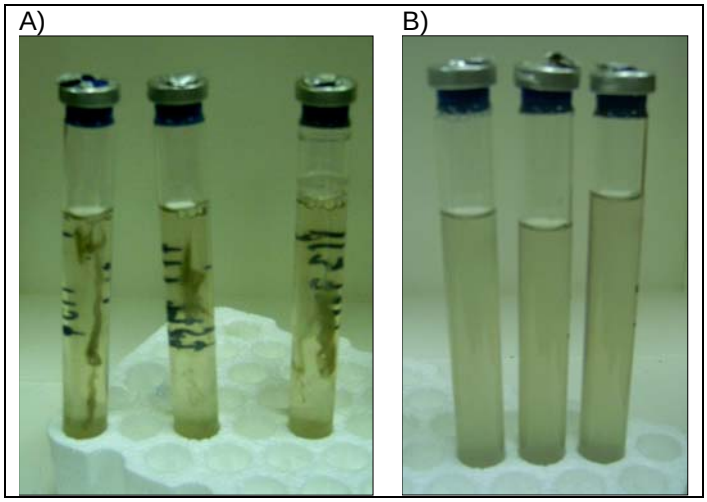


**Figure 5.6:** *Desulfovibrio desulfuricans* (A) and SRB consortium (B) cultures grown under identical conditions. Detached biofilm 'streamers' are clearly visible in (A). The SRB consortium cultures contained only a small amount of floc particles that settled to the bottom of the tube (not visible).

Despite the absence of visible biofilm formation, the consortium was not expected to exhibit nearly negligible immobilization potential. The recent literature had reported the successful use of similarly enriched SRB consortia in packed bed bioreactors (Baskaran and Nemati, 2006; Alvarez et al., 2006). The low observed immobilization potential may have been a result of an insufficient circulation period. It was clear though that the consortium did not immobilize nearly as well as *Desulfovibrio desulfuricans.* In a manner similar to the trend observed in Figure 5.1, the addition of even small fractions of consortium to the inoculum was apparently sufficient for the consortium to become the dominant population, sharply decreasing the immobilization potential.

Sulfate reducing bacteria are well known to produce biofilms in their natural environment. Their tendency to adhere to surfaces allows them to be significant nuisances with regard to pipeline corrosion and clogging (Chen et al., 1994). This suggests that the environmental sample from which the consortium was enriched may have originally contained SRB with greater immobilization potential. The serial transfer enrichment process may have inadvertently selected for SRB with poor biofilm tendencies. Transfers were performed using syringes that collected suspended growth species rather than those attached to the glass surfaces. The serial transfer method also selected for kinetically superior species as previously demonstrated by the consortium's greater growth rates. Biofilm forming SRB may be at a disadvantage in this regard. An organism that directs a greater proportion of energy and carbon source towards extracellular products (e.g. EPS, biofilm) would have a slower growth rate to that of a competitor that devoted the majority its resources towards cellular replication.

Recognizing the consortium's poor immobilization capabilities, an attempt was made to re-enrich for kinetically superior SRB species with good attached growth properties. The original enrichment received from the University of Calgary was used to inoculate culture tubes containing PC media and packed with R-635 pellets. Several transfers failed to produce a consortium that exhibited similar biofilm properties to *Desulfovibrio desulfuricans* as measured qualitatively by observation and simple biofilm staining techniques. This failure was attributed to the Calgary consortium having already undergone four serial transfers that enriched for suspended growth species before its delivery to Queen's. The presence of increased surface area alone was also unlikely to enrich for biofilm producers, even if they had been present. In order to impose the correct selective pressure, enrichment should have occurred in a continuous flow reactor that would washout the suspended species while retaining the biofilm prone species. Furthermore, it is also unlikely that the addition of surface area to a closed system would induce a 'poor' biofilm producer to modify its phenotype. Christy (2001) observed similar results with an SRB consortium, similarly enriched from wastewater that exhibited poor immobilization potential in the presence of pall ring packing material.

The consortium's attached growth properties could not be readily improved, thus it was decided that an inoculum composition of approximately 5 % consortium and balance *Desulfovibrio desulfuricans* would be ideal for use in future PBR fermentations, the rationale being that the initial establishment of a substantial biofilm foundation in a packed bed is vital to stable bioreactor operation. The EPS produced by the

*Desulfovibrio desulfuricans* biofilm foundation would serve to immobilize the rapidly growing consortium. Continuous flow conditions would then naturally select for the optimal balance between the slower growing *Desulfovibrio desulfuricans* and the faster growing consortium. This hypothesis was confirmed qualitatively by inoculating a serum bottle culture with a sample from a PBR after 11 d of operation with an initial ~5% consortium inoculum. The serum bottle culture exhibited sulfate reducing activity, but did not form the characteristic biofilms of *Desulfovibrio desulfuricans*, suggesting it was no longer the dominant species.

In summary, it was found that while the consortium had superior kinetics its immobilization potential was relatively poor. Literature studies that used similarly enriched cultures have reported extended bioreactor startup times which may be due in part to the poor immobilization potential of their suspended growth enriched consortia. Carrier material evaluation is a common method of improving packed bed bioreactor design and Celite™ R-635 diatomaceous earth pellets were found to have the best performance of the materials tested. Rational design of an inoculum containing both kinetically favoured and attached growth (biofilm) prone species is a novel approach to SRB bioprocess improvement and may offer significant advantages with regards to decreasing bioreactor startup time and increasing volumetric productivities.

## 5.4 PBR Fermentation #1

The first continuous PBR experiment was conducted to characterize the system behaviour, evaluate its response to step changes in the feed rate, and obtain high volumetric productivities with a minimal start-up period. Volumetric productivity was calculated based on the TDS concentration at port 3 (bioreactor outlet), the liquid feed rate, and total reactor volume (615 mL). The volumetric productivity-time course plot is shown in Figure 5.7. Concentration-time course plots for the bioreactor's three sampling ports are shown in Figure 5.8.

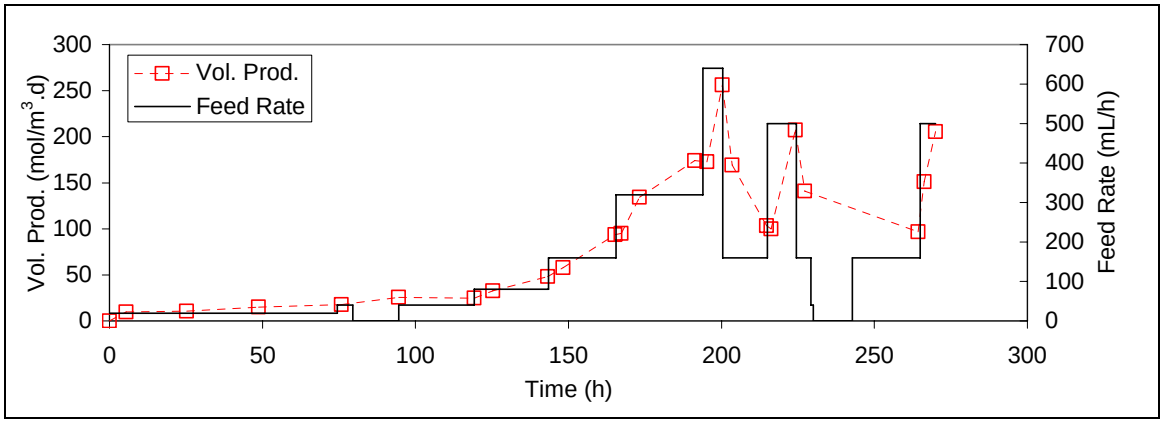


**Figure 5.7:** Volumetric sulfide productivity-time course plot for PBR fermentation #1.

Figure 5.7 shows that an increase in the liquid feed rate ($L$, ml/h) was accompanied by a proportional increase in the volumetric productivity. The direct relationship between volumetric productivity and feed rate was due to the bioreactor's ability to maintain relatively stable substrate, product, and suspended biomass concentrations despite changes to the feed rate.

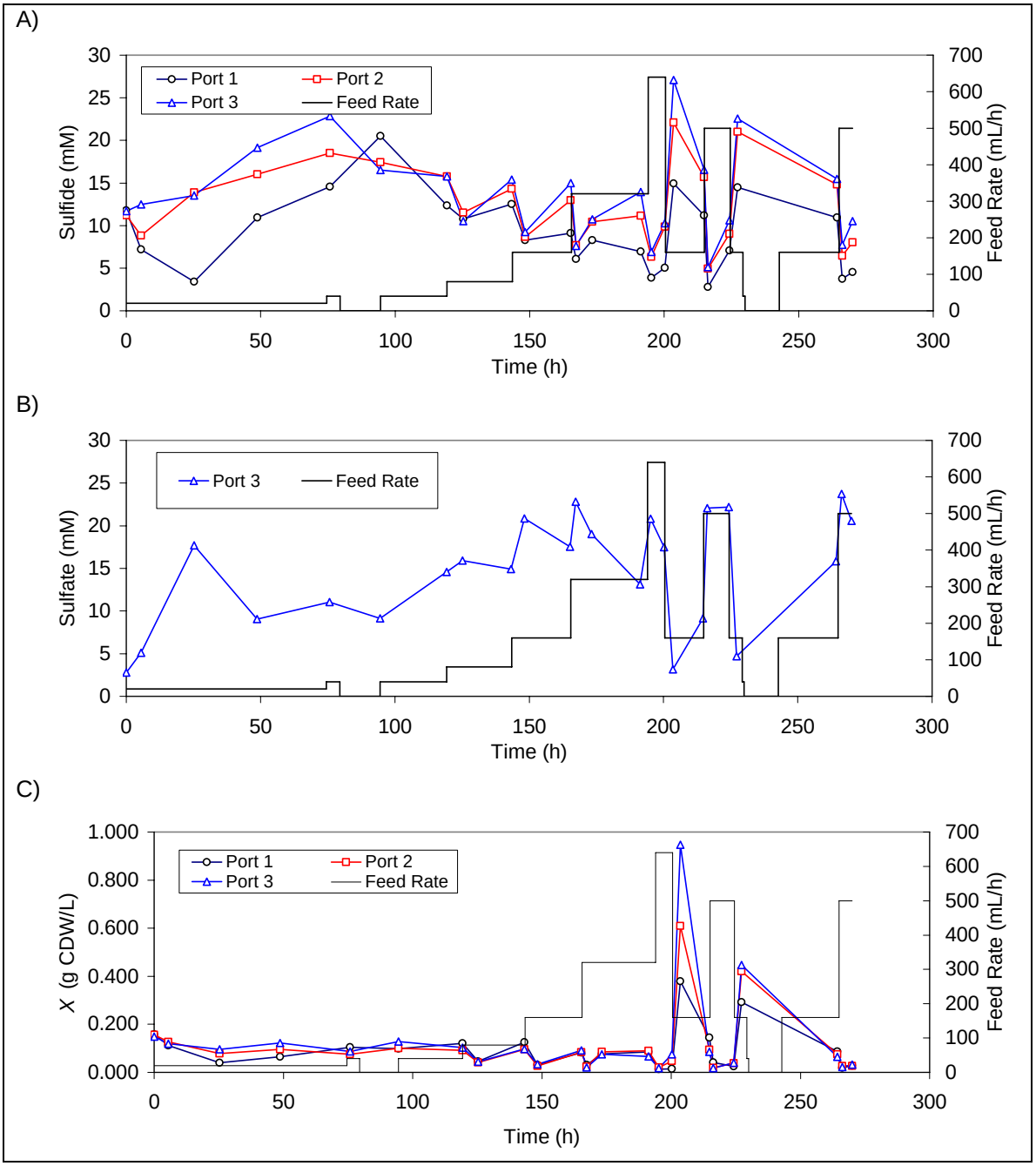


**Figure 5.8:** Concentration-time course plot for total dissolved sulfide (A), sulfate (B), and suspended biomass (C) concentrations for PBR fermentation #1. Port 3 corresponds to the reactor's outlet.

Figure 5.8 shows that as step increases were made to the feed rate, the product (TDS and suspended biomass) concentrations decreased briefly and the substrate (sulfate) concentration increased briefly. These transient responses were due to the minor dilution effect of increasing the feed rate. After a few column volumes had passed, steady-state concentrations were re-established. The behaviour of the PBR could be described in some respects as analogous to a chemostat stirred tank bioreactor. Whereas a chemostat responds to feed fluctuations by regulating its suspended biomass concentration to maintain constant substrate/product concentrations, the PBR likely regulated its immobilized biomass inventory to maintain state-state conditions. The PBR differed from the chemostat in that the steady-state TDS concentration always approached the inhibitory range (15-20 mM) and was practically independent of the feed rate. In contrast, the steady-state concentrations in a chemostat are a function of the feed rate at conditions that approach washout ($D = \mu$).

The TDS product concentration profile increased along the length of the bioreactor (Figure 5.8A). Likewise the sulfate substrate concentration decreased along the length of the bioreactor, behavior typical of a PBR configuration. The TDS concentration profile indicated that the majority of the biological activity was occurring within a small portion of the bioreactor between the inlet and the first sampling port. By the time the liquid had reached the first sampling port, the TDS concentration had reached at least 50 % of the final exiting concentration. The upper two-thirds of the bioreactor were thus only contributing marginally to total product formation and represented an inefficient use of bioreactor volume under the evaluated operating conditions. Chen et al. (1994) observed

similar results in their sand packed SRB PBR. Daugulis and Swaine (1987) presented a model that predicted identical behaviour for an ethanol inhibited PBR system. As product concentration increases along the length of the bioreactor, kinetic rates and conversion efficiency are expected to decrease rapidly. The highest immobilized biomass concentrations would thus be expected at the bioreactor inlet where substrate concentrations are high and product inhibition is minimal. In densely packed systems it is not uncommon for excessive microbial overgrowth to lead to clogging and pressure drops across the column (Daugulis et al., 1985).

Concomitant spikes in the suspended biomass and TDS concentrations were observed after large decreases to the feed rate were imposed at ~200 h and ~230 h. The spike in TDS concentration was attributed to transient product accumulation due to the decrease in the feed (dilution) rate. The increase in suspended biomass however was considered too great to be attributed solely to product biomass accumulation. Adverse bioreactor conditions may have induced partial biofilm sloughing although this link was uncertain and the subject of further investigation in the second PBR fermentation.

Experimental conditions in the first PBR fermentation were such that bioreactor clogging was not an issue and biofilm coverage of the R-635 pellets was apparent as dark discolourations on the packing material near the bioreactor inlet. The assumption that the first third of the bioreactor length contained a disproportionately high concentration of immobilized biomass that was responsible for the majority of biological activity was confirmed by SEM analysis. Figure 5.9, Figure 5.10, and Figure 5.11 are typical SEM

images of R-635 pellets taken from the inlet, middle, and outlet of the bioreactor after an 11 d fermentation. The R-635 from the inlet was covered in a dense layer of bacterial cells and the carrier surface was barely visible. R-635 pellets from the middle of the reactor were observed to have clusters of immobilized cells but did not have the layered topology of inlet pellets' biofilm. The majority of the carrier surface was bacteria free. R-635 pellets from the bioreactor's outlet had the least amount of immobilized biomass and only a few scattered bacteria were observed on the carrier surface. These observations were consistent with the assumption that bioreactor inlet had the most favourable growth conditions and as a result the most immobilized biomass.

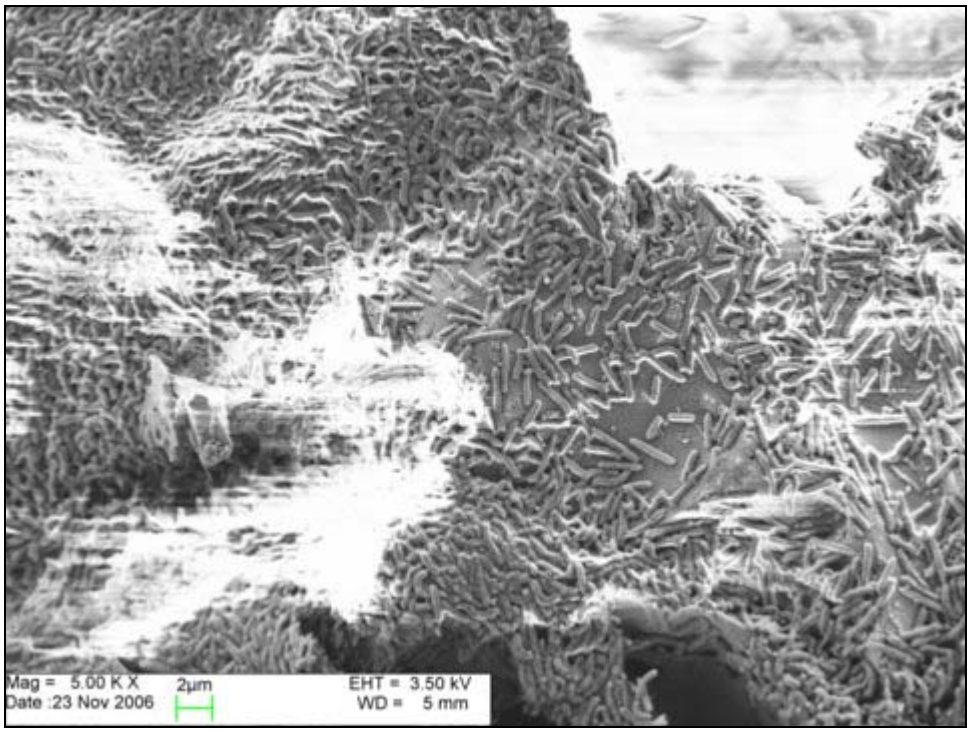


**Figure 5.9:** Scanning electron micrograph (5000x) of the surface of a Celite™ R-635 pellet retrieved from the bioreactor inlet after an 11 d fermentation. Scale bar shows 2 $\mu$m.

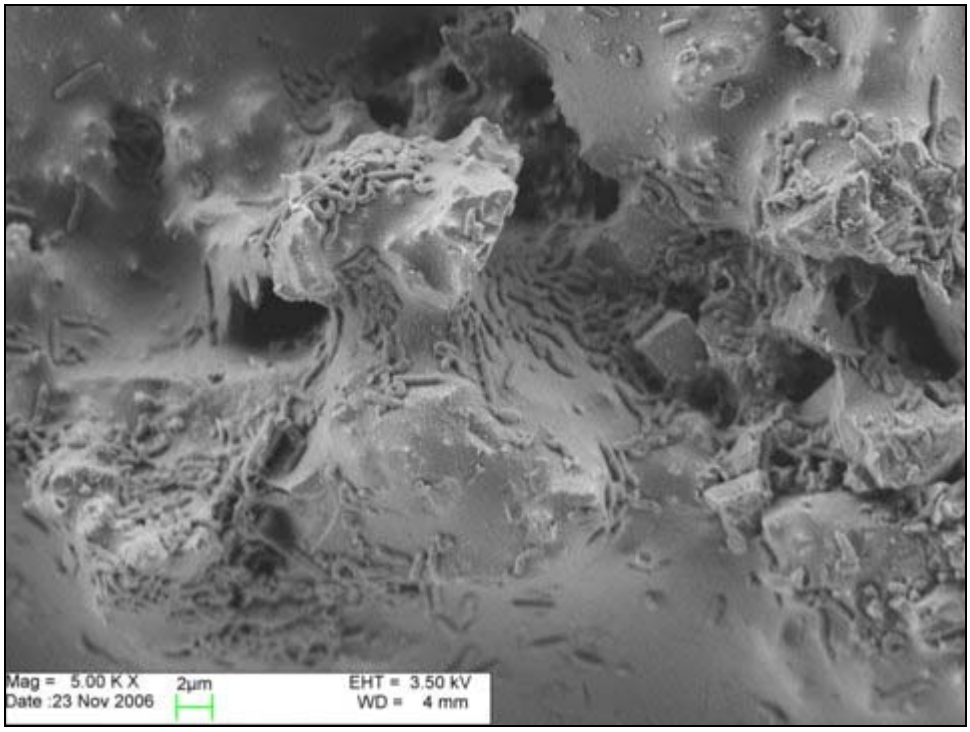


**Figure 5.10:** Scanning electron micrograph (5000x) of the surface of a Celite™ R-635 pellet retrieved from the midpoint of the bioreactor after an 11 d fermentation. Scale bar shows 2 $\mu$m.

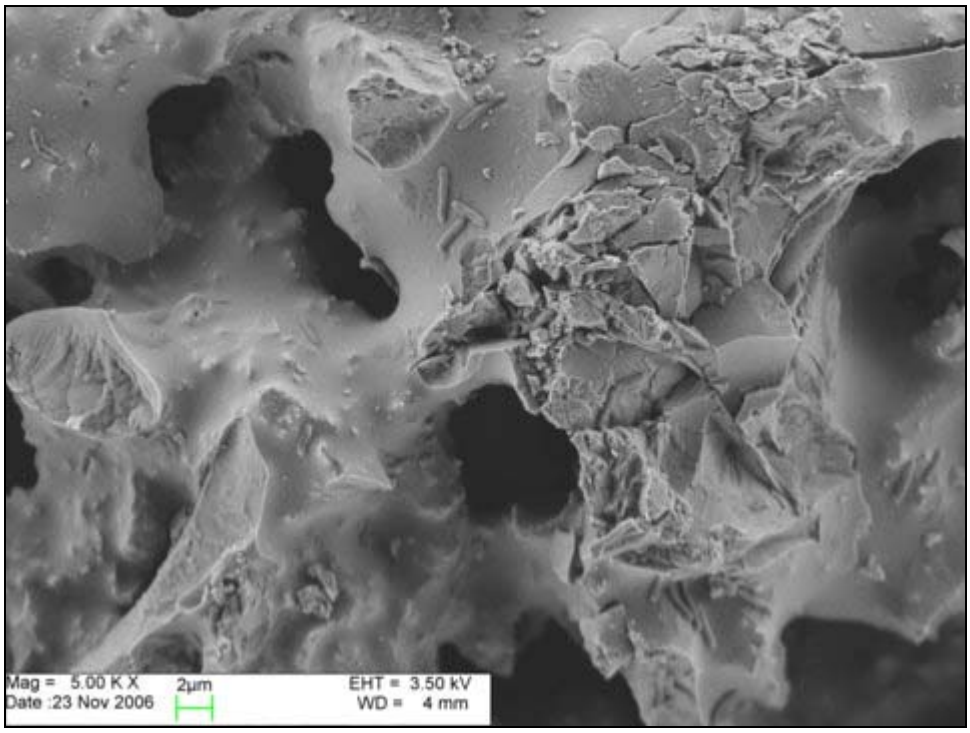


**Figure 5.11:** Scanning electron micrograph (5000x) of the surface of a Celite™ R-635 pellet retrieved from the bioreactor outlet after an 11 d fermentation. Scale bar shows 2 $\mu$m.

As noted previously, the TDS concentration profile increased along the length of the bioreactor. This pattern was consistently observed except after the bioreactor had been briefly shutdown for 15 h (after ~80 h of fermentation time). After the shutdown a reverse profile was observed (highest TDS concentration near the inlet). This phenomenon was due to the PBR behaving essentially as a series of static batch reactors with concentrations of biomass (i.e. biocatalyst) decreasing from bottom to top. After the liquid feed had been resumed and a few column volumes had passed, the typical concentration profile associated for a continuous flow regime was re-established.

The highest volumetric productivity for the bioreactor was observed when the feed rate was at its highest value ($L$ = 640 mL/h; HRT = 0.63 h; $D$ = 1.6 $h^{-1}$; $t$ = 200 h ≈ 8 d). At these conditions the volumetric productivity based on the outlet (port 3) concentration was 257 $mol/m^3.d$. The TDS concentrations at the second and third ports were 9.9 and 10.3 mM respectively. If only the first half of the bioreactor is considered, the calculated volumetric productivity increases to 493 $mol/m^3.d$. These volumetric rates are comparable to the highest values reported in literature (Table 5.3) and occurred at TDS concentrations close to the inhibitory concentration range (15-20 mM). Had the bioreactor been allowed to operate longer at 640 mL/h it is likely that higher volumetric productivities would have been obtained due to the TDS concentration approaching 20 mM. Continuous operation at this feed rate was not feasible due to the excessive volumes of media required. This was a limitation of laboratory logistics and not intrinsic to the bioreactor system.

While the highest volumetric productivity achieved in this experiment was below the highest value reported in literature [(493 mol/$m^3$.d) < (677 mol/$m^3$.d)] it is important to consider the conditions under which these values were obtained. The high volumetric productivities obtained by Stucki et al. (1993) and Selvaraj et al. (1997) were achieved using more elaborate PBR systems that included recycle loops and online pH controllers. This study was able to achieve comparable volumetric productivities using a simple PBR configuration without an external pH control loop and a drastically reduced startup period of 8 d compared to 150 d for the case of the highest literature value. Growth medium and temperature variation may be partially responsible for the differences in system performance but it is more likely that the use of a superior carrier material (Celite™ R-635) and critical inoculum design were the key factors that improved biomass retention and overall bioreactor performance. Baskaran and Nemati's (2006) experience with a similar system further supports this hypothesis. Their suspended growth enriched consortium was not supplemented with an SRB species prone to biofilm formation and their packing materials lacked a microporous structure. Despite operating under otherwise similar conditions over several months they were only able to achieve volumetric productivities between 3-57 mol/$m^3$.d.

**Table 5.3:** Summary of relevant volumetric productivities reported in literature for sulfate reducing bioreactors.

| Carbon Substrate | HRT (h) | Carrier Material | Temp. ($^{o}$C) | Volumetric Productivity (mol/m$^3$.d) | Reference |
|---|---|---|---|---|---|
| acetate | not reported | polyurethane foam | 35 | 576 | Stucki et al., 1993 |
| acetate | not reported | sintered glass beads | 35 | 677 | Stucki et al., 1993 |
| **lactate** | **0.63** | **Celite™ R-635** | **38** | **257** | **This study** |
| **lactate** | **0.32** | **Celite™ R-635** | **38** | **493** | **This study** |
| anaerobically digested municipal sewage solids | 3.4 | BioSep™ activated charcoal impregnated polymer | 30 | 456 | Selvaraj et al., 1997 |
| lactate | 0.5 | sand | 22 | 57 | Baskaran and Nemati, 2006 |
| lactate | 5.3 | scouring pad foam | 22 | 29 | Baskaran and Nemati, 2006 |
| lactate | 28.6 | glass beads | 22 | 3 | Baskaran and Nemati, 2006 |

## 5.5 PBR Fermentation #2

The first PBR fermentation showed that the bioreactor system was capable of high volumetric productivities within a relatively short startup period. The objectives of the second PBR fermentation were to evaluate sustained operation at a high feed rate ($L$ = 250 mL/h; HRT = 1.6 h; $D$ = 0.63 h$^{-1}$), evaluate the ability of the bioreactor to recover from a 24 h shutdown, and to further investigate the relationship between adverse bioreactor conditions and biofilm sloughing. The volumetric productivity-time course plot is shown in Figure 5.12. Concentration-time course plots for the bioreactor's three sampling ports are shown in Figure 5.13.

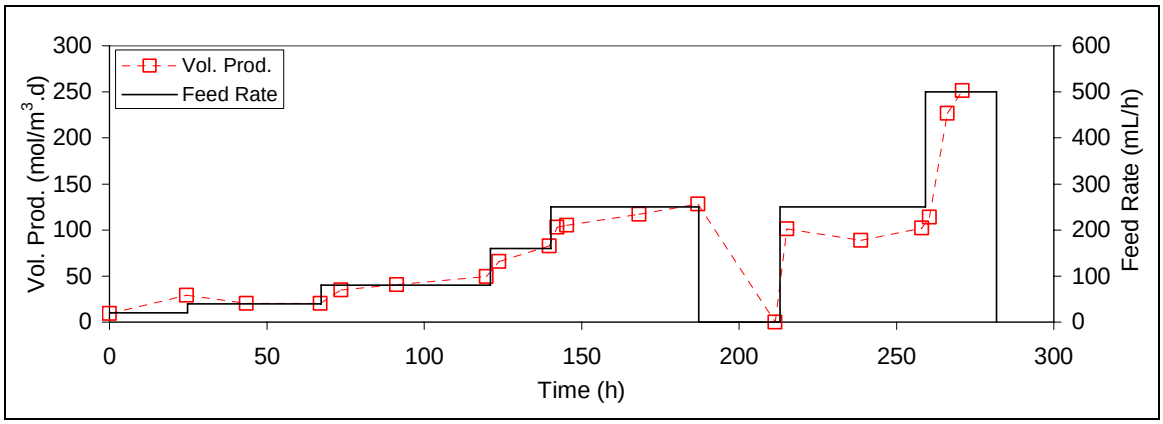


**Figure 5.12:** Volumetric sulfide productivity-time course plot for PBR fermentation #2.

Figure 5.12 shows a similar trend to the first PBR fermentation where changes in the liquid feed rate result in proportional changes to volumetric productivity. At the highest feed rate (500 mL/h) the volumetric productivity based on the port 3 TDS concentration was 252 mol/$m^3$.d. Volumetric productivity based on a half reactor volume and port 2 TDS concentration was 448 mol/$m^3$.d. By operating the bioreactor for a longer period at 500 mL/h, the TDS concentrations were closer to the inhibitory range than in the first PBR fermentation when the bioreactor was operated for a shorter period at 640 mL/h. Due to the increased TDS concentrations in the second PBR fermentation, comparable volumetric productivities were achieved at lower feed rates. In either case, TDS concentrations would likely have increased to the 15-20 mM range given sufficient time but extended operation at these high flowrates was not feasible due to laboratory logistics.

**Table 5.4:** Summary of highest volumetric productivities observed for PBR fermentations #1 and #2.

| PBR Fermentation | *L*, Feed Rate (mL/h) | Port 2 TDS Conc. (mM) | Port 2 Vol. Prod. (mol/$m^3$.d) | Port 3 TDS Conc. (mM) | Port 3 Vol. Prod. (mol/$m^3$d.) |
|---|---|---|---|---|---|
| #1 | 640 mL/h | 9.9 | 493 | 10.3 | 257 |
| #2 | 500 mL/h | 11.5 | 448 | 12.9 | 252 |

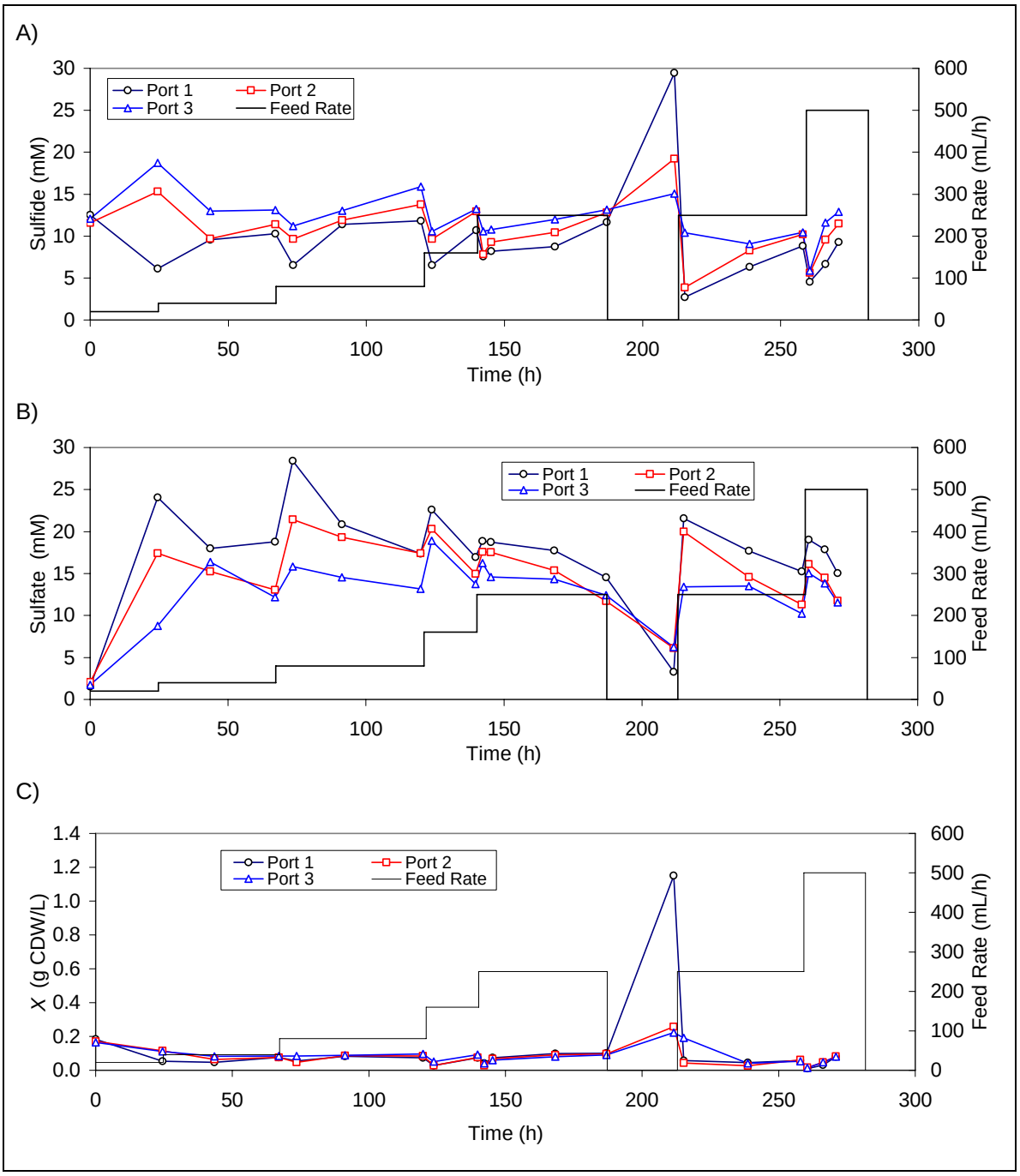


**Figure 5.13:** Concentration-time course plot for total dissolved sulfide (A), sulfate (B), and suspended biomass (C) concentrations for PBR fermentation #2. Port 3 corresponds to the bioreactor's outlet.

Concentrations profiles in the second PBR fermentation were similar to those observed in the previous fermentation. Sustained operation at a relatively high feed rate of 250 mL/h showed relatively stable TDS and sulfate concentration profiles. After the transient TDS decrease due to increasing the feed from 160 mL/h to 250 mL/h at 140 h, the TDS concentration slowly reestablished a relatively steady value near the inhibitory range. At 250 mL/h the equivalent dilution rate was 0.63 $h^{-1}$, nearly twice the commonly reported $\mu$ values at non-inhibited growth conditions (Okabe et al., 1992; Konishi et al., 1996) and over four times the observed $\mu$ values observed experimentally in the kinetics experiments. The sustained operation at this dilution rate for the equivalent of 30 column volumes confirmed the system's ability for biomass retention and that the majority of the biological activity was due to immobilized rather than suspended biomass.

After 187 h of continuous operation, the bioreactor was shutdown. The liquid feed was halted and the bioreactor was allowed to cool to ambient temperature. After 24 h, sulfate and TDS concentrations were measured at each port (Figure 5.13A, B). Sulfate concentrations were found to have been reduced to approximately 5 mM along the entire column, indicating complete conversion of the stoichiometric limiting lactate carbon source. Very high TDS concentrations of 30, 19, and 15 mM at the inlet, middle, and outlet respectively were observed. The decreasing TDS profile along the bioreactor length was similar to that observed in the first fermentation after a shutdown period. In both cases this was attributed to the immobilized biomass concentration profile that also decreased along the bioreactor length.

The combination of substrate depletion and highly inhibitory TDS concentrations produced an adverse environment for the immobilized biomass. During continuous bioreactor operation the steady-state suspended biomass concentration had an upper limit of 0.100 g CDW/L. After the 24 h shutdown period, suspended biomass concentrations at the inlet, middle, and outlet ports were 1.515, 0.258, and 0.225 g CDW/L respectively. This represents a considerable increase in the suspended biomass that cannot be due to synthesis alone and was likely due to biomass sloughing from the carrier material under the adverse conditions. Calculations were performed using synthesis yield coefficients ($Y_{X/S}$) obtained from earlier experiments and literature values to calculate the maximum concentration of biomass that could be produced in the case of complete substrate utilization (Table 5.5).

**Table 5.5:** Maximum theoretical suspended biomass concentrations assuming complete conversion of substrate to biomass according to the equation [$X = (Y_{X/S})(S_0)$]. The initial sulfate concentration is 32 mM but only 27 mM can be reduced due to a stoichiometric limiting amount of lactate.

| $Y_{X/S}$ **Synthesis Yield Coefficient** | $S_0$ **Initial Substrate Concentration** | $X$ **Theoretical Maximum Biomass Concentration (g CDW/L)** |
|---|---|---|
| 0.11 g CDW/g $SO_4$ (from this study) | 2.60 g/L, (27 mM) $SO_4$ | 0.286 |
| 0.03 g CDW/g lactate (Okabe et al., 1995) | 4.86 g/L, (54 mM)lactate | 0.146 |

Table 5.5 shows that even if all the substrate present in the bioreactor were converted to biomass during the shutdown period, it would not be sufficient to account for the measured concentrations. The calculated values are considered conservative estimates. The biomass yields under the given conditions would likely have approached 0 due to the highly inhibitory sulfide concentration that would have exerted considerable maintenance energy requirements. These calculations suggest that the combination of high sulfide

concentration and substrate limitation had an adverse effect on the system and induced considerable sloughing of immobilized biomass.

To test the bioreactor's robustness and ability to recover from the shutdown, the feed rate was resumed at the previous value of 250 mL/h ($t$ = 213 h, Figure 5.12). The bioreactor rapidly recovered and within 48 h the volumetric productivity had returned to 102 mol/$m^3$.d with an outlet TDS concentration of 10.5 mM (both 80 % of the pre-shutdown values). The bioreactor was operated at 250 mL/h for 46 h (29 column volumes) and then was further challenged by doubling the feed rate to 500 mL/h for a further 23 h (28 column volumes). The bioreactor adapted successfully and achieved a volumetric productivity of 448 mol/$m^3$.d as described in Table 5.4. The observed robustness of the system and swift recovery after shutdown was remarkable. After experiencing such adverse conditions and considerable loss of biomass it was thought that restoration of the feed rate to 250 mL/h may have led to complete biomass washout or at least require a longer, more gradual recovery process. The system's rapid 48 h recovery and subsequent feed rate doubling highlighted the bioreactor's capacity for biomass immobilization and ability to sustain microbial growth under adverse conditions. The resiliency of the biomass to TDS concentrations well beyond the known inhibitory level (30 mM) may be due partially to the consortium enrichment method that continuously exposed the transfers to high TDS concentrations as previously discussed.

In summary, two PBR fermentations were conducted to characterize the system behaviour and achieve high rates of volumetric sulfide production. It was found that the

majority of the immobilized biomass and thus most of the biological activity was located within the first third of the bioreactor. The bioreactor was able to respond to changes in feed rates by adjusting its biomass inventory to maintain relatively constant TDS concentrations near the inhibitory level of approximately 15 mM. The combination of a superior carrier material (Celite™ R-635) and critical inoculum design resulted in excellent biomass immobilization. This facilitated rapid bioreactor startup, achievement of high volumetric productivities, and the ability to recover from shutdown periods concomitant with highly adverse conditions of substrate depletion and sulfide inhibition. This relatively simple bioreactor system was able to achieve volumetric productivities comparable to more complex systems reported in the literature while requiring a startup period on the scale of 10 d rather than 100 d (Stucki et al., 1993; Selvaraj et al., 1997; Baskaran and Nemati, 2006).

## 5.6 PBR Fermentation #3

The objective of the third PBR fermentation was to characterize the system behaviour while operating with an $N_2$ strip gas. The sulfide product does not readily transfer to the gas phase due to its high aqueous solubility. This was observed experimentally and reported in the literature under similar conditions (Baskaran and Nemati, 2006; Alvarez et al., 2007) where practically all the sulfide product was measured in the dissolved phase. A strip gas was therefore considered an essential element of product recovery. $CH_4$ in comparison is highly insoluble ($H_{CH4}$ = 37,600 atm @ 20 $^{o}$C) and is easily recovered as a gas phase product without the need for additional stripping. $CH_4$ saturation concentrations (1.5 mM, 18 mg/L) are readily achieved as $CH_4$ is not inhibitory to anaerobic bacteria. In contrast, $H_2S$ is roughly two orders of magnitude more soluble in

solution ($H_{H2S}$ = 483 atm @ 20 $^{o}$C). Due to its inhibitory nature, biologically produced dissolved sulfide concentrations have an upper limit of about 20 mM (640 mg/L), far below the saturation concentration of 115 mM (3910 mg/L). pH effects further hinder $H_2S$ recovery since at biologically favourable pH values (6-8) significant fractions of dissolved sulfides are present as the non-strippable ion $HS^-$ (Figure 2.4).

The results of the PBR fermentation with a constant feed rate ($L$ = 80 mL/h) and a varying $N_2$ ($G$, mL/min) flow rate are shown in Figure 5.14. Strip rates were reported as the normalized volumetric stripping ratio $G/L$ ($m^3/m^3$).

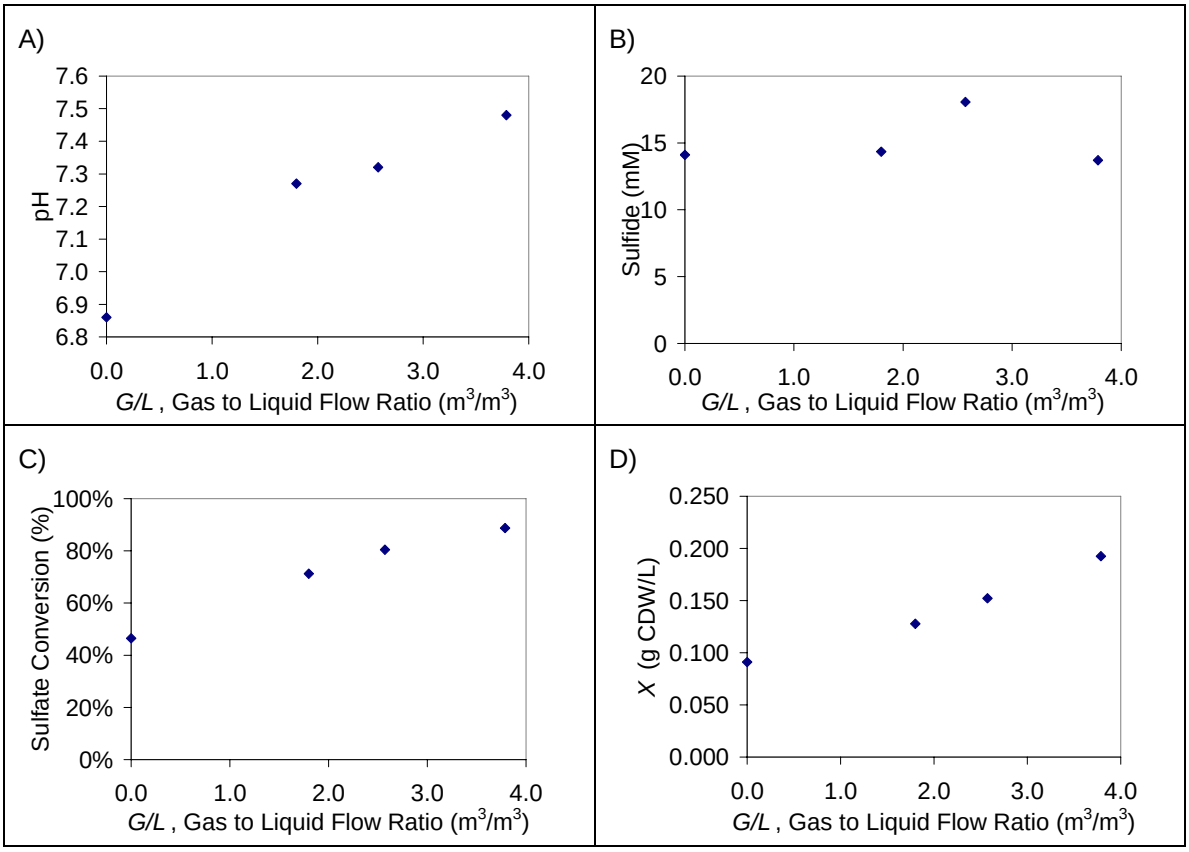


**Figure 5.14:** Results of a PBR experiment at constant liquid flow (80 mL/h) and a varying $N_2$ strip gas flow rate (reported as a normalized *G/L* ratio). pH (A), total dissolved sulfide (B), sulfate conversion (C), and suspended biomass concentration (D) were measured at port 3 (outlet) of the bioreactor.

A direct relationship between *G/L* and the effluent pH was observed (Figure 5.14A). Even in the absence of stripping a rise in pH from an initial value of 6.50 to 6.86 was observed. This intrinsic pH increase was due to the production of bicarbonate by SRB. Adding a strip gas to the system had a twofold effect on increasing the pH. First, the removal of the inhibitory sulfide product increased sulfate conversion (Figure 5.14C) which was concomitant with increased metabolic activity and bicarbonate production. Secondly, the removal of $CO_2$ and $H_2S$ from the system shifted the equilibrium relationships shown in Equations (16) and (17) to the right, resulting in free proton consumption.

$$HCO_3^- + H^+ \leftrightarrow H_2CO_3 \leftrightarrow H_2O + CO_2 \quad (16)$$

$$HS^- + H^+ \leftrightarrow H_2S \quad (17)$$

The TDS concentration remained relatively constant in the inhibitory range of 15-20 mM (Figure 5.14B) despite large increases in the sulfate conversion from 47 % to 89 % (Figure 5.14C). The additional sulfide that was produced was later confirmed to be leaving the bioreactor with the strip gas. The molar ratio of TDS to sulfate was 0.95 mol/mol in the absence of stripping. This confirmed that without the $N_2$ strip gas, the majority of the sulfide product remained in the dissolved phase.

It was assumed that the increase in conversion (i.e. metabolic activity) was due to a similar increase in immobilized biomass. Although the suspended biomass had a minor contribution to the overall metabolic activity, it was used as an indicator of the amount of immobilized biomass present. The basis for this correlation was that when operating at washout conditions ($D > \mu$) suspended cells are overwhelmingly due to steady-state sloughing rather than suspended cell replication. It would then be anticipated that an increase in immobilized biomass would be accompanied by a proportional increase in the steady-steady sloughing. Figure 5.14C,D shows this direct relationship between *G/L*, conversion, and suspended biomass concentration.

Additional *G/L* ratios were evaluated and gas phase samples were analyzed to confirm that the increase in reduced sulfate could be attributed to the removal of sulfide as $H_2S_{(g)}$ in the strip gas. Table 5.6 shows the relative partitioning of total sulfides ($H_2S_{(g)}$, $H_2S_{(aq)}$, $HS^-_{(aq)}$) between the dissolved and gas phases and the ratio between total sulfide produced

and sulfate reduced.

**Table 5.6:** Results of a PBR experiment with stripping at various *G/L* ratios and the resulting partitioning of sulfide between dissolved and gas phases. The molar sulfur mass balance is also reported as total sulfide produced per sulfate reduced (mol/mol).

| ***L*** **(mL/h)** | ***G*** **(mL/min)** | ***G/L*** **($m^3/m^3$)** | **Fraction of Total Sulfides in Dissolved Phase ($H_2S_{(aq)}$, $HS^-_{(aq)}$)** | **Gas Phase $H_2S$ Conc. (mol %)** | **Total Sulfide Produced/Sulfate Reduced (mol/mol)** |
|---|---|---|---|---|---|
| 80 | 5.1 | 3.8 | 0.82 | 2.7 | 0.93 |
| 40 | 1.7 | 2.5 | 0.81 | 5.0 | 0.94 |
| 40 | 1.7 | 2.5 | 0.85 | 3.7 | 0.85 |
| 40 | 4.1 | 6.2 | 0.66 | 3.3 | 0.86 |

The composition of the strip gas varied within the range of 2.7-5.0 mol % $H_2S$. This composition range matched well with the equilibrium $H_2S$ partial pressures calculated to be 2.7-7.0 mol % $H_2S$ for the experimental conditions assuming $P_T$ = 1 atm. At the *G/L* values evaluated, the majority (66-85 %) of the total sulfide produced remained in the aqueous phase. Most of the reduced sulfate could be accounted for in the total sulfide produced (86-94 %). The small amount of unaccounted sulfide was attributed to the product's volatile and reactive nature which may have resulted in some losses during handling of the liquid and gas samples despite attempts to minimize such losses. Small amounts of sulfur species may also have been incorporated into biomass and/or formed metal sulfide precipitates (e.g. FeS) that were responsible for black discolouration of the biofilm. Baskaran and Nemati (2006) also reported that measured sulfate reduction rates were up to 15 % greater than measured sulfide production rates using a similar PBR system. Volumetric sulfide production rates are thus considered the conservative approach to reporting volumetric productivity.

## 5.7 Basic Model for PBR Operation with Stripping

The third PBR fermentation suggested that a strip gas could improve volumetric productivity by increasing the bioreactor's sulfate conversion. A simple model (Appendix D) was created that calculated bioreactor volumetric productivity based upon assumed values for the liquid feed, gas strip rate, temperature, pH, and a constant effluent TDS concentration of 20 mM. The assumption of a constant TDS concentration of 20 mM was based on previous observations that the system was capable of adjusting its biomass inventory to maintain the sulfide concentration in the inhibitory range despite changes in operating conditions. The purpose of the model was to evaluate the effect of pH and *G/L* ratios on volumetric productivity and sulfide product partitioning. The results of a simulation for a 600 mL void volume PBR operating at a constant liquid feed rate of 80 mL/h are shown in Figure 5.15 and Table 5.7. Volumetric sulfide production was calculated using the total bioreactor volume. *G/L* values from 0 to 3.8 and pH values from 6 to 8 were evaluated.

**Table 5.7:** Distribution of 20 mM total dissolved sulfide and the equilibrium $H_2S$ partial pressure at 37 $^oC$ for the pH range 6-8.

| | | TDS Distribution | | |
|---|---|---|---|---|
| **pH** | **TDS (mM)** | **$HS^-_{(aq)}$ (mM)** | **$H_2S_{(aq)}$ (mM)** | **$P_{H2S}$ (atm)** |
| 6 | 20 | 3.6 | 16.6 | 0.21 |
| 7 | 20 | 13.6 | 6.4 | 0.08 |
| 8 | 20 | 19 | 1 | 0.01 |

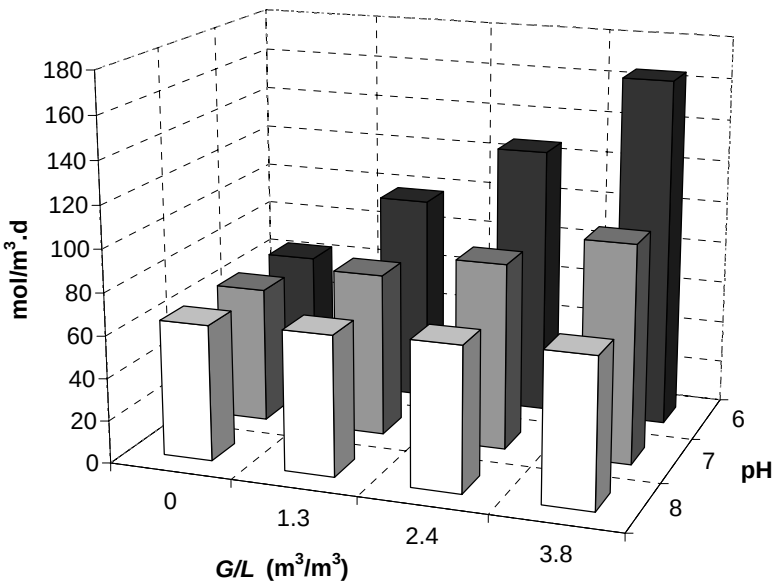


**Figure 5.15:** Predicted volumetric sulfide production (mol/$m^3$.d) for a PBR with reactor volume of 600 mL and liquid feed rate of 80 mL/h. Effluent conditions were assumed to be 37 $^oC$ and 20 mM TDS. *G/L* is the ratio of strip gas to liquid feed. Volumetric productivities were calculated using total reactor volume.

The results of the simulation illustrate the importance of pH on stripping effectiveness. At pH 8, the majority (95.6 %) of dissolved sulfides are in the non-strippable $HS^-_{(aq)}$ form. An increase in the *G/L* ratio from 0 to 3.8 at pH 8 results in a small volumetric productivity change from 64 to 70 mol/$m^3$.d due to the difficulty with which the dissolved sulfide is stripped. At a pH of 6, the majority (82 %) of the dissolved sulfides are present in the strippable $H_2S_{(aq)}$ form. An increase in the *G/L* ratio from 0 to 3.8 now results in a large volumetric improvement from 64 mol/$m^3$.d to 165 mol/$m^3$.d. Operating at a pH of 6 rather than a pH of 8 not only increases the volumetric productivity, but also increases the partial pressure of $H_2S$ in the strip gas (Table 5.7).

## 5.8 PBR Fermentation Experiment #4

The objectives of the fourth PBR fermentation were to experimentally evaluate the effect of pH and higher *G/L* ratios on the bioreactor performance. Due to the anticipated increase in conversion at higher *G/L* ratios, the medium nutrient concentration was doubled to prevent substrate limitation as described in Methods and Materials. A phosphate buffer system was used to mitigate the pH increases that were observed in the previous fermentations. 153 mM of phosphate salts were used to buffer the medium to a pH of 6.1. During the fermentation it was observed that magnitude of the pH shift was roughly halved but not eliminated. For conditions at pH 7, the concentration of phosphate salts was increased to 208 mM which further reduced, but did not eliminate the pH shift. Observed pH changes operating at *G/L* ratios of 0 and 3 are shown in Table 5.8. Further increases in the phosphate salt concentrations were not attempted as the $K^+$ concentration was already approaching levels that may have imposed salt stress on the SRB.

**Table 5.8:** Observed changes in pH during the fourth PBR fermentation with potassium phosphate buffered media.

| *G/L* ($m^3/m^3$) | Initial pH | Effluent pH |
|---|---|---|
| 0 | 6.10 | 6.30 |
| 3 | 6.10 | 6.57 |
| 0 | 7.00 | 7.02 |
| 3 | 7.00 | 7.23 |

Figure 5.16A shows the effect of the *G/L* ratio on the sulfate conversion at various pH and liquid feed rates. Figure 5.16B shows the effect of the *G/L* ratio on the TDS concentration at the same pH and feed rates.

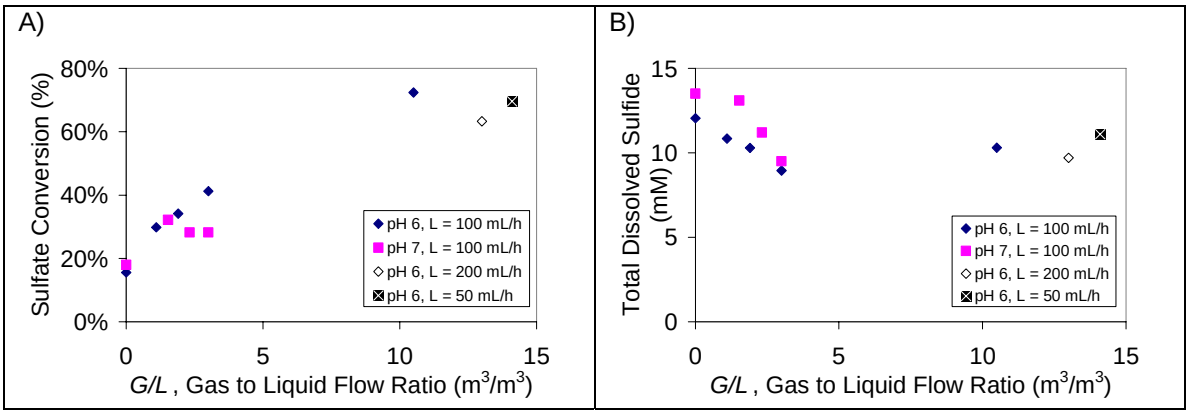


**Figure 5.16:** Results of a PBR fermentations at various feed rates and pH values showing the effect of *G/L* ratio on sulfate conversion (A) and total dissolved sulfide concentration (B). All measurements were based on port 3 (outlet) samples.

The trend observed in Figure 5.16A was that sulfate conversion (and thus volumetric productivity) was directly related to the *G/L* ratio as anticipated. The trend observed in Figure 5.16B was that the TDS concentration remained relatively constant in the range of 10-15 mM. Initially *G/L* ratios were evaluated between 0 and 3 but within this range the trends were somewhat ambiguous. *G/L* ratios as high as 14 were then evaluated to confirm the trends over a greater *G/L* range. For the *G/L* ratios between 10 and 15, different absolute feed rates were used (*L* = 50, 100, 200 mL/h). By evaluating similar *G/L* ratios at different absolute *G* and *L* values, *G/L* was confirmed to be a suitable dimensionless ratio for scaling the process.

The steady state TDS concentrations (Figure 5.16B) observed in this fermentation were slightly lower (10-15 mM) than those observed in previous fermentation experiments (15-20 mM). This trend was observed at both pH 6 and 7 and may have been due to modifications in the medium formulation. Depletion of the higher substrate concentrations (e.g. lactate) was accompanied by higher concentrations of acetate by-

product. Unlike the sulfide product that was being removed by the strip gas, the dissolved acetate accumulated in the liquid phase. Acetate in its undissociated form (acetic acid) is inhibitory to SRB (Reis et al., 1992) and may have had the net effect of decreasing the SRB's ability to cope with higher sulfide concentrations. Another factor that may have decreased the SRB's resistance to sulfide is the increased $Na^+$ and $K^+$ concentrations in the medium. Doubling the concentration of substrates (sodium lactate, $Na_2SO_4$) and extensive use of potassium phosphate buffers may had contributed to salt stress on the SRB. Lactate and sulfate substrates supplied 234 mM $Na^+$ and the phosphate buffer supplied at least 200 mM $K^+$ (depending on the pH value being buffered). Mukhopadhyay et al. (2006) reported significant inhibition effects of *Desulfovibrio vulgaris* (Hildenborough) at $Na^+$ and $K^+$ concentrations greater than 250 mM. Mukhopadhyay et al. (2006) also reported prominent elongation of the cell morphology under salt stress conditions. This phenomenon may explain the qualitative observation (by phase contrast microscopy) of greater numbers of elongated cells in samples taken from the bioreactor. Salt tolerance varies among SRB species however and since the composition of the consortium was unknown, it is difficult to gauge the full effect of salt stress on overall bioreactor performance. It is possible that acetate and salt stress both played a role in decreasing the SRB's sulfide resistance. Despite the small decrease in the steady-state TDS range, the bioreactor's ability to sustain TDS concentrations at stripping rates 14 times the liquid feed demonstrates the system robustness and potential for operation at higher rates.

According to previous simulation calculations, conversion at pH 6 should have been

higher than at pH 7. Experimentally this relationship was not clearly observed (Figure 5.16). The conversion trends at pH 7 could be interpreted as either being equal to or less than those at pH 6. The similarity in conversion may have been due to the pH shifts which had the net result of producing smaller differences in effluent pH (e.g. 6.57 v. 7.23) than desired. Despite these results, even if conversion (i.e. volumetric productivity) was independent between pH 6 and 7, there would still be a significant advantage to operating at pH 6 with regard to sulfide product recovery. As previously discussed, the lower pH values shift the dissolved sulfide equilibrium towards $H_2S_{(aq)}$ allowing for higher $H_2S_{(g)}$ partial pressures. This was confirmed experimentally. The average $H_2S$ composition of the strip gas was 5.8 mol % at initial pH 6 compared to 3.6 mol % at initial pH 7.

The PBR experiments with stripping were conducted by running the bioreactor continuously for a period of approximately 100 d at feed rates between 20 and 200 mL/h and strip gas rates as high as 43.5 mL/min ($G/L$ = 13 $m^3/m^3$). During the course of the fermentation visible accumulation of black biomass was observed along the bioreactor. The black biofilm was thickest at the reactor inlet and decreased along the bioreactor length. With such a large biomass accumulation and high gas strip rates there were concerns of biofilm shearing, increased backpressure due to clogging, and decreased biofilm-liquid mass transfer due to gas hold-up. Fortunately none of these issues was apparent during the course of the experiment, indicating the system had good long-term stability and the potential to operate at more aggressive flow conditions. The only notable problem with long-term operation was the inability to measure suspended

biomass concentrations. The usual method of obtaining liquid samples by syringe resulted in perturbation of the thick biofilm layers and contamination of the translucent colloidal suspended cell sample with thick, black, viscous biofilm.

The highest observed rate of volumetric sulfide production during the stripping fermentation experiments was 261 mol/$m^3$.d and occurred at the highest feed rate ($L$ = 200 mL/h) and a $G/L$ ratio of 13. Table 5.9 summarizes the operating conditions for the highest volumetric productivities (based on port 3 conditions) for the first, second, and fourth PBR fermentations. By doubling the feed concentration and using a strip gas to remove the sulfide product, higher conversions were achieved than previously possible. Had all the sulfide in the fourth fermentation remained in solution, the TDS concentration would have been 33 mM, well beyond the inhibitory range. The volumetric productivity attained in the fourth fermentation was nearly identical to values obtained in earlier fermentations but at a liquid feed rate of 200 mL/h rather than 500-640 mL/h. Operating at lower feed rates is desirable to minimize fluid shear and sloughing of the immobilized biomass.

**Table 5.9:** Summary of highest volumetric productivities (based on total reactor volume and port 3 outlet concentrations) from separate fermentations in this study. The volumetric productivity for the fourth fermentation accounts for both dissolved and gas phase sulfide product streams.

| PBR Fermentation | *L* (mL/h) | *G* (mL/min) | *G/L* ($m^3/m^3$) | $H_2S$ in Strip Gas (mol %) | Port 3 TDS Conc. (mM) | Port 3 Vol. Prod. (mol/$m^3$d.) |
|---|---|---|---|---|---|---|
| #1 | 640 | - | - | - | 10.3 | 257 |
| #2 | 500 | - | - | - | 12.9 | 252 |
| #4 | 200 | 43.5 | 13 | 4.5 | 9.7 | 261 |

The $G/L$ dimensionless ratio had been shown to be a suitable basis for scaling the process and if the conditions at a $G/L$ = 13 were scaled to a liquid feed of 640 mL/h, the resulting

productivity would be 835 mol/$m^3$.d. This value represents a 20 % increase over the highest volumetric productivity reported literature (Stucki et al., 1993). This was not attempted experimentally due to logistical limitations but all previous experience in this study suggested that such a scale-up was feasible.

In summary, PBR fermentation experiments were conducted using an $N_2$ strip gas for *in situ* removal of the sulfide product. The removal of the inhibitory product allowed for higher conversions and volumetric productivities to be achieved at lower feed rates than previously possible. Operating at the lower end of the biologically acceptable pH range (~6), increased the stripping effectiveness and the $H_2S$ composition of the strip gas. Long term, stable operation of the bioreactor at various *G/L* ratios suggests that further improvements in volumetric productivity are attainable with appropriate scale-up.

# Chapter 6: Sulfide Product Recovery Considerations

## 6.1 $H_2S$ and $CO_2$ Partitioning Simulation

The experimental portion of this study has shown that an $N_2$ strip gas is capable of recovering the dissolved sulfide product from the liquid to gas phase. Concomitant biological production of sulfide and carbonate species results in a strip gas containing $N_2$, $H_2S$, and $CO_2$. As a downstream gas separation unit operation will be necessary to purify the $H_2S$, it is desirable to have an estimate of the possible strip gas compositions over a range of temperature and pH values. An equilibrium closed system model was developed (Figure 6.1) to estimate gas phase composition by taking into account dissolved phase ionization and vapour-liquid equilibria relationships. The closed system was assumed to contain a fixed 100 mL liquid volume and a fixed 100 mL gas volume composed initially of $N_2$ at 1 atm. It was assumed that the $N_2$ was insoluble in solution. 20 mM of total sulfide species was assumed to be present with the stoichiometric amount of total carbonate species (40 mM). A closed system model was required to calculate the partitioning of species between fixed volume gas and liquid phases. The closed system model is considered an approximation of behaviour within an open bioreactor system with stripping occurring at equilibrium conditions. Equations describing the vapour-liquid equilibria and dissolved phase ionization equilibria within the range of typical operating conditions ($T$ = 10-50 $^{o}$C, pH = 6-8) formed the basis of the steady-state model as described below.

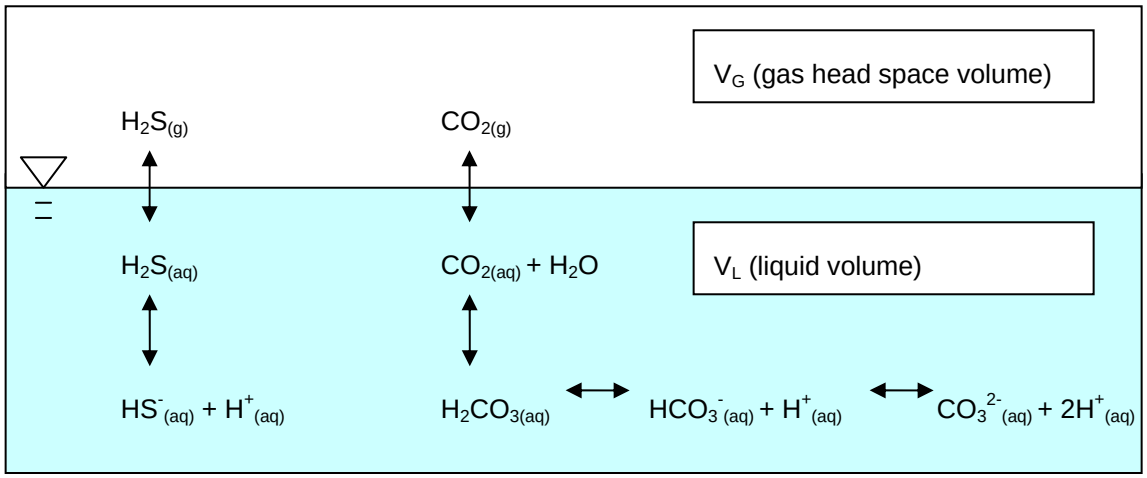


**Figure 6.1:** Diagrammatic representation of a closed system model describing sulfide and carbonate dissolved phase ionization and vapour-liquid equilibrium.

### 6.1.1 Sulfide Equilibrium

The sulfide equilibrium was described by a system of four equations. The four unknown values were molar quantity of each sulfide species ($H_2S_{(g)}$, $H_2S_{(aq)}$, $HS^-_{(aq)}$) and the partial pressure of $H_2S$ in the head space. Nomenclature is shown in Table 6.1.

**Table 6.1:** Nomenclature for sulfide equilibrium calculations.

| Parameter | Description | Units |
|---|---|---|
| $P_g$ | $H_2S$ gas partial pressure | atm |
| $H$ | Henry's constant | atm |
| $x$ | Mole fraction of total dissolved sulfides in solution | mol/mol |
| $n_g$ | Moles of gas phase $H_2S$ | mol |
| $n_d$ | Moles of dissolved $H_2S$ | mol |
| $n_{HS}$ | Moles of dissolved $HS^-$ | mol |
| $R$ | Universal gas constant | L.atm/mol.K |
| $T$ | Temperature | K |
| $V_G$ | Volume of gas head space | L |
| $V_L$ | Volume of liquid | L |
| $n_w$ | Moles of liquid (water) | mol |
| $[H^+]$ | Free proton concentration = $10^{(-pH)}$ | mol/L |
| $\alpha$ | Fraction of unionized ($H_2S$) dissolved sulfide | mol/mol |
| $K_a$ | First $H_2S$ dissociation constant | mol/L |

Henry's Law describes the relationship between the partial pressure of a gas ($P_g$) in equilibrium with its mole fraction ($x$) dissolved in solution. The dissolved gas was

assumed to sufficiently dilute such that $n_d << n_w$. Henry's Law then simplifies to Equation (19)

$$P_g = Hx = H\left(\frac{n_d}{n_d + n_w}\right) \cong H\left(\frac{n_d}{n_w}\right) \tag{18}$$

$$P_g - \frac{H}{n_w} n_d = 0 \tag{19}$$

The ideal gas law describes the number of moles of a gas that occupy a given headspace volume at a stated partial pressure [Equation (21)].

$$P_g = \frac{n_g RT}{V_G} \tag{20}$$

$$P_g - n_g \frac{RT}{V_G} = 0 \tag{21}$$

By conservation of mass in a closed system, the sum of moles of sulfide in the gas and dissolved phases is constant [Equation (22)].

$$n_g + n_d + n_{HS} = n_t \tag{22}$$

The dissolved sulfide equilibrium is described be Equation (25). The fraction (*frac*) of total dissolved sulfide that exists as $H_2S$ is proportional to temperature (via $K_a$) and inversely proportional to pH. Values of $K_a$ were obtained from tabulated data (Metcalf and Eddy, 2003).

$$K_a = \frac{[HS^-][H^+]}{[H_2S]} \rightarrow \frac{[HS^-]}{[H_2S]} = \frac{K_a}{[H^+]} \tag{23}$$

$$\alpha = \frac{n_d}{n_d + n_{HS}} = \left(\frac{[H_2S]}{[H_2S] + [HS^-]}\right)\left(\frac{[H_2S]^{-1}}{[H_2S]^{-1}}\right) = \frac{1}{1 + K_a/[H^+]} \tag{24}$$

$$n_d \frac{(1-\alpha)}{\alpha} - n_{HS} = 0 \tag{25}$$

The four equations [(19), (21, (22), and (25)] were arranged into a matrix of the form $Ax = b$ [Equation (26)]. Both sides of the equation were multiplied by the inverse of $A$. The four unknowns ($P_g$, $n_g$, $n_d$ and $n_{HS}$) were then solved using Microsoft Excel software.

$$A = \begin{bmatrix} 1 & 0 & -\frac{H}{n_w} & 0 \\ 1 & -\frac{(R)(T)}{V_G} & 0 & 0 \\ 0 & 1 & 1 & 1 \\ 0 & 0 & \frac{(1-\alpha)}{\alpha} & -1 \end{bmatrix} x = \begin{bmatrix} P_g \\ n_g \\ n_d \\ n_{HS} \end{bmatrix} b = \begin{bmatrix} 0 \\ 0 \\ n_t \\ 0 \end{bmatrix} \quad (26)$$

$$A^{-1}Ax = A^{-1}b$$

$$x = A^{-1}b$$

### 6.1.2 Carbonate Equilibrium

$CO_2$ exhibits equilibrium properties similar to $H_2S$ for gas-liquid systems. When dissolved, it theoretically is present as either dissolved $CO_{2(aq)}$ or hydrolyzed to carbonic acid ($H_2CO_3$):

$$CO_{2(aq)} + H_2O_{(l)} \leftrightarrow H_2CO_{3(aq)} \quad (27)$$

In practice $CO_{2(aq)}$ and $H_2CO_{3(aq)}$ cannot be measured separately and are considered as a single dissolved species in equilibrium with $CO_{2(g)}$ as described by Henry's Law.

In a similar manner to the ionization of $H_2S$, $H_2CO_3$ ionizes at low pH and high temperature due to proton transfer:

$$H_2CO_{3(aq)} \xleftrightarrow{K_{a1}} HCO_3^-{}_{(aq)} + H^+{}_{(aq)} \xleftrightarrow{K_{a2}} CO_3^{2-}{}_{(aq)} + 2H^+{}_{(aq)} \quad (28)$$

The carbonate equilibrium was described and solved using a system of five equations [(29), (30), (32), (34), and (35)]. Nomenclature for the calculations is shown in Table 6.2.

**Table 6.2:** Nomenclature for carbonate equilibrium equations.

| Parameter | Description | Units |
|---|---|---|
| $P_{CO2}$ | $CO_2$ gas partial pressure | atm |
| $H_{CO2}$ | Henry's constant | atm |
| $x$ | Mole fraction of $CO_2$ and $H_2CO_3$ in solution | mol/mol |
| $n_{CO2}$ | Moles of gas phase $CO_2$ | mol |
| $n_{H2CO3}$ | Moles of dissolved $CO_2$ & $H_2CO_3$ | mol |
| $n_{HCO3}$ | Moles of dissolved $HCO_3^-$ | mol |
| $n_{HCO3}$ | Moles of dissolved $CO_3^{2-}$ | mol |
| $n_{H+}$ | Moles of free protons (based on pH) | mol |
| [ ] | Molar concentration value | mol/L |
| $R$ | Universal gas constant | L.atm/mol.K |
| $T$ | Temperature | K |
| $V_G$ | Volume of gas head space | L |
| $V_L$ | Volume of liquid | L |
| $n_w$ | Moles of liquid (water) | mol |
| $K_{a1,H2CO3}$ | First $H_2CO_3$ dissociation constant | mol/L |
| $K_{a2,H2CO3}$ | Second $H_2CO_3$ dissociation constant | mol/L |

Henry's Law:

$$P_{CO_2} - \frac{H_{CO_2}}{n_w} n_{H_2CO_3} = 0 \tag{29}$$

Ideal Gas Law:

$$P_{CO_2} - n_{CO_2} \frac{RT}{V_G} = 0 \tag{30}$$

First Ionization Equilibrium:

$$K_{a1,H_2CO_3} = \frac{[n_{H^+}][n_{HCO_3^-}]}{[n_{H_2CO_3}]} \tag{31}$$

$$-\frac{(n_{H^+})}{V_L^2}(n_{HCO_3^-}) + \frac{(K_{a1,H_2CO_3})}{V_L}(n_{H_2CO_3}) = 0 \tag{32}$$

Second Ionization Equilibrium:

$$K_{a2,H_2CO_3} = \frac{[n_{H^+}][n_{CO_3^{2-}}]}{[n_{HCO_3^-}]} \tag{33}$$

$$\frac{(K_{a2,H_2CO_3})}{V_L}(n_{HCO_3^-}) - \frac{(n_{H^+})}{V_L^2}(n_{CO_3^{2-}}) = 0 \tag{34}$$

Total Carbonate Mass Balance:

$$n_{CO_2} + n_{HCO_3^-} + n_{CO_3^{2-}} + n_{H_2CO_3} = n_{tc} \tag{35}$$

Matrix $Ax = b$:

$$A = \begin{bmatrix} 1 & 0 & 0 & 0 & -\frac{H_{CO_2}}{n_w} \\ 1 & -\frac{(R)(T)}{V_G} & 0 & 0 & 0 \\ 0 & 0 & \frac{-n_{H^+}}{V_L^2} & 0 & \frac{K_{a1,H_2CO_3}}{V_L} \\ 0 & 0 & \frac{K_{a2,H_2CO_3}}{V_L} & \frac{-n_{H^+}}{V_L^2} & 0 \\ 0 & 1 & 1 & 1 & 1 \end{bmatrix} \quad x = \begin{bmatrix} P_{CO_2} \\ n_{CO_2} \\ n_{HCO_3^-} \\ n_{CO_3^{2-}} \\ n_{H_2CO_3} \end{bmatrix} \quad b = \begin{bmatrix} 0 \\ 0 \\ 0 \\ 0 \\ n_{tc} \end{bmatrix} \tag{36}$$

### 6.1.3 Simulation Results

The equilibrium partial pressure values from the simulation were normalized to calculate the mol % of $H_2S$ and $CO_2$ in the gas head space. The results are shown in Figure 6.2.

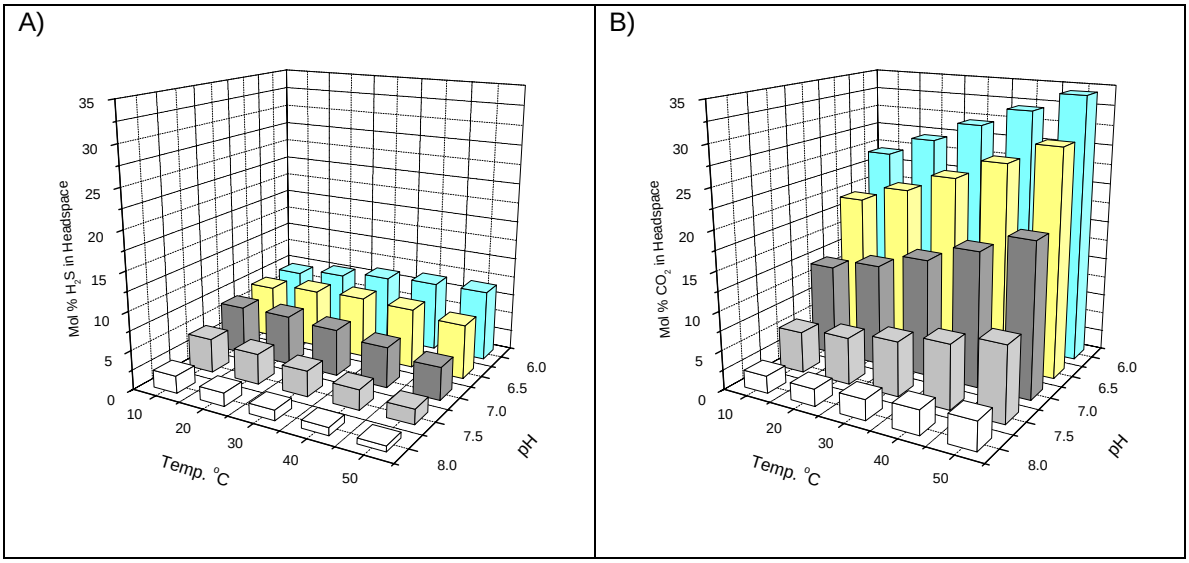


**Figure 6.2** Effect of temperature and pH on the mol % of $H_2S$ (A) and mol % of $CO_2$ (B) in a closed system. The system was assumed to have a liquid volume of 100 mL, headspace volume of 100 mL (with $N_2$ at 1 atm), and 20 mM of total sulfide ($H_2S_{(g)}$, $H_2S_{(aq)}$, $HS^-_{(aq)}$) and 40 mM total carbonate ($CO_{2(g)}$, $H_2CO_{3(aq)}$, $HCO_3^-$(aq), $CO_3^{2-}{}_{(aq)}$).

$H_2S$ and $H_2CO_3$ are both mild acids and respond to pH changes in a similar manner. A decrease in pH shifts the equilibrium to their fully protonated form with the net result of increasing equilibrium partial pressure. Lower pH values are therefore desirable for maximizing the $H_2S$ content of the gas phase. With regard to temperature dependence, the sulfide system exhibits some seemingly contradictory trends depending on the pH. At pH 8 (Figure 6.2A) $H_2S$ mol % decreases with temperature. This trend is due to the majority of sulfide being in the dissolved phase and the sensitivity of sulfide ionization to temperature (Figure 6.3A). At pH 6 the majority of dissolved sulfide is present in the

strippable $H_2S_{(aq)}$ form such that temperature dependent vapour-liquid equilibrium dominates. Overall, the temperature effect on gas phase composition is relatively minor compared to the pH effect. Temperature shifts from 10 $^oC$ to 50 $^oC$ result in marginal differences in gas phase composition. The most efficient means of partitioning the product to the gas phase would be to shift the pH below 6.

The carbonate system is not nearly as sensitive to temperature dependent ionization as the sulfide system (Figure 6.3B). As a result, temperature and mol % $CO_2$ in the gas phase are directly related across pH values of 6-8. In a manner similar to the sulfide system, $CO_2$ gas phase partitioning is much more sensitive to changes in pH than temperature.

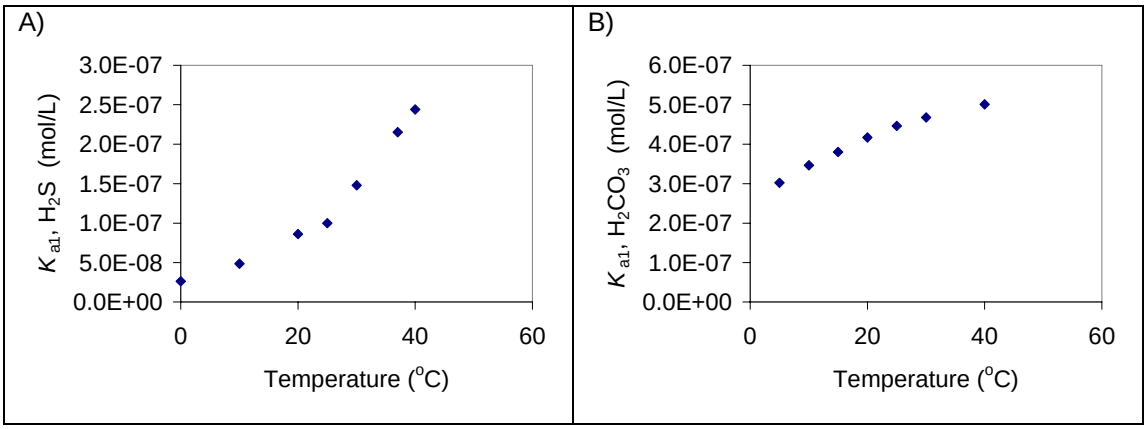


**Figure 6.3:** Temperature dependence of the first dissociation equilibrium constants for $H_2S_{(aq)}$ and $CO_2/H_2CO_{3(aq)}$ (B).

Another important factor that affects the head space gas composition is the relative volatility of $H_2S$ and $CO_2$. $CO_2$ is approximately three times as volatile as $H_2S$ ($H_{H2S}$ = 483 atm, $H_{CO2}$ = 1420 atm at 20 $^oC$), therefore any changes to temperature or pH that increase the partial pressure of $H_2S$, will increase the partial pressure of $CO_2$ to a greater extent.

In summary, a model was developed to provide estimations of the strip gas composition under varying pH and temperature conditions. Due to dissolved phase molecule ionization and vapour-liquid equilibrium effects, the highest partial pressures and mol % of $H_2S$ and $CO_2$ in nitrogen strip gas are obtained at pH values less than 6 and at elevated temperatures. For a bioreactor system with an $N_2$ strip gas operating at biologically relevant conditions (pH = 6; $T$ = 37 $^{o}$C, total sulfides = 20 mM) the strip gas will have an approximate composition of 9 mol % $H_2S$, 31 mol % $CO_2$, and 60 mol % $N_2$. These values are consistent with the experimental trends of this study and those reported in the literature for an acidified stripping column that recovered biologically produced sulfide (Stucki et al., 1993).

## 6.2 Downstream Sulfide Product Recovery

Regardless of whether *in situ* stripping is applied, the bioreactor liquid effluent will contain a significant concentration of total dissolved sulfide (in the range of 10-20 mM). It is desirable to recover these dissolved sulfides in a downstream stripping process to maximize the $H_2$ yield of the overall process. The following section outlines the initial design considerations for such a unit operation.

### 6.2.1 Design Equations and Mass Balance

A counter-current stripping column is the most appropriate unit operation for downstream sulfide recovery. Counter-current design maximizes both the amount of sulfide recovered and the concentration of $H_2S$ in the exiting strip gas. The overall mass balance on a stripping column can be described by the following general word statement:

| Moles of solute entering in liquid stream | + | Moles of solute entering in gas stream | = | Moles of solute leaving in liquid stream | + | Moles of solute leaving in gas stream |
|---|---|---|---|---|---|---|

The stripping column mass balance is illustrated in Figure 6.4. Individual analysis of the internal column stage equilibria can be accomplished by more advanced methods but present calculations will be limited to an overall mass balance (nomenclature described in Table 6.3).

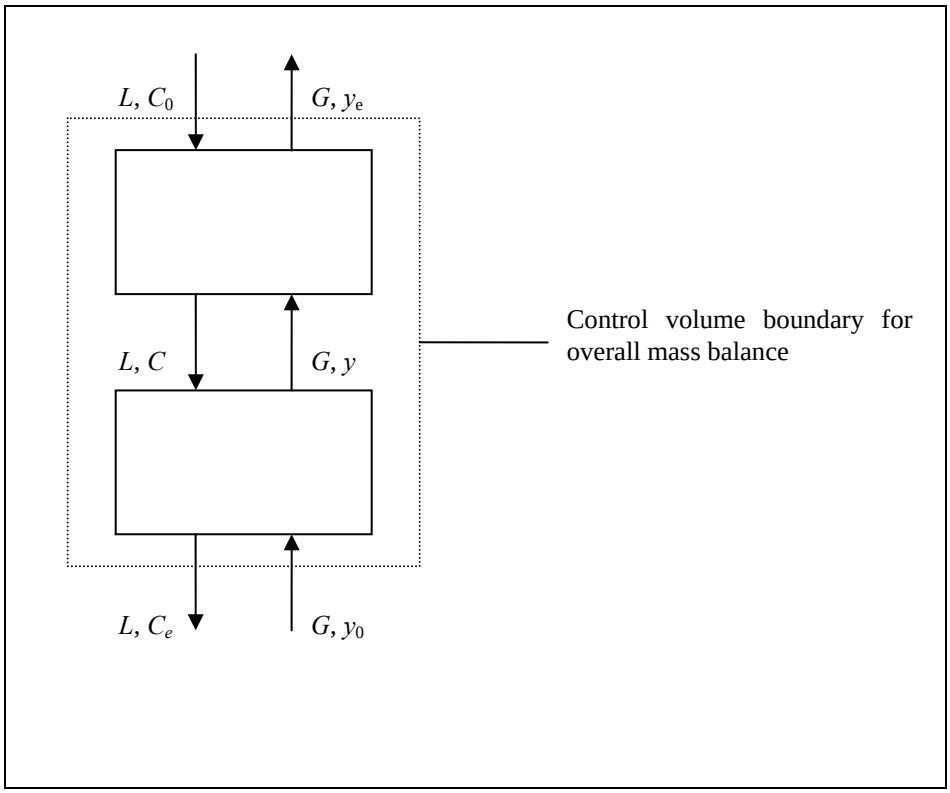


**Figure 6.4:** Diagram for mass balance analysis of a counter-current gas stripping column (adapted from Metcalf and Eddy, 2003). Nomenclature described in Table 6.3.

**Table 6.3:** Nomenclature for stripping column analysis. It is assumed that the solute is sufficiently dilute in the liquid phase that its molar fraction and mole concentration are equivalent (i.e. $C_i = x_i$).

| Parameter | Description | Units |
|---|---|---|
| $L$ | molar liquid flow | mol/min |
| $G$ | molar gas flow | mol/min |
| $y_0$ | mole fraction of solute in gas entering the column | mol solute/mol (solute free) gas |
| $y_e$ | mole fraction of solute in gas exiting the column | mol solute/mol (solute free) gas |
| $y$ | mole fraction of solute in gas at a given point in the column | mol solute/mol (solute free) gas |
| $C_0$ | concentration of solute in liquid entering the column | mol solute/mol liquid |
| $C_e$ | concentration of solute in liquid exiting the column | mol solute/mol liquid |
| $C$ | concentration of solute in liquid at a given point in the column | mol solute/mol liquid |
| $C'_0$ | concentration of solute in liquid at equilibrium with the gas exiting the column | mol solute/mol liquid |
| $H$ | Henry's constant | atm |
| $P_T$ | Total pressure (usually 1 atm) | atm |
| $G/L$ | Theoretical molar (volumetric) strip gas to liquid ratio | mol/mol, $m^3/m^3$ |

The overall solute mass balance is written as:

$$LC_0 + Gy_0 = LC_e + Gy_e \tag{37}$$

Combining terms the mass balance is re-written as:

$$(y_0 - y_e) = \frac{L}{G}(C_e - C_0) \tag{38}$$

Assuming the strip gas entering the column contains no solute ($y_0 = 0$) the mass balance becomes:

$$y_e = \frac{L}{G}(C_0 - C_e) \tag{39}$$

The exit gas mole fraction ($y_e$) can also be described by Henry's law:

$$y_e = \frac{H}{P_T} C_0^{'} \tag{40}$$

Substituting Henry's Law (40) into Equation (39) and isolating for $C^{'}_0$:

$$C_0^{'} = \frac{L}{G}\frac{P_T}{H}(C_0 - C_e) \tag{41}$$

Assuming that the concentration of solute in the liquid entering the column ($C_0$) is equilibrium with the exiting gas (i.e. $C^{'}_0 = C_0$), Equation (41) becomes:

$$\frac{G}{L} = \frac{P_T}{H}\frac{(C_0 - C_e)}{C_0} \tag{42}$$

Where *G/L* is the theoretical molar ratio of strip gas to liquid required for operation at assumed values of $C_0$, $C_e$, $y_e$, and $y_0$ at equilibrium. In practice, 1.5 to 3 times the theoretical value of *G/L* is applied in stripping column design (Metcalf and Eddy, 2003).

### 6.2.2 Gas to Liquid (*G/L*) Requirements for Dissolved Sulfide Recovery

#### 6.2.2.1 Use of Fresh $N_2$ Strip Gas

Figure 6.5 shows the results of calculations to estimate the *G/L* ratios required to strip a bioreactor effluent containing 20 mM of dissolved sulfides. It was assumed that the pH of effluent was lowered sufficiently (pH < 5.0) such that all of the dissolved sulfides were in the strippable $H_2S_{(aq)}$ form and that sulfide ionization due to temperature effects was negligible. It was also assumed that $N_2$ was insoluble in liquid and contained no $H_2S$ before entering the stripping column ($y_0 = 0$). *G/L* requirements were evaluated at 20 $^oC$ (293 K) and 37 $^oC$ (310 K).

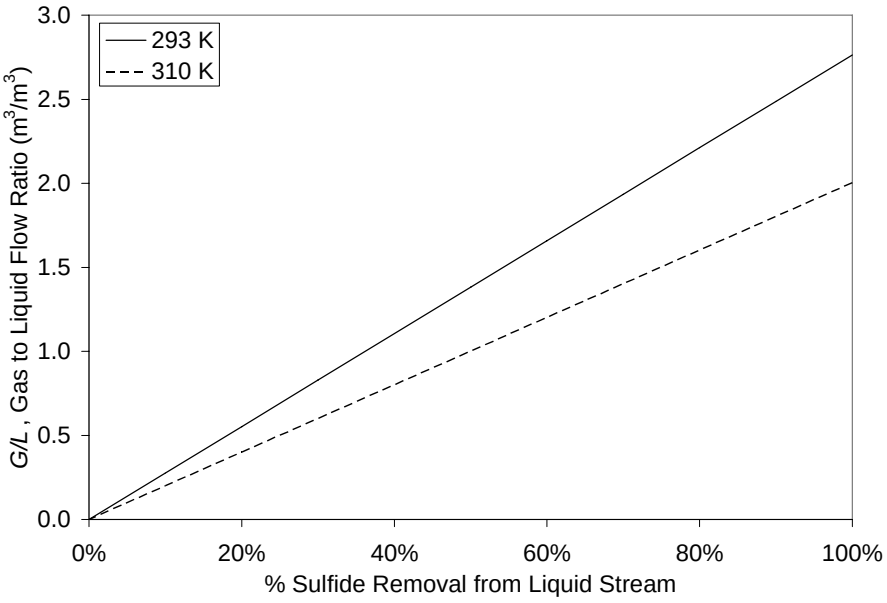


**Figure 6.5:** Gas to liquid ratios *(G/L*, $m^3/m^3$) required to remove varying % dissolved sulfide from a liquid stream (20 mM) at 20 $^oC$ (293 K) and 37 $^oC$ (310 K). It was assumed that the pH was sufficiently low (pH < 5.0) that all of the dissolved sulfides were in the strippable $H_2S_{(aq)}$ form and that temperature dependent ionization was negligible.

Due to the temperature dependence of Henry's constant, the solute is more readily

stripped at higher temperatures resulting in lower *G/L* ratios to remove equal amounts of sulfide. Operating at elevated temperature also has the benefit of producing a strip gas with a higher partial pressure of $H_2S$. For conditions evaluated in Figure 6.5 the equilibrium partial pressure of $H_2S$ in the exiting strip gas is 0.17 atm (at 20 $^oC$/293 K) and 0.25 atm (at 37 $^oC$/310 K).

#### 6.2.2.2 Use of Bioreactor Strip Gas

The gas fed to the downstream stripping column need not be $H_2S$ free and may be substituted with the gas from *in situ* bioreactor stripping. Assuming that the bioreactor effluent pH is decreased before being sent to the stripping column, the bioreactor gas should be suitable for use downstream column use (Figure 6.6). Figure 6.7 shows the *G/L* ratios required to strip 100 % of the dissolved sulfides from a 20 mM liquid stream as a function of initial $H_2S$ partial pressure in the strip gas. *G/L* requirements were evaluated at 20 $^oC$ (293 K) and 37 $^oC$ (310 K).

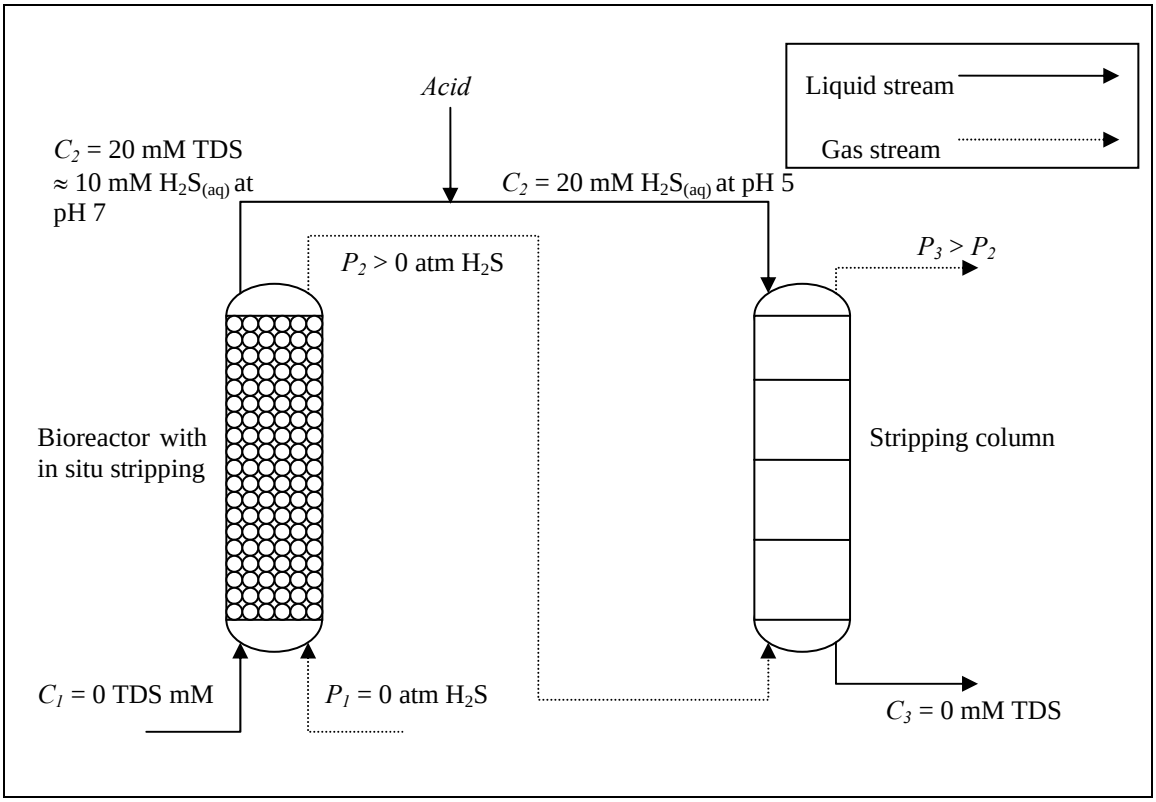


**Figure 6.6:** Process flow diagram of a possible process where an $H_2S$ free strip gas is first fed to bioreactor to strip a portion of $H_2S$ *in situ*. The liquid is then acidified to convert the residual total dissolved sulfides (TDS) to the strippable $H_2S_{(aq)}$ species which are removed in a countercurrent stripping column using gas from the bioreactor. $C_i$ = liquid phase concentration (mM); $P_i$ = gas phase $H_2S$ partial pressure (atm).

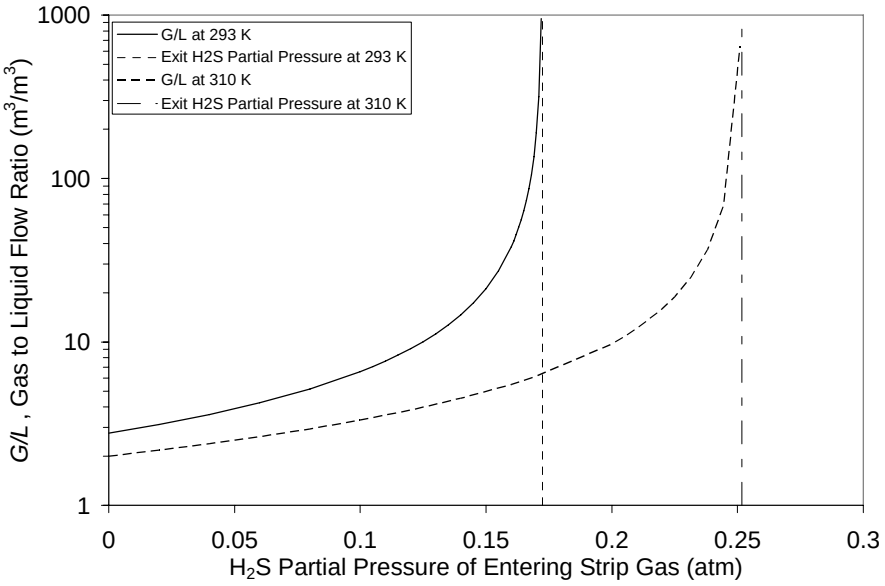


**Figure 6.7:** Gas to liquid (*G/L*, $m^3/m^3$) ratios required to remove 100% dissolved sulfide from a liquid stream (20 mM) using strip gases of varying initial $H_2S$ partial pressures (atm). *G/L* values were evaluated at 20 $^oC$ (293 K) and 37 $^oC$ (310 K). The equilibrium $H_2S$ partial pressure in the exiting gas ($P_e = P_3$) is 0.17 atm at 293 K (vertical dotted line) and 0.25 atm at 310 K (vertical dotted-dashed line). It was assumed that the pH was sufficiently low (pH < 5.0) that all of the dissolved sulfides were in the strippable $H_2S_{(aq)}$ form and that temperature dependent ionization was negligible. $H_2S$ partial pressure of entering strip gas will likely be in the range of 0.04-0.21 atm.

Figure 6.7 shows that if the initial partial pressure of $H_2S$ increases, greater *G/L* ratios are required to remove the same amount of dissolved sulfide. When the inlet $H_2S$ partial pressure equals the equilibrium $H_2S$ partial pressure at the top of the column, *G/L* requirements rise to infinity as there is no longer a concentration difference to serve as a stripping driving force. Again there are advantages associated with operating at elevated temperatures due to the higher equilibrium partial pressures. This is illustrated in Figure 6.7 where a strip gas entering with a $H_2S$ partial pressure of 0.17 cannot remove any dissolved sulfides ($G/L \rightarrow \infty$) at 20 $^oC$ (293 K), but requires only a *G/L* ratio of 6.2 to remove 100 % of the dissolved sulfides at 37 $^oC$ (310 K).

The calculations shown (Figure 6.5 and Figure 6.7) have not considered the simultaneous stripping of $CO_2$ from the liquid stream which would result in a reduction of the mole fraction of $H_2S$ in the product stream (i.e. $y_{H2S} < 0.17\text{-}0.25$). This is due to gas partial pressures being independent of the presence of other gases whereas gas mole fractions are not.

The *G/L* values required for complete sulfide recovery under the given conditions when practical design considerations are applied (*G/L* = 3-9) are within the same range as those applied experimentally *in situ* to the bioreactor. Use of the strip gas from the bioreactor (expected to have $H_2S$ partial pressures between 0.04-0.21 atm) will result in only moderate increases in *G/L* values (*G/L* = 12-36) assuming the stripping column is operated at elevated temperatures ($T$ = 37 $^{o}$C/310 K). The required *G/L* ratios are consistent with experimental values reported by Stucki et al. (1993) for recovery of biogenic sulfide in a stripping column operated at similar conditions. These *G/L* ratios are relatively low compared to the requirements for other common wastewater applications such as ammonia stripping. *G/L* ratios for ammonia removal from wastewater are often in the order of $10^3$ (Metcalf and Eddy, 2003).

Complete stripping column design requires the selection of an appropriate packing material to allow for calculation of the corresponding column height, cross sectional area, pressure drop, and other design parameters. These initial calculations have shown that dissolved sulfide can be recovered using reasonable volumes of stripping gas (either fresh or from the bioreactor) and that more detailed calculations would be an important part of

future work regarding this key product recovery unit operation.

# Chapter 7: Conclusions

This study has developed a sulfate reducing packed bed bioreactor as part of a multi-step process to convert organic waste to $H_2$. Key findings with respect to carrier material selection, inoculum composition, and operating protocols have advanced the current state-of-the-art for sulfate reducing bioreactor technology and set the standard for attainable volumetric productivity as high as 830 mol/$m^3$.d. Experimental and theoretical gas stripping work has highlighted the challenges associated with the recovery of the soluble sulfide product. Although further work is required to develop the overall $H_2$ production process, many of this study's conclusions are relevant to existing sulfate reducing bioreactor applications.

Results from this study have demonstrated the largely unrecognized importance of critical inoculum design for improving the performance of sulfate reducing bioreactors. The standard method of suspended growth serial transfers enriched for a kinetically favourable SRB consortium with a specific sulfate reduction rate of 1.2 g $SO_4^{2-}$/g CDW.h that was nearly double that of the benchmark species. Unfortunately the consortium exhibited negligible immobilization potential. *Desulfovibrio desulfuricans* (ATCC 7757) was the benchmark species and despite its slower kinetics, it was capable of visible biofilm formation and had superior immobilization potential. By combining these two microbial systems, a mixed inoculum was designed that exploited the advantages of the individual cell lines. Celite™ R-635 diatomaceous earth pellets were shown, for the first time, to be a suitable carrier material for SRB and outperformed other known SRB carrier

materials such as Poraver™ porous glass beads and polyurethane foam.

Using an inoculum with an initial composition of 96 % *Desulfovibrio desulfuricans* and 4 % consortium, a Celite™ R-635 filled PBR was able to achieve a volumetric sulfide production rate of 493 mol/$m^3$.d (HRT = 38 min; $D$ = 1.6 $h^{-1}$) after only 8 d of operation. This represents an order of magnitude decrease in start-up time compared to other PBR studies that achieved similar volumetric rates after approximately 100 d with more elaborate bioreactor systems involving recycle loops and online pH control (Stucki et al., 1993; Selvaraj et al., 1997). Baskaran and Nemati (2006) employed a single-pass, sand filled PBR system similar to this study's but was only able to obtain a volumetric sulfate reduction rate of 57 mol/$m^3$.d after 100 d of operation. The relatively poor performance of the similar system was likely due to the poor immobilization potential of the SRB consortium that was employed.

The bioreactor exhibited continuous stable operation for extended experimental periods (100 d) with steady-state effluent TDS concentrations were in the range of 15-20 mM. These values were consistent with the recent literature that reported maximum TDS concentrations of 16 mM from Poraver™ filled PBRs supplied lactate (Alvarez et al., 2006) and organic waste (Alvarez et al., 2007). Partial biofilm detachment during a 24 h shutdown period was attributed to a combination of sulfide inhibition and substrate limitation. The bioreactor's ability to recover from the adverse shutdown conditions in only 48 h was attributed to the rapid kinetics and excellent immobilization potential imparted by the initial inoculum and the effectiveness of Celite™ R-635 as a carrier

material.

Implementing an $N_2$ strip gas in the bioreactor was an effective method of increasing the sulfate conversion and recovering the sulfide product in the gas phase. Feed substrate concentrations were doubled to exploit the bioreactor's increased operating capacity and sulfate conversions as high as 33 mM were achieved while maintaining sub-inhibitory concentrations of TDS (< 20 mM). The net result was attainment of volumetric productivities at liquid feed rates lower than previously possible which allows for more quiescent hydrodynamic conditions and decreased sloughing. Similar values of the *G/L* ratio were evaluated at different absolute feed rates and *G/L* was shown to be an appropriate design parameter for process scale-up. From the various experimental conditions evaluated, a volumetric productivity of at least 830 $mol/m^3.d$ was considered easily attainable but not attempted due to practical limitations of the current bench-scale bioreactor setup.

Decreasing the pH of the liquid feed was effective in partitioning greater fractions of the sulfide product to the gas phase. By lowering the initial pH from a value of 7 to 6, the $H_2S$ composition of the strip gas was observed to increase from 3.6 mol % to 5.8 mol %. An undesirable effect of decreasing the pH is an associated increase in the $CO_2$ content of the strip gas. A simple mathematical model that incorporated ionization and vapour-liquid equilibria indicated that under ideal conditions, a strip gas composition of approximately 9 mol % $H_2S$, 31 mol % $CO_2$, and 60 mol % $N_2$ can be obtained from a bioreactor producing a pH 6 effluent with 20 mM TDS.

Due to the nature of co-current bioreactor stripping, the effluent is expected to contain 15-20 mM of TDS. The residual dissolved sulfides can be recovered if the effluent is acidified to below pH 5.0 and fed to the top of a counter-current abiotic stripping column. Model results indicated that a *G/L* ratio of around 2.0 is required for 100 % sulfide recovery with a fresh $N_2$ strip gas. A *G/L* ratio of around 12.0 is required if the bioreactor strip gas is used, assuming its feed $H_2S$ partial pressure is below 0.21 atm.

The biological methanogenic and sulfate reducing processes were evaluated and found to be similar with regard to current bioreactor technology performance. The methods developed in this preliminary study to enhance bioreactor performance suggest that sulfate reducing bioreactor technology is capable of considerably outpacing its methanogenic counterpart with regard to volumetric productivity. More detailed comparisons of the thermochemical conversion processes to $H_2$ are required to determine the feasibility of the overall process. The potential for large improvements in sulfate reducing bioreactor technology is a key contributing factor to the competitiveness of the $H_2S$ based process. Finally, the insights from this study will find immediate application in improving existing SRB bioreactor technology for the bioremediation of acid mine drainage, destruction of xenobiotics, and the treatment of sulfate-laden waste streams.

# Chapter 8: Future Work

Due to the preliminary nature of the current study, several areas of investigation remain open for further exploration. These include the use of complex organic substrates and the integration of an $SO_2$ gas stream. Modification of the carrier material, addition of growth factors to the liquid feed, and further characterization and refinement of the SRB inoculum are also recommended to further enhance bioreactor performance.

Several potential sources of organic waste were listed in the literature review (Table 2.5) but a more thorough examination of the literature and possible experimental work is required to identify a feedstock that exhibits the optimal balance of degradable COD, cost, and availability. Fermentative heterotrophs will be required to breakdown the complex substrate to lactate and other substrates suitable for SRB. The fermentative bacteria can be co-cultured with the SRB (Selvaraj et al., 1997) but there may be advantages to operating a separate upstream bioreactor dedicated to hydrolysis and fermentation. The upstream bioreactor could utilize an alumina ceramic carrier material which immobilizes hydrolytic and fermentative bacteria preferentially over SRB (Silva et al., 2006). Concerns regarding sulfide inhibition of the fermentative process would also be eliminated.

Due to the metabolism of the incompletely oxidizing SRB, the effluent from the sulfate reducing bioreactor will contain considerable concentrations of acetate. Mineralization of the residual acetate to $H_2S$ and $CO_2$ can be accomplished in additional downstream

bioreactors seeded with acetotrophic SRB as described by Deswaef et al. (1996). If organic waste is completely degraded to $H_2S$ and $CO_2$ then the theoretical feedstock requirements will be 48 g COD/mol $SO_2$ or 64 g COD/mol $SO_4^{2-}$.

Ideally the $SO_2$ stream can be blended with the $N_2$ bioreactor strip gas so that it dissolves gradually along the length of the column. $SO_2$ is 1000x more soluble than $N_2$ in aqueous solution and it may be possible to design the $SO_2/N_2$ ratio in a manner that 100 % of the $SO_2$ transfers to solution before the strip gas exits the bioreactor. This method of $SO_2$ delivery avoids inhibition concerns due to high sulfite concentrations and provides a degree of pH moderation. Protons for sulfide hydrolysis to $H_2S$ are provided by sulfurous acid ($H_2SO_3$) rather than an alkalinity generating reaction. Additional methods of pH control may also be required if sufficiently high conversions are obtained.

Immediate improvements in bioreactor volumetric productivity can be obtained by using previously tested *G/L* ratios but increasing the absolute feed rate values. This is a relatively simple matter of laboratory logistics (e.g. increasing the medium reservoir volume, upgrading pump capacity, etc.). More fundamental improvements to bioreactor design may be accomplished by further refining the inoculum composition and reducing the size of the Celite™ R-635 pellets to provide increased surface area. Molecular methods can be applied to track changes in microbial population during the course of bioreactor operation. Identification of the kinetically superior SRB species will allow for the development of a defined consortium that can be distributed and reproduced with consistent results. The effect of cofactors such as $Ni^{2+}$ should be investigated as a

method of improving biofilm adhesion as proposed by Lopes et al. (2006). If the kinetically superior SRB species could be induced to form biofilms, it would reduce the need for *Desulfovibrio desulfuricans* but more importantly would allow for the selective induction of replication and biofilm growth modes. This would serve as valuable tool for rapid bioreactor start-up and recovery from shutdown periods.

# Chapter 9: References

Alvarez MT, Crespo C, Mattiasson B. Precipitation of Zn(II), Cu(II) and Pb(II) at bench-scale using biogenic hydrogen sulfide from the utilization of volatile fatty acids. Chemosphere. 2007; 66(9): 1677-83.

Alvarez MT, Pozzo T, Mattiasson B. Enhancement of sulphide production in anaerobic packed bed bench-scale biofilm reactors by sulphate reducing bacteria. Biotechnology Letters. 2006; 28(3): 175-81.

Ammary BY. Treatment of olive mill wastewater using an anaerobic sequencing batch reactor. Desalination. 2005; 177(1-3): 157-65.

Andersson J, Björnsson L. Evaluation of straw as a biofilm carrier in the methanogenic stage of two-stage anaerobic digestion of crop residues. Bioresource Technology. 2002; 85(1): 51-6.

Angenent LT, Karim K, Al-Dahhan MH, Wrenn BA, Domiguez-Espinosa R. Production of bioenergy and biochemicals from industrial and agricultural wastewater. Trends in Biotechnology. 2004; 22(9): 477-85.

Annachhatre AP, Suktrakoolvait S. Biological sulfate reduction using molasses as a carbon source. Water Environment Research. 2001; 73(1): 118-26.

Azabou S, Mechichi T, Sayadi S. Zinc precipitation by heavy-metal tolerant sulfate-reducing bacteria enriched on phosphogypsum as a sulfate source. Minerals Engineering. 2007; 20(2): 173-8.

Azabou S, Mechichi T, Sayadi S. Sulfate reduction from phosphogypsum using a mixed culture of sulfate-reducing bacteria. International Biodeterioration & Biodegradation. 2005; 56(4): 236-42.

Baskaran V, Nemati M. Anaerobic reduction of sulfate in immobilized cell bioreactors, using a microbial culture originated from an oil reservoir. Biochemical Engineering Journal. 2006; 31(2): 148-59.

Battaglia-Brunet F, Foucher S, Denamur A, Ignatiadis I, Michel C, Morin DE. Reduction

of chromate by fixed films of sulfate-reducing bacteria using hydrogen as an electron source. Journal of Industrial Microbiology and Biotechnology. 2002; 28(3): 154-9.

Bertin L, Berselli S, Fava F, Petrangeli-Papini M, Marchetti L. Anaerobic digestion of olive mill wastewaters in biofilm reactors packed with granular activated carbon and "Manville" silica beads. Water Research. 2004; 38(14-15): 3167-78.

Beyenal H, Lewandowski Z. Dynamics of lead immobilization in sulfate reducing biofilms. Water Research. 2004; 38(11): 2726-36.

Boopathy R, Kulpa CF, Manning J. Anaerobic biodegradation of explosives and related compounds by sulfate-reducing and methanogenic bacteria: a review. Bioresource Technology. 1998; 63(1): 81-9.

Borja R, Banks CJ, Zhengjian W. Effect of organic loading rate on anaerobic treatment of slaughterhouse wastewater in a fluidised-bed reactor. Bioresource Technology. 1995; 52(2): 157-62.

Borja R, Gonzalez E, Raposo F, Millan F, Martin A. Performance evaluation of a mesophilic anaerobic fluidized-bed reactor treating wastewater derived from the production of proteins from extracted sunflower flour. Bioresource Technology. 2001; 76(1): 45-52.

Boshoff G, Duncan J, Rose PD. Tannery effluent as a carbon source for biological sulphate reduction. Water Research. 2004a; 38(11): 2651-8.

Boshoff G, Duncan J, Rose PD. The use of micro-algal biomass as a carbon source for biological sulphate reducing systems. Water Research. 2004b; 38(11): 2659-66.

Cadavid DL, Zaiat M, Foresti E. Performance of horizontal-flow anaerobic immobilized sludge (HAIS) reactor treating synthetic substrate subjected to decreasing COD to sulfate ratios. Water Science and Technology. 1999; 39(10-11): 99-106.

Calli B, Mertoglu B, Roest K, Inanc B. Comparison of long-term performances and final microbial compositions of anaerobic reactors treating landfill leachate. Bioresource Technology. 2006; 97(4): 641-7.

Cattony EBM, Chinalia FA, Ribeiro R, Zaiat M, Foresti E, Varesche MBA. Ethanol and toluene removal in a horizontal-flow anaerobic immobilized biomass reactor in the

presence of sulfate. Biotechnology and Bioengineering. 2005; 91(2): 244-53.

Chang BV, Shiung LC, Yuan SY. Anaerobic biodegradation of polycyclic aromatic hydrocarbon in soil. Chemosphere. 2002; 48(7): 717-24.

Chang IS, Shin PK, Kim BH. Biological treatment of acid mine drainage under sulphate-reducing conditions with solid waste materials as substrate. Water Research. 2000; 34(4): 1269-77.

Chauhan A, Ogram A. Evaluation of support matrices for immobilization of anaerobic consortia for efficient carbon cycling in waste regeneration. Biochemical and Biophysical research communications. 2005; 327(3): 884-93.

Chen CI, Taylor RT. Thermophilic biodegradation of BTEX by two consortia of anaerobic bacteria. Applied Microbiology and Biotechnology. 1997; 48(1): 121-8.

Chen C, Mueller RF, Griebe T. Kinetic analysis of microbial sulfate reduction by *Desulfovibrio desulfuricans* in an anaerobic upflow porous media biofilm reactor. Biotechnology and Bioengineering. 1994; 43(4): 267-74.

Christensen B, Laake M, Lien T. Treatment of acid mine water by sulfate-reducing bacteria; results from a bench scale experiment. Water Research. 1996; 30(7): 1617-24.

Christy BCP. Effect of hydraulic retention time and attachment media on sulfide production by sulfate reducing bacteria (MASc thesis). University of Windsor. 2001.

Coetser S, Pulles W, Heath R, Cloete TE-. Chemical characterisation of organic electron donors for sulfate reduction for potential use in acid mine drainage treatment. Biodegradation. 2006.

Cohen RRH. Use of microbes for cost reduction of metal removal from metals and mining industry waste streams. Journal of Cleaner Production. 2006; 14(12-13): 1146-57.

Colleran E, Finnegan S, Lens PE-. Anaerobic treatment of sulphate-containing waste streams. Antonie van Leeuwenhoek. 1995; 67(1): 29-46.

Cord-Ruwisch R. A quick method for the determination of dissolved and precipitated sulfides in cultures of sulfate-reducing bacteria. Journal of Microbiological Methods. 1985; 4(1): 33-6.

Costerton JW, Lewandowski Z, Caldwell DE, Korber DR, Lappin-Scott HM. Microbial biofilms. Annual Review of Microbiology. 1995; 49: 711-45.

Costerton WJ, Wilson M. Introducing biofilms. Biofilms. 2004; 1(1): 1-4.

D'Alessandro PL, Characklis WG, Kessick MA, Ward CH. Developments in industrial microbiology. Washington, DC: American Institute of Biological Sciences; 1974.

Daugulis AJ, Krug TA, Choma CET. Filament formation and ethanol production by *Zymomoas mobilis* in adsorbed cell bioreactors. Biotechnology and Bioengineering. 1985; 27: 626-31.

Daugulis AJ, Swaine DE. Examination of substrate and product inhibition kinetics on the production of ethanol by suspended and immobilized cell reactors. Biotechnology and Bioengineering. 1987; 24: 639-45.

de Ory I, Romero LE, Cantero D. Optimization of immobilization conditions for vinegar production. Siran, wood chips and polyurethane foam as carriers for *Acetobacter aceti*. Process Biochemistry. 2004; 39(5): 547-55.

de Smul. A combined biotechnological and physico-chemical process for the desulfurization of waste waters (PhD thesis). University of Ghent. 1998.

de Smul A, Goethals L, Verstraete W. Effect of COD to sulphate ratio and temperature in expanded-granular-sludge-blanket reactors for sulphate reduction. Process Biochemistry. 1999; 34(4): 407-16.

del Pozo R, Diez V, Beltrán S. Anaerobic pre-treatment of slaughterhouse wastewater using fixed-film reactors. Bioresource Technology. 2000; 71(2): 143-9.

Deswaef S, Salmon T, Hiligsmann S, Taillieu X, Milande N, Thonart P, et al. Treatment of gypsum waste in a two stage anaerobic reactor. Water Science and Technology. 1996; 34(5-6): 367-74.

Dries J, De Smul A, Goethals L, Grootaerd H, Verstraete W. High rate biological treatment of sulfate-rich wastewater in an acetate-fed EGSB. Biodegradation. 1998; 9(2): 103-11.

du Preez LA, Maree JP. Pilot-scale biological sulphate and nitrate removal utilizing

producer gas as energy source. Water Science and Technology. 1994; 30(12): 275-85.

Durham DR, Marshall LC, Miller JG, Chmurny AB. Characterization of inorganic biocarriers that moderate system upsets during fixed-film biotreatment processes. Applied Environmental Microbiology. 1994; 60(9): 3329-35.

Dutta S, Chowdhury R, Bhattacharya P. Stability and response of bioreactor: An analysis with reference to microbial reduction of $SO_2$. Chemical Engineering Journal. 2007; 133(1-3): 343-54.

Fedorovich V, Greben M, Kalyuzhnyi S, Lens P, Hulshoff Pol L. Use of hydrophobic membranes to supply hydrogen to sulphate reducing bioreactors. Biodegradation. 2000; 11(5): 295-303.

Foucher S, Battaglia-Brunet F, Ignatiadis I, Morin D. Treatment by sulfate-reducing bacteria of Chessy acid-mine drainage and metals recovery. Chemical Engineering Science. 2001; 56(4): 1639-45.

Fukui M, Takii S. Kinetics of sulfate respiration by free-living and particle-associated sulfate-reducing bacteria. FEMS Microbiology Ecology. 1994; 13(4): 241-7.

Gibert O, de Pablo J, Cortina JL, Ayora C. Municipal compost-based mixture for acid mine drainage bioremediation: Metal retention mechanisms. Applied Geochemistry. 2005; 20(9): 1648-57.

Gibert O, de Pablo J, Luis Cortina J, Ayora C. Chemical characterisation of natural organic substrates for biological mitigation of acid mine drainage. Water Research. 2004; 38(19): 4186-96.

Glombitza F. Treatment of acid lignite mine flooding water by means of microbial sulfate reduction. Waste Management. 2001; 21(2): 197-203.

Grover R, Marwaha SS, Kennedy JF. Studies on the use of an anaerobic baffled reactor for the continuous anaerobic digestion of pulp and paper mill black liquors. Process Biochemistry. 1999; 34(6-7): 653-7.

Hammack RW, Edenborn HM, Dvorak DH. Treatment of water from an open pit copper mine using biogenic sulfide and limestone: a feasibilty study. Water Resources. 1994; 28: 2321-9.

Han S, Kim S, Shin H. UASB treatment of wastewater with VFA and alcohol generated during hydrogen fermentation of food waste. Process Biochemistry. 2005; 40(8): 2897-905.

Hao JH, Chen JM, Huang L, Buglass RL. Sulfate-reducing bacteria. Critical Reviews in Environmental Science and Technology. 1996; 26(1): 155-87.

Harendranath CS, Anuja K, Singh A, Gunaseelan A, Satish K, Lala K. Immobilization in fixed film reactors: An ultrastructural approach. Water Science and Technology. 1996; 33(8): 7-15.

Haridas A, Suresh S, Chitra KR, Manilal VB. The Buoyant Filter Bioreactor: a high-rate anaerobic reactor for complex wastewater--process dynamics with dairy effluent. Water Research. 2005; 39(6): 993-1004.

Hauser JY, Holder GA. Iron availability in mixed cultures of sulfate-reducing bacteria. Biotechnology and Bioengineering. 1986; 28(1): 101-6.

Held C, Wellacher M, Robra K, Gubitz GM. Two-stage anaerobic fermentation of organic waste in CSTR and UFAF-reactors. Bioresource technology. 2002; 81(1): 19-24.

Henry JG, Prasad D. Anaerobic treatment of landfill leachate by sulfate reduction. Water Science and Technology. 2000; 41(3): 239-46.

Hiligsmann S, Deswaef S, Taillieu X, Crine M, Milande N, Thonart P. Production of sulfur from gypsum as an industrial byproduct. Applied Biochemistry and Biotechnology. 1996; 57/58: 959-969.

Hofvendahl K, Hahn-Hagerdal B. Factors affecting the fermentative lactic acid production from renewable resources. Enzyme and Microbial Technology. 2000; 26(2-4): 87-107.

Hulshoff Pol LW. New developments in reactor and process technology for sulfate reduction. Water science and technology. 2001; 44(8): 67.

Huysman P, Van Meenen P, Van Assche P, Verstraete W. Factors affecting the colonization o fnon porous and porous packing material in model upflow methane reactors. Biotechnology Letters. 1983; 5(9): 643-8.

Icgen B, Harrison S. Exposure to sulfide causes populations shifts in sulfate-reducing consortia. Research in Microbiology. 2006; 157(8): 784-91.

Ince O, Ince K, Donnelly T. Attachment, strength and performance of a porous media in an upflow anaerobic filter treating dairy wastewater. Water Science and Technology. 2000; 41(4-5): 261-70.

Jong T, Parry DL. Removal of sulfate and heavy metals by sulfate reducing bacteria in short-term bench scale upflow anaerobic packed bed reactor runs. Water Research. 2003; 37(14): 3379-89.

Joo-Hwa T, S. J, Kuan-Yeow S. Performance of anaerobic packed-bed system with different media characteristics. Water Science and Technology. 1996; 34(5-6): 453-9.

Kaksonen AH, Plumb JJ, Robertson WJ, Riekkola-Vanhanen M, Franzmann PD, Puhakka JA. The performance, kinetics and microbiology of sulfidogenic fluidized-bed treatment of acidic metal- and sulfate-containing wastewater. Hydrometallurgy. 2006; 83(1-4): 204-13.

Kaksonen AH, Riekkola-Vanhanen M-, Puhakka JA. Optimization of metal sulphide precipitation in fluidized-bed treatment of acidic wastewater. Water Research. 2003a; 37(2): 255-66.

Kaksonen AH, Franzmann PD, Puhakka JA. Effects of hydraulic retention time and sulfide toxicity on ethanol and acetate oxidation in sulfate-reducing metal-precipitating fluidized-bed reactor. Biotechnology and Bioengineering. 2004; 86(3): 332-43.

Kaksonen AH, Franzmann PD, Puhakka JA. Performance and ethanol oxidation kinetics of a sulfate-reducing fluidized-bed reactor treating acidic metal-containing wastewater. Biodegradation. 2003b; 14(3): 207-17.

Kaksonen AH, Plumb JJ, Franzmann PD, Puhakka JA. Simple organic electron donors support diverse sulfate-reducing communities in fluidized-bed reactors treating acidic metal- and sulfate-containing wastewater. FEMS Microbiology Ecology. 2004; 47(3): 279-89.

Kapdan IK, Kargi F. Bio-hydrogen production from waste materials. Enzyme and Microbial Technology. 2006; 38(5): 569-82.

Kim HW, Han SK, Shin HS. Simultaneous treatment of sewage sludge and food waste by the unified high-rate anaerobic digestion system. Water Science and Technology. 2006; 53(6): 29-35.

Kim J, Oh K, Lee S, Kim S, Hong S. Biodegradation of phenol and chlorophenols with defined mixed culture in shake-flasks and a packed bed reactor. Process Biochemistry. 2002; 37(12): 1367-73.

Koku H, Eroglu I, Gunduz U, Yucel M, Turker L. Aspects of the metabolism of hydrogen production by *Rhodobacter sphaeroides*. International Journal of Hydrogen Energy. 2002; 27: 1315-29.

Kolmert A, Henrysson T, Hallberg R, Mattiasson B. Optimization of sulphide production in an anaerobic continuous biofilm process with sulphate reducing bacteria. Biotechnology Letters. 1997; 19(10): 971-5.

Kolmert A, Johnson DB. Remediation of acidic waste waters using immobilised, acidophilic, sulfate-reducing bacteria. Journal of Chemical Technology and Biotechnology. 2001; 76(8): 836-43.

Kolmert A, Wikstrom P, Hallberg KB. A fast and simple turbidimetric method for the determination of sulfate in sulfate-reducing bacterial cultures. Journal of Microbiological Methods. 2000; 41(3): 179-84.

Kondo T, Arakawa M, Waakayama T, Miyake J. Hydrogen production by combining two types of photosynthetic bacteria with different characteristics. International Journal of Hydrogen Energy. 2002; 27: 1303-8.

Konishi Y, Yoshida N, Asai S. Desorption of dydrogen sulfide duringbatch growth and the sulfate-reducing bacterium *Desulfovibrio desulfuricans*. Biotechnology Progress. 1996; 12(3): 322-30.

Krug TA, Daugulis AJ. Ethanol production using *Zymomonas mobilis* immobilized on an ion exchange resin. Biotechnology Letters (Historical Archive). 1983; 5(3): 159-64.

Kuo W, Shu T. Biological pre-treatment of wastewater containing sulfate using anaerobic immobilized cells. Journal of hazardous materials. 2004; 113(1-3): 147-55.

La H, Kim K, Quan Z, Cho Y, Lee SE-. Enhancement of sulfate reduction activity using

granular sludge in anaerobic treatment of acid mine drainage. Biotechnology Letters. 2003; 25(6): 503-8.

Lacayo M, van Bavel B, Mattiasson B. Degradation of toxaphene in water during anaerobic and aerobic conditions. Environmental Pollution. 2004; 130(3): 437-43.

Lee CM, Chen PC, Wang CC, Tung YC. Photohydrogen production using purple non-sulfur bacteria with hydrogen fermentation reactor effluent. International Journal of Hydrogen Energy. 2002; 1308(1314).

Lee AK, Buehler MG, Newman DK. Influence of a dual-species biofilm on the corrosion of mild steel. Corrosion Science. 2006; 48(1): 165-78.

Lefebvre O, Vasudevan N, Torrijos M, Thanasekaran K, Moletta R. Anaerobic digestion of tannery soak liquor with an aerobic post-treatment. Water Research. 2006; 40(7): 1492-500.

Lens P, Vallerol M, Esposito G, Zandvoort M. Perspectives of sulfate reducing bioreactors in environmental biotechnology. Reviews in Environmental Science and Biotechnology. 2002; 1(4): 311-25.

Lens PNL, Gastesi R, Lettinga G. Use of sulfate reducing cell suspension bioreactors for the treatment of $SO_2$ rich flue gases. Biodegradation. 2003; 14(3): 229-40.

Liamleam W, Annachhatre AP. Electron donors for biological sulfate reduction. Biotechnology Advances. 2007; 25(5): 452-63.

Lin C, Jo C. Hydrogen production from sucrose using an anaerobic sequencing batch reactor process. Journal of Chemical Technology & Biotechnology. 2003; 78(6): 678-84.

Lopes FA, Morin P, Oliveira R, Melo LF. Interaction of *Desulfovibrio desulfuricans* biofilms with stainless steel surface and its impact on bacterial metabolism. Journal of Applied Microbiology. 2006; 101(5): 1087-95.

Lopes FA, Morin P, Oliveira R, Melo LF. The influence of nickel on the adhesion ability of *Desulfovibrio desulfuricans*. Colloids and Surfaces B: Biointerfaces. 2005; 46(2): 127-33.

Luinstra EA. Hydrogen from $H_2S$: technologies and economics. Calgary, Alberta:

Sulfotech; 1995.

Luptakova A, Kusnierova M. Bioremediation of acid mine drainage contaminated by SRB. Hydrometallurgy. 2005; 77(1-2): 97-102.

Madigan MT, Martinko JM, Parker J editors. Brock biology ofmicroorganisms, 8th Ed. Upper Saddle River, NJ: Prentice Hall; 1997.

Maree JP, Strydom WF. Biological sulphate removal from industrial effluent in an upflow packed bed reactor. Water Resources. 1987; 21: 141-6.

Metcalf and Eddy Inc., Tchobanoglous G., Burton FL, Stensel HD editors. Wastewater engineering: treatment and reuse. New York, NY: McGraw Hill; 2003.

Moosa S, Nemati M, T. L. Harrison S. A kinetic study on anaerobic reduction of sulphate, part I: Effect of sulphate concentration. Chemical Engineering Science. 2002; 57(14): 2773-80.

Moosa S, Nemati M, Harrison STL. A kinetic study on anaerobic reduction of sulphate, part II: incorporation of temperature effects in the kinetic model. Chemical Engineering Science. 2005; 60(13): 3517-24.

Mukhopadhyay A, He Z, Alm EJ, Arkin AP, Baidoo EE, Borglin SC, et al. Salt stress in *Desulfovibrio vulgaris* Hildenborough: an integrated genomics approach. The Journal of Bacteriology. 2006; 188(11): 4068-78.

Muthumbi W, Boon N, Boterdaele R, De Vreese I, Top EM, Verstraete W. Microbial sulfate reduction with acetate: process performance and composition of the bacterial communities in the reactor at different salinity levels. Applied Microbiology and Biotechnology. 2001; 55(6): 787-93.

Nagpal S, Chuichulcherm S, Livingston A, Peeva L. Ethanol utilization by sulfate-reducing bacteria: An experimental and modeling study. Biotechnology and Bioengineering. 2000a; 70(5): 533-43.

Nagpal S, Chuichulcherm S, Peeva L, Livingston A. Microbial sulfate reduction in a liquid-solid fluidized bed reactor. Biotechnology and Bioengineering. 2000b; 70(4): 370-80.

Nanninga HJ, Gottschal JC. Properties of *Desulfovibrio carbinolicus* sp. nov. and other sulfate-reducing bacteria isolated from an anaerobic-purification plant. Applied and Environmental Microbiology. 1987; 53(4): 802-9.

Nath K, Das DE-. Improvement of fermentative hydrogen production: various approaches. Applied Microbiology and Biotechnology. 2004; 65(5): 520-9.

Nedwell DB, Reynolds PJ. Treatment of landfill leachate by methanogenic and sulphate-reducing digestion. Water research. 1996; 30(1): 21-8.

Ni M, Leung DYC, Leung MKH, Sumathy K. An overview of hydrogen production from biomass. Fuel Processing Technology. 2006; 87(5): 461-72.

O'Flaherty V. Microbial interactions during anaerobic treatment of sulphate-containing wastewaters (PhD thesis). National University of Ireland. 1997.

Ohkouchi Y, Inoue Y. Impact of chemical components of organic wastes on L(+)-lactic acid production. Bioresource Technology. 2007; 98(3): 546-53.

Okabe S, Characklis WG. Effects of temperature and phosphorus concentration on microbial sulfate reduction by *Desulfovibrio desulfuricans*. Biotechnology and Bioengineering. 1992; 39: 1031-42.

Okabe S, Neilson PH, Characklis WG. Factors affecting microbial sulfate reduction by Desulfovibrio desulfuricans in continuous culture: limiting nutrients and sulfide concentration. Biotechnology and Bioengineering. 1992; 40: 725-34.

Okabe S, Nielsen PH, Jones WL, Characklis WG. Sulfide product inhibition of *Desulfovibrio desulfuricans* in batch and continuous cultures. Water Research. 1995; 29(2): 571-8.

Oliveira SVWB, Moraes EM, Adorno MAT, Varesche MBA, Foresti E, Zaiat M. Formaldehyde degradation in an anaerobic packed-bed bioreactor. Water Research. 2004; 38(7): 1685-94.

Omil F, Lens P, Pol LWH, Lettinga G. Characterization of biomass from a sulfidogenic, volatile fatty acid-degrading granular sludge reactor. Enzyme and Microbial Technology. 1997; 20(3): 229-36.

Parawira W, Murto M, Zvauya R, Mattiasson B. Comparative performance of a UASB reactor and an anaerobic packed-bed reactor when treating potato waste leachate. Renewable Energy. 2006; 31(6): 893-903.

Patel H, Madamwar D. Effects of temperatures and organic loading rates on biomethanation of acidic petrochemical wastewater using an anaerobic upflow fixed-film reactor. Bioresource Technology. 2002; 82(1): 65-71.

Picanco AP, Vallero MVG, Gianotti EP, Zaiat M, Blundi CE. Influence of porosity and composition of supports on the methanogenic biofilm characteristics developed in a fixed bed anaerobic reactor. Water Science and Technology. 2001; 44(4): 197-204.

Postgate JR. The sulphate-reducing bacteria. London: Cambridge University Press; 1984.

Ohashi H, Ohya, H, Aihara, H. Hydrogen production from hydrogen sulfide using membrane reactor integrated with porous membranes having thermal and corrosion resistance. Journal of Membrane Science. 1998; 146: 39-42.

Quereshi N, Annous BA, Ezeji TC, Karcher P, Maddox IS. Biofilm reactors for industrial bioconversion processes: employing potential of enhanced reaction rates. 2005; 4(24): BioMed Online Journal.

Rabus R, Hansen T, Widdel F. Dissimilatory sulfate- and sulfur-reducing prokaryotes. 2000; Available at: http://141.150.157.117:8080/prokPUB/chaprender/jsp/showchap.jsp?chapnum=274&initsec=04_00. Accessed 08/01, 2005.

Ramasamy EV, Gajalakshmi S, Sanjeevi R, Jithesh MN, Abbasi SA. Feasibility studies on the treatment of dairy wastewaters with upflow anaerobic sludge blanket reactors. Bioresource Technology. 2004; 93(2): 209-12.

Reis MAM. Effect of hydrogen sulfide on growth of sulfate reducing bacteria. Biotechnology and bioengineering. 1992; 40(5): 593.

Reis MAM, Lemos PC, Almeida JS, Carrondo MJTE-. Evidence for the intrinsic toxicity of $H_2S$ to sulphate-reducing bacteria. Applied Microbiology and Biotechnology. 1991; 36(1): 145-7.

Ribeiro R, Varesche MBA, Foresti E, Zaiat M. Influence of the carbon source on the

anaerobic biomass adhesion on polyurethane foam matrices. Journal of Environmental Management. 2005; 74(2): 187-94.

Sa CSA, Boaventura RAR. Biodegradation of phenol by *Pseudomonas putida* DSM 548 in a trickling bed reactor. Biochemical Engineering Journal. 2001; 9(3): 211-9.

Sarner E. Removal of sulphate and sulphite in an anaerobic tricking (Antric) filter. Water Science and Technology. 1990; 22: 395-404.

Selvaraj PT, Little MH, Kaufman EN. Biodesulfurization of flue gases and other sulfate/sulfite waste streams using immobilized mixed sulfate-reducing bacteria. Biotechnology Progress. 1997; 13: 583-9.

Senthuran A, Senthuran V, Hatti-Kaul R, Mattiasson B. Lactic acid production by immobilized Lactobacillus casei in recycle batch reactor: a step towards optimization. Journal of Biotechnology. 1999; 73(1): 61-70.

Seth R, Goyal SK, Handa BK. Fixed film biomethanation of distillery spentwash using low cost porous media. Resources, Conservation and Recycling. 1995; 14(2): 79-89.

Sheoran AS, Sheoran V. Heavy metal removal mechanism of acid mine drainage in wetlands: A critical review. Minerals Engineering. 2006; 19(2): 105-16.

Silva AJ, Hirasawa JS, Varesche MB, Foresti E, Zaiat M. Evaluation of support materials for the immobilization of sulfate-reducing bacteria and methanogenic archaea. Anaerobe. 2006; 12(2): 93-8.

Silva AJ, Varesche MB, Foresti E, Zaiat M. Sulphate removal from industrial wastewater using a packed-bed anaerobic reactor. Process Biochemistry. 2002; 37(9): 927-35.

Sorial GA, Smith FL, Suidan MT, Pandit A, Biswas P, Brenner RC. Evaluation of trickle bed Air biofilter performance for BTEX removal. Journal of Environmental Engineering. 1997; 123(6): 530-7.

Sorial GA, Smith FL, Suidan MT, Pandit A, Biswas P, Brenner RC. Evaluation of trickle-bed air biofilter performance for styrene removal. Water Research. 1998; 32(5): 1593-603.

Speece RE. Anaerobic biotechnology. Nashville, Tennessee: Archae Press; 1996.

Sreenath HK, Moldes AB, Koegel RG, Straub RJE-. Lactic acid production from agriculture residues. Biotechnology Letters. 2001; 23(3): 179-84.

Stucki G, Hanselmann KW, Hurzeler RA. Biological sulfuric acid transformation: reactor design and process optimization. Biotechnoloy and Bioengineering. 1993; 41: 303-15.

Torre AD, Stephanopoulos G. Simulation study of anaerobic digestion control. Biotechnology and Bioengineering. 1986; 28(8): 1138-53.

Traore AS, Hatchikian CE, Le Gall J, Belaich JP. Microcalorimetric studies of the growth of sulfate-reducing bacteria: comparison of the growth parameters of some *Desulfovibrio species*. Journal of Bacteriology. 1982; 149(2): 606-11.

Tsukamoto TK, Killion HA, Miller GC. Column experiments for microbiological treatment of acid mine drainage: low-temperature, low-pH and matrix investigations. Water Research. 2004; 38(6): 1405-18.

Tursman JF, Cork DJ. Influence of sulfate and sulfate-reducing bacteria on anaerobic digestion technology. In: Mizhari A, editor. Advances in biotechnological processes. New York, NY: A.R. Liss Inc.; 1989. p. 273-285.

Vallero MVG, Lettinga G, Lens PNL. High rate sulfate reduction in a submerged anaerobic membrane bioreactor (SAMBaR) at high salinity. Journal of Membrane Science. 2005; 253(1-2): 217-32.

van Houten RT, Elferink SJWHO, van Hamel SE, Pol LWH, Lettinga G. Sulphate reduction by aggregates of sulphate-reducing bacteria and homo-acetogenic bacteria in a lab-scale gas-lift reactor. Bioresource Technology. 1995; 54(1): 73-9.

van Houten RT, Hulshoff Pol LW, Lettinga G. Biological sulphate reduction using gas-lift reactors fed with hydrogen and carbon dioxide as energy and carbon source. Biotechnology and Bioengineering. 1994; 44(5): 586-94.

van Houten RT, van der Spoel H, van Aelst AC, Hulshoff Pol LW, Lettinga G. Biological sulfate reduction using synthesis gas as energy and carbon source. Biotechnology and Bioengineering. 1996; 50(2): 136-44.

van Houten RT, Yun SY, Lettinga G. Thermophilic sulphate and sulphite reduction in lab-scale gas-lift reactors using $H_2$ and $CO_2$ as energy and carbon source. Biotechnology

and Bioengineering. 1997; 55(5): 807-14.

Van Loosdrecht MCM, Heijnen SJ. Biofilm bioreactors for waste-water treatment. Trends in Biotechnology. 1993; 11(4): 117-21.

Viera M, Curutchet G, Donati E. A combined bacterial process for the reduction and immobilization of chromium. International Biodeterioration & Biodegradation. 2003; 52(1): 31-4.

Waybrant KR, Ptacek CJ, Blowes DW. Treatment of mine drainage using permeable reactive barriers: column experiments. Environmental Science & Technology. 2002; 36(6): 1349-56.

Weijma J, Chi TM, Hulshoff Pol LW, Stams AJM, Lettinga G. The effect of sulphate on methanol conversion in mesophilic upflow anaerobic sludge bed reactors. Process Biochemistry. 2003; 38(9): 1259-66.

Widdel F. Microbiology and ecology of sulfate- and sulfur-reducing bacteria. In: Zehnder AJB, editor. Biology of anaerobic microorganisms. New York: John Wiley and Sons; 1988. p. 469-585.

Wiszniowski J, Surmacz-Górska J, Robert D, Weber J-. The effect of landfill leachate composition on organics and nitrogen removal in an activated sludge system with bentonite additive. Journal of Environmental Management. 2007; 85(1): 59-68.

Wright WF. Transient response of vapor-phase biofilters. Chemical Engineering Journal. 2005; 113(2-3): 161-73.

Yamaguchi T, Harada H, Hisano T, Yamazaki S, Tseng I. Process behavior of UASB reactor treating a wastewater containing high strength sulfate. Water Research. 1999; 33(14): 3182-90.

Yang Y, Tada C, Tsukahara K, Sawayama S. Methanogenic community and performance of fixed- and fluidized-bed reactors with reticular polyurethane foam with different pore sizes. Materials Science and Engineering: C. 2004; 24(6-8): 803-13.

Ye F, Chen Y, Feng X. Advanced start-up of anaerobic attached film expanded bed reactor by pre-aeration of biofilm carrier. Bioresource Technology. 2005; 96(1): 115-9.

Yeh, E. Raw sludge as substrate for sulphate-reducing bacteria (MASc thesis). University of Toronto. 1999.

Zagury GJ, Kulnieks VI, Neculita CM. Characterization and reactivity assessment of organic substrates for sulphate-reducing bacteria in acid mine drainage treatment. Chemosphere. 2006; 64(6): 944-54.

Zellner G, Neudorfer F, Diekmann H. Degradation of lactate by an anaerobic mixed culture in a fluidized-bed reactor. Water Research. 1994; 28(6): 1337-40.

Zinatizadeh AAL, Mohamed AR, Najafpour GD, Hasnain Isa M, Nasrollahzadeh H. Kinetic evaluation of palm oil mill effluent digestion in a high rate up-flow anaerobic sludge fixed film bioreactor. Process Biochemistry. 2006; 41(5): 1038-46.

# Chapter 10: Appendices

## 10.1 Appendix A: Prediction of Volumetric $CH_4$ Production

Procedure for calculating volumetric $CH_4$ production in a bioreactor with a known COD removal efficiency. Adapted from Metcalf and Eddy (2003).

1. The sum of the $CH_4$ yield ($Y_{CH4}$) and volumetric COD removal rate is the volumetric $CH_4$ production rate.

$$\frac{\text{mol CH4}}{\text{m}^3\text{.d}} = \left(\frac{\text{mol CH}_4}{\text{g COD}_{\text{removed}}}\right)\left(\frac{\text{g COD}_{\text{removed}}}{\text{m}^3\text{.d}}\right)$$

2. To determine the $CH_4$ yield, the numerator (moles of $CH_4$ produced) and denominator (g COD removed) for the entire process must be individually calculated.

3. A COD mass balance on the process is performed. The $COD_{removed}$ is the product of $COD_{in}$ and removal efficiency $\eta$. $COD_{removed}$ can also be expressed by two alternate and equal relationships. The removal of COD in a methanogenic processe occurs via the synthesis of cells (VSS) and $CH_4$.

$$\begin{aligned}\text{COD}_{\text{removed}} &= \text{COD}_{\text{in}} \cdot \eta \\ &= \text{COD}_{\text{in}} - \text{COD}_{\text{out}} \\ &= \text{COD}_{\text{VSS}} + \text{COD}_{\text{CH4}}\end{aligned}$$

4. Determine the amount of COD converted to cells. Typically 0.08 g of cells (VSS) are synthesized from each g $COD_{removed}$. Assuming an average cell composition of $C_5H_7NO_2$, each g of VSS has a COD content of 1.42 g.

$$\text{g COD}_{\text{VSS}} = \left(\frac{1.42\text{ g COD}_{\text{VSS}}}{\text{g VSS}}\right)\left(\frac{0.08\text{ g VSS}}{\text{g COD}_{\text{removed}}}\right)\cdot \text{g COD}_{\text{removed}}$$

5. The amount of COD converted to $CH_4$ can now be calculated.

$$\text{COD}_{\text{CH4}} = \left(\text{COD}_{\text{in}} - \text{COD}_{\text{out}}\right) - \text{COD}_{\text{VSS}}$$

6. Calculate the amount of $CH_4$ produced from $COD_{CH4}$. Based upon the theoretical oxygen demand of methane, (1 mol of $CH_4$ = 64 g COD). This corresponds to 0.40 L $CH_4$ produced per g COD at 35 $^{o}$C which correlates well with experimental values from literature.

$$\text{mol CH}_4 = \frac{\text{mol CH}_4}{64\text{ g COD}}\cdot \text{g COD}_{\text{CH4}}$$

All necessary values for the methane yield have now been obtained.

## 10.2 Appendix B: Volumetric Sulfate Reduction Rates from Literature

**Table 10.1:** Volumetric sulfate reduction rates (mol $SO_4^{2-}/m^3.d$) from recent SRB literature. Abbreviations: CSTR - continuous stirred tank reactor; UASB, upflow anaerobic sludge blanket; PBR - packed bed reactor; FBR - fluidized bed reactor; WW - wastewater.

| Substrate | Reactor Type | Carrier Material | Temp. ($^oC$) | mol $SO_4^{2-}$ $/m^3.d$ | Reference |
|---|---|---|---|---|---|
| lactate, organic waste | PBR | pyrite, sand, wood chips | NR | 1 | Waybrant, et al., 2002 |
| lactate | PBR | glass beads | 22 | 3 | Baskaran and Nemati , 2006 |
| lactate/ethanol/glycerol | PBR | Poraver porous glass beads | NR | 3 | Kolmert and Johnson, 2001 |
| tannery effluent | CSTR | - | NR | 3 | Boshoff et al., 2004a |
| glucose | PBR | polymer entrapment | NR | 4 | Kuo and Shu et al., 2004 |
| methanol | UASB | - | 30 | 4 | Weijma et al., 2003 |
| tannery effluent | trench reactor | - | NR | 4 | Boshoff et al., 2004a |
| lactate | PFR | - | ambient | 4 | Hammack et al., 1994 |
| $H_2$ | CSTR | - | 30 | 5 | Lens et al., 2003 |
| tannery effluent | UASB | - | NR | 6 | Boshoff et al., 2004a |
| lactate | PBR | polypropylene pall rings | ambient | 7 | Christy, 2001 |
| ethanol, toluene | horizontal PBR | polyurethane foam | 30 | 7 | Cattony et al., 2005 |
| $H_2/CO_2$ | membrane | - | 30 | 9 | Fedorovich et al., 2000 |
| glucose, methanol, acetate | horizontal PBR | polyurethane foam | 26 | 11 | Cadavid et al., 1999 |
| CO | PBR | pelletized ash | 35 | 13 | du Preeze and Maree, 1995 |
| acetate | CSTR | - | 35 | 19 | Moosa et al., 2005 |
| lactate | FBR | silicate | 35 | 21 | Kaksonen et al., 2003a |
| $H_2$/CO | PBR | pelletized ash | 35 | 25 | du Preeze and Maree, 1995 |
| lactate | PBR | scouring pad foam | 22 | 29 | Baskaran and Nemati , 2006 |
| lactate | PBR | pool filter silica sand | 25 | 32 | Jong and Parry, 2003 |
| methanol | PBR | porous ceramic | ambient | 33 | Glombitza, 2001 |
| organic peroxide wastewater | PBR | polyurethane foam | NR | 34 | Silva et al., 2002 |
| cheese whey | PBR | Plasdek PVC | 35 | 36 | Deswaef et al., 1996 |
| AD-MSS | PBR | k-carrageenan gel | 30 | 41 | Selvaraj et al., 1997 |
| acetate | CSTR | - | 35 | 43 | Moosa et al., 2002 |
| molasses | UASB | - | 30 | 45 | Annachhatre and Suktrakoolvait, 2001 |
| ethanol | FBR | silicate | 35 | 45 | Kaksonen et al., 2004 |

| | | | | | |
|---|---|---|---|---|---|
| $H_2/CO_2$ | PBR | "special packing" | 30 | 50 | Foucher et al., 2001 |
| anaerobically digested municipal sewage sludge | CSTR with recycle | - | 30 | 50 | Selvaraj et al., 1997 |
| lactate | PBR | sand | 22 | 57 | Baskaran and Nemati , 2006 |
| ethanol | UASB | - | 35 | 63 | Kalyuhnyi |
| cheese whey | PBR | Plasdek PVC | 35 | 64 | Hiligsmann et al, 1996 |
| ethanol | FBR | Poraver porous glass beads | ambient | 66 | Nagpal et al., 2000b |
| molasses | PBR | N/A | 31 | 68 | Maree and Strydom, 1987 |
| acetate, ethanol | membrane | - | 33 | 69 | Vallero et al., 2005 |
| ethanol | EGSB | - | 35 | 92 | de Smul et al., 1997 |
| acetate | EGSB | - | 33 | 92 | Dries et al., 1998 |
| acetate, propionate, butyrate | UASB | - | 30 | 94 | Omil et al., 1996 |
| acetate | EGSB | - | 35 | 99 | de Smul, 1998 |
| acetate | EGSB | - | 35 | 100 | de Smul, 1998 |
| $H_2/CO_2/CO$ | FBR/gas lift | pumice | 35 | 104 | van Houten et al., 1996 |
| $H_2/CO_2$ | gas-lift | pumice | 55 | 116 | van Houten et al., 1997 |
| ethanol | EGSB | - | 33 | 131 | de Smul et al., 1999 |
| acetate | UASB | - | 32 | 146 | Muthumbi et al., 2001 |
| acetate | PBR | textile fiber | 35 | 155 | Stucki et al., 1993 |
| acetate | PBR | porous lava rock | 35 | 156 | Stucki et al., 1993 |
| $H_2/CO_2$ | FBR/air lift | basalt | 30 | 186 | van Houten et al., 1994 |
| $H_2/CO_2$ | FBR/air lift | pumice | 30 | 260 | van Houten et al., 1995 |
| $H_2/CO_2$ | FBR/air lift | pumice | 30 | 313 | van Houten et al., 1994 |
| molasses | PBR | granular activated carbon | 35 | 320 | Gasiorek, 1994 |
| anaerobically digested municipal sewage sludge | PBR | BioSep | 30 | 456 | Selvaraj et al., 1997 |
| acetate | PBR | polyurethane foam | 35 | 576 | Stucki et al., 1993 |
| acetate | PBR | sintered glass beads | 35 | 677 | Stucki et al., 1993 |

## 10.3 Appendix C: Calibration Curves for Analytical Methods

### 10.3.1 Calibration Curve for Dissolved Sulfide

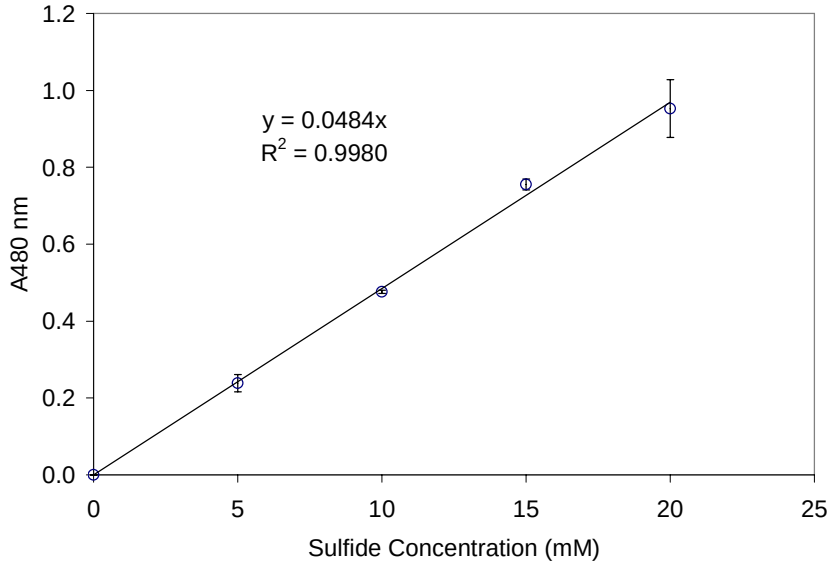


**Figure 10.1:** Linear relationship between $A_{480\ nm}$ and total dissolved sulfide concentration (mM). Data points are mean values of triplicate analysis and the vertical error bars are standard deviation.

### 10.3.2 Calibration Curve for Dissolved Sulfate

The relationship between dissolved sulfate and $A_{420}$ nm was described by a 3rd order polynomial of the form $y = ax^3 + bx^2 + cx + d$. (Figure 10.2). Coefficient values were $a$ = -1.49598E-05, $b$ = 9.72374E-04, $c$ = 2.37134E-02, and $d$ = 6.71879E-02 with an $R^2$ value of 0.997.

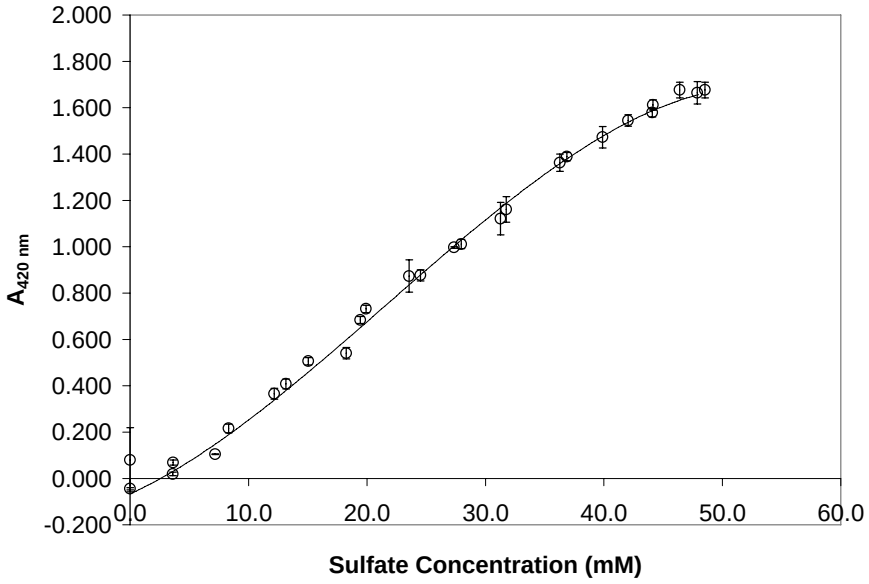


**Figure 10.2:** Relationship between $A_{420\ nm}$ and total dissolved sulfide concentration (mM). Data points are mean values of triplicate analysis and the vertical error bars are standard deviation.

### 10.3.3 Calibration Curve for Gas Phase $H_2S$

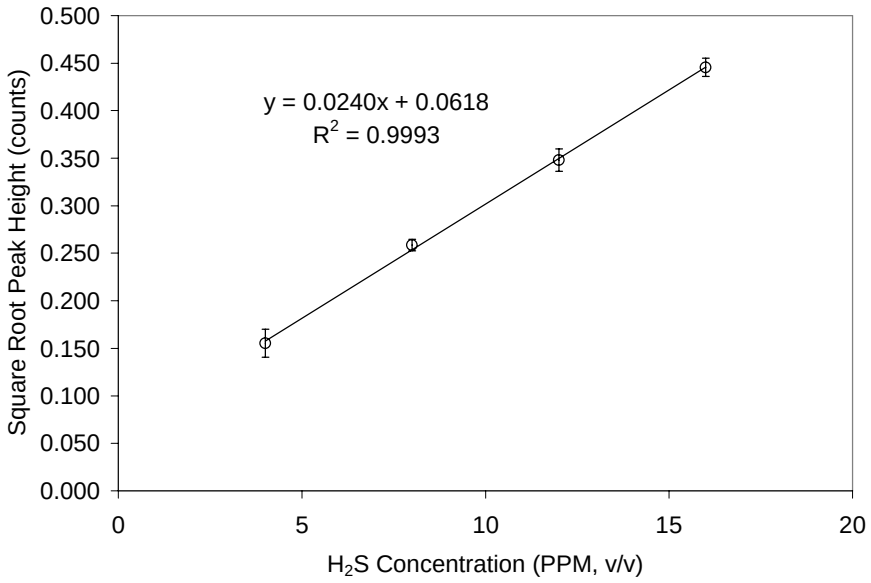


**Figure 10.3:** Relationship between square root peak height (counts) and gas phase $H_2S$ concentration (PPM, v/v). Data points are mean values of triplicate analysis and the vertical error bars are standard deviation.

### 10.3.4 Calibration Curves for Dissolved Lactate and Acetate

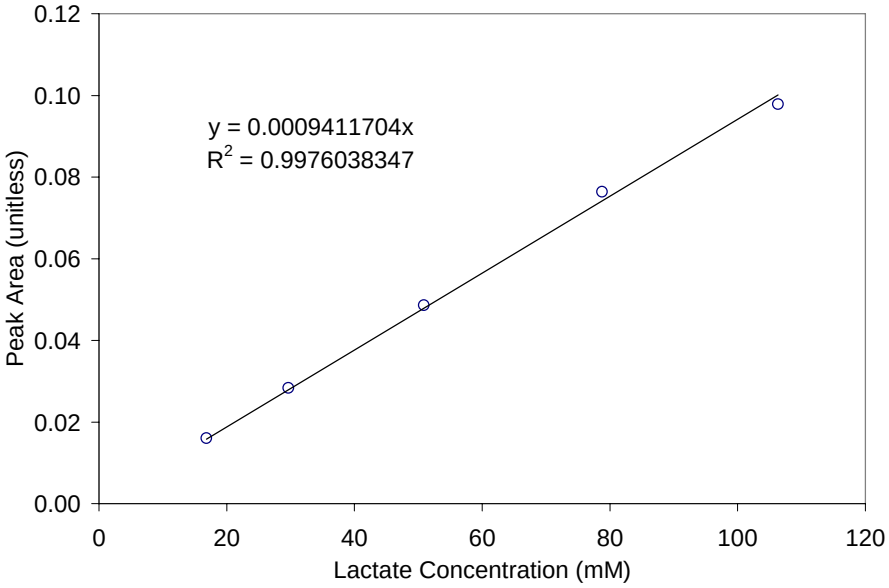


**Figure 10.4:** Relationship between peak area and dissolved lactate concentration (mM).

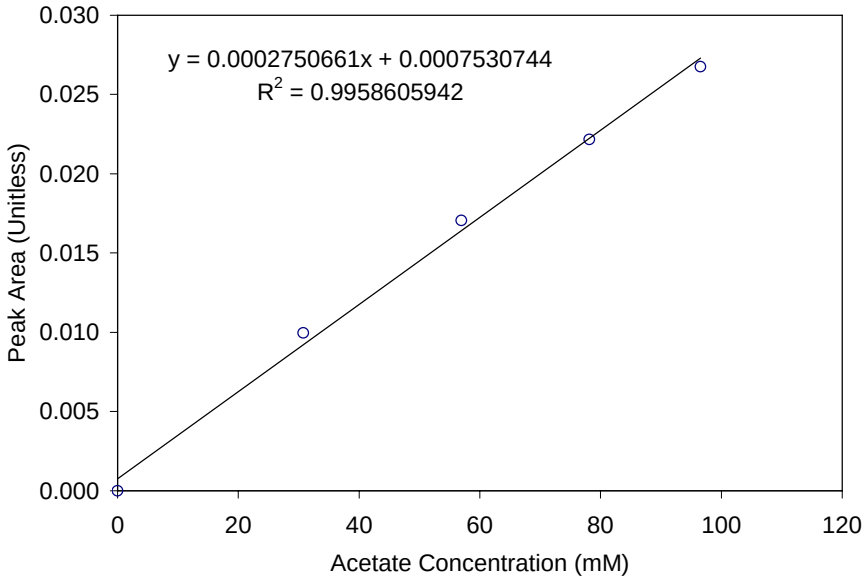


**Figure 10.5:** Relationship between peak area and dissolved acetate concentration (mM).

### 10.3.5 Calibration Curve for Suspended Cell Concentration

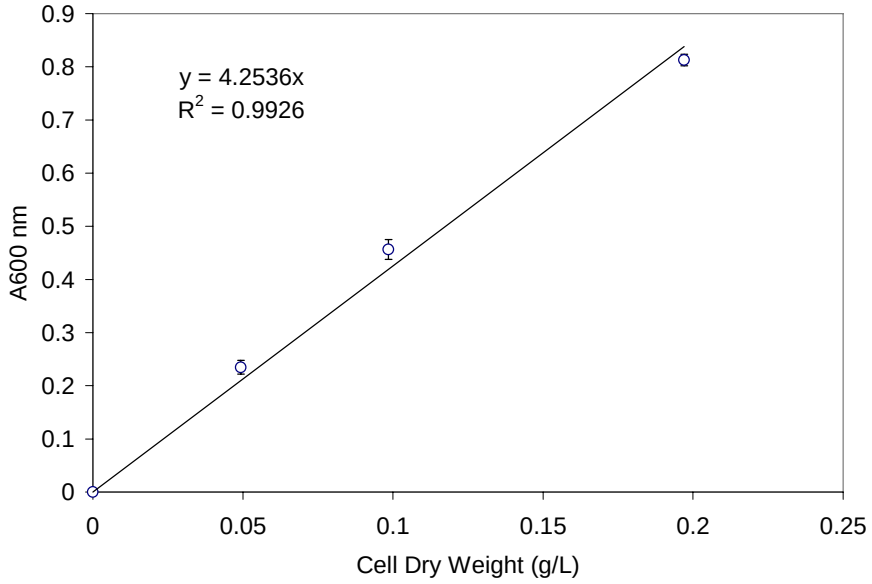


**Figure 10.6:** Relationship between $A_{600\ nm}$ and suspended cell biomass measured as cell dry weight (CDW g/L).

## 10.4 Appendix D: Basic PBR Model Description

**Table 10.2:** Nomenclature for basic PBR model for volumetric productivity based on equilibrium relationships.

| Parameter | Description | Value/Relationship | Units |
|---|---|---|---|
| $dP/dt$ | Volumetric sulfide production | [43] | mol/m$^3$.d |
| $n_{total}$ | Total molar sulfide flow rate | [44] | mol/h |
| $n_{TDS}$ | Dissolved molar sulfide flow rate | 0.00160 | mol/h |
| $n_{H2S(g)}$ | Gaseous molar sulfide flow rate | [46] | mol/h |
| $P_{H2S}$ | $H_2S$ partial pressure | [47] | atm |
| $V$ | Bioreactor volume | 600 x 10$^{-6}$ | m$^3$ |
| $R$ | Universal gas constant | 0.082 | L.atm/mol.K |
| $T$ | Temperature | 310 | K |
| [TDS] | Moles of total dissolved sulfide per L $H_2O$ | 0.020 | mol/L |
| [$H_2S_{(aq)}$] | Moles of dissolved $H_2S$ per L $H_2O$ | [48] | mol/L |
| [$H_2O$] | Moles of $H_2O$ per L $H_2O$ | 55.6 | mol/L |
| $H$ | Henry's Constant at 37 $^oC$ | 708 | atm |
| $K_a$ | First $H_2S$ dissociation constant | 2.512 x 10$^{-7}$ | mol/L |

Volumetric productivity is calculated as the rate of sulfide production divided by the bioreactor volume:

$$\frac{dP}{dt} = \frac{n_{\text{total}}}{V}\frac{24\,\text{h}}{\text{d}} \tag{43}$$

The total rate of sulfide production is the sum of sulfide in the aqueous and gas phases:

$$n_{\text{TDS}} + n_{\text{H2S}_{(g)}} = n_{\text{total}} \tag{44}$$

Constant liquid flow rate and TDS concentration results in a constant value for $n_{TDS}$:

$$n_{\text{TDS}} = (20\,\text{mM})\frac{0.080\,\text{L}}{\text{h}}\frac{\text{mol}}{1000\,\text{mmol}} = 0.00160\,\text{mol/h} \tag{45}$$

The flow rate of $H_2S$ is the gas phase is a function of the equilibrium $H_2S$ partial pressure:

$$n_{\text{H2S}_{(g)}} = \frac{P_{H2S}V}{RT} \tag{46}$$

The equilibrium partial pressure is defined by Henry's Law and a function of the concentration of $H_2S$ in the aqueous phase:

$$P_{H2S} = Hx \cong H\left(\frac{[H_2S_{(aq)}]}{[H_2O]}\right) \tag{47}$$

The concentration of $H_2S$ in the aqueous phase is a function of pH:

$$[H_2S_{(aq)}] = [TDS]\frac{1}{1 + K_a/[H^+]} \tag{48}$$